PB85-156248

Auto-Oxidation Potential of Raw and Retorted Oil Shale

Research Triangle Inst.
Research Triangle Park, NC

Prepared for

Environmental Protection Agency, Cincinnati, OH

Sep 84

U.S. Department of Commerce
National Technical Information Service
NTIS

PB85-156248

EPA/600/2-84/153
September 1984

AUTO-OXIDATION POTENTIAL OF RAW AND RETORTED OIL SHALE

by

D. A. Green
Research Triangle Institute
Post Office Box 12194
Research Triangle Park, North Carolina 27709

EPA Contract No. 68-02-3170-73

Project Officer
Edward R. Bates
Hazardous Waste Engineering Research Laboratory
Cincinnati, Ohio 45268

HAZARDOUS WASTE ENGINEERING RESEARCH LABORATORY
OFFICE OF RESEARCH AND DEVELOPMENT
U.S. ENVIRONMENTAL PROTECTION AGENCY
CINCINNATI, OH 45268

REPRODUCED BY
NATIONAL TECHNICAL
INFORMATION SERVICE
U.S. DEPARTMENT OF COMMERCE
SPRINGFIELD, VA. 22161

TECHNICAL REPORT DATA

(Please read Instructions on the reverse before completing)

1. REPORT NO. EPA/600/2-84/153	2.	3. RECIPIENT'S ACCESSION NO. PB85 156248 /AS
4. TITLE AND SUBTITLE Auto-Oxidation Potential of Raw and Retorted Oil		5. REPORT DATE September 1984
		6. PERFORMING ORGANIZATION CODE
7. AUTHOR(S) D.A. Green		8. PERFORMING ORGANIZATION REPORT NO.
9. PERFORMING ORGANIZATION NAME AND ADDRESS D.A. Green Research Triangle Institute RTP, NC 27709		10. PROGRAM ELEMENT NO.
		11. CONTRACT/GRANT NO. 68-02-3170-73
12. SPONSORING AGENCY NAME AND ADDRESS Hazardous Waste Engineering Research Laboratory Environmental Protection Agency Office of Research and Development Cincinnati, OH 45268		13. TYPE OF REPORT AND PERIOD COVERED Project Report/ Summary
		14. SPONSORING AGENCY CODE EPA/600-12

15. SUPPLEMENTARY NOTES

16. ABSTRACT

This paper discusses an EPA sponsored study to asses the potential environmental impacts of leachates from raw mined western oil shales. The study was undertaken as a cooperative effort of the Environmental Protection Agency, Colorado State University, Rio Blanco Oil Shale Company, Cathedral Bluffs Shale Oil Company, and the Oil Shale Project Office of the Bureau of Land Management. This paper presents the results of three years evaluation of the quantity and chemical characterization of leachates generated from onsite field collectors along with laboratory shake tests on raw mined oil shales from the C-a and C-b Federal lease tracts in western Colorado. The findings are indicators of the levels of common and trace species that can be expected to occur in field generated raw shale leachates.

17. KEY WORDS AND DOCUMENT ANALYSIS

a. DESCRIPTORS	b. IDENTIFIERS/OPEN ENDED TERMS	c. COSATI Field/Group

18. DISTRIBUTION STATEMENT Release Unlimited	19. SECURITY CLASS *(This Report)* Unclassified	21. NO. OF PAGES 163
	20. SECURITY CLASS *(This page)* Unclassified	22. PRICE

NOTICE

This document has been reviewed in accordance with U.S. Environmental Protection Agency policy and approved for publication. Mention of trade names or commercial products does not constitute endorsement or recommendation for use.

FOREWORD

When energy and material resources are extracted, processed, converted, and used, the related pollutional impacts on our environment and even on our health often require that new and increasingly more efficient pollution control methods be used. The Industrial Environmental Research Laboratory -- Cincinnati (IERL-CI) assists in developing and demonstrating new and improved methodologies that will meet these needs both efficiently and economically.

David G. Stephen, Director

Cincinnati

ABSTRACT

A study was conducted to assess the potential spontaneous combustion hazard of solid waste streams produced in the processing of oil shale. In addition, the utility and precision of various test methods to assess this hazard were determined. The best methods that were found involved a differential scanning calorimetry test and a nonadiabatic oxygen absorption test. In both cases, the sample was slowly heated in air. In the former case, exothermic activity (i.e., heat release) was monitored; in the latter, changes in exhaust gas composition were monitored.

The carbonaceous retorted oil shale samples appear to present less hazard of spontaneous combustion than bituminous coal. None of the raw shales were found to present as great a hazard as Wyoming subbituminous coal. However, the two raw Utah shale samples tested were found to present hazards exceeding those of less reactive bituminous coals. These materials represent a potential hazard, but if stored and disposed of under conditions suitable for long-term storage of reactive coals, should not spontaneously combust.

The codisposal of raw and retorted shale should be approached cautiously and preferably be avoided if possible because the presence of raw shale increases the energy contents of the mixture and, in some cases, decreased the temperature at which exothermic activity was observed. Codisposal of byproduct sulfur with retorted shale appears to cause no increase in risk of spontaneous combustion (but may lead to leaching problems).

It must be noted that the results reported here are based on a very limited number of samples of raw and retored shale. Substantial variations in composition of raw shales occur with geographic and stratigraphic location. The retorted shale samples came from pilot plant operations which may not be completely representative of commercial operations. Hence, it is strongly recommended that actual samples of waste materials proposed for field disposal be tested to determine their actual spontaneous combustion hazard.

TABLE OF CONTENTS

Section		Page
	Foreword	iii
	Abstract	iv
	Figures	vii
	Tables	viii
1	Relating Characteristics of Solids to Storage Pile	1
	1.0 Introduction	1
	1.1 Empirical Ranking	1
	1.2 Analytical Model	3
	1.3 Computer Simulation	7
	1.4 Application of Solid-Gas Reaction Models	8
	1.5 Effects of Pore and Particle Size Upon Adsorption	9
	1.6 Chemistry of Low-Temperature Oxidation	12
2	Description of Samples	13
3	Differential Scanning Calorimetry Testing and Nonadiabatic Oxygen Absorption Testing	17
	3.1 Differential Scanning Calorimetry	17
	3.2 Nonadiabatic Oxygen Absorption Testing	24
	3.2.1 Introduction	24
	3.2.2 Method: Phase I Samples	27
	3.2.3 Apparatus: Phase I Samples	27
	3.2.4 Method and Apparatus: Phase II Samples	30
	3.2.5 Results	30
	3.2.6 Interpretation	32
4	Other Experimental Methods	34
	4.1 Thermogravimetric Analysis	34
	4.1.1 Introduction	34
	4.1.2 Experimental	34
	4.1.3 Results	36
	4.2 Peroxide Test	38
	4.3 Adiabatic Oxygen Absorption Test	38
	4.4 Pressure Differential Scanning Calorimetry	39

TABLE OF CONTENTS (continued)

Section		Page
5	Quality Assurance	40
	5.0 Introduction	40
	5.1 DSC Testing	40
	5.2 Nonadiabatic Oxygen Absorption Testing	40
	5.3 Specific Heat Determination	41
	5.4 Heating Value, Sulfur, and Organic Carbon Determination	41
6	Conclusions	43
	REFERENCES	46
	APPENDIX A	A-1
	APPENDIX B	A-12
	APPENDIX C	A-62

FIGURES

Number		Page
1	Spontaneous heating of dry, stage-crushed, 0- to 14-inch coal in an adiabatic calorimeter	2
2	Acceptable and unsatisfactory combinations of M and N by van Doornum's model	6
3	Limiting cases of the grain model for solid-gas reactions	10
4	Representation of general case of a grain model for a storage pile where both reaction and diffusion control the rate	11
5	DSC cell cross section	19
6	Effect of adding raw Utah (28 GPT) shale to Paraho retorted shale (2° C/min heating ramp)	25
7	Effect of adding sulfur to raw/retorted shale mixture (2° C/min heating ramp)	26
8	Nonadiabatic test apparatus	28
9	TGA Diagram	35

TABLES

Number		Page
1	The Relative Tendency of Coals To Heat Spontaneously in Storage	4
2	Total Sulfur Content of Samples (Weight %)	15
3	Higher Heating Values of Samples (Btu/lb)	15
4	Organic Carbon Content of Materials Tested (Weight Percent on Dry Basis)	16
5	Mean Heat Capacity of Coal and Shale Materials Based on Initial Sample Weight (J/G)	16
6	Exothermic Onset Temperature Observed in Oxidation of Coal, Oil Shale, and Retorted Oil Shale (2° C/Minute Heating Ramp)	21
7	Magnitude of Exothermic Reaction of Coal, Oil Shale, and Retorted Oil Shale (2° C/Minute Heating Ramp)	22
8	Spontaneous Combustion Index and Calculation Parameters of Materials Subjected to Nonadiabatic Test	33
9	Weight Losses Observed at 300° C and 500° C During Thermogravimetric Analysis (2° C/Minute Heating Ramp, Dry Air)	37
10	Sulfur Contents of Test Materials	42
11	Summary of Results From Differential Scanning Calorimetry and Nonadiabatic Oxygen Absorption Testing	45

APPENDIX TABLES

Number		Page
A-1	Heat Capacity of C-a Raw Shale based on Initial Sample Weight (-325 mesh)	A-1
A-2	Heat Capacity of Lurgi Retorted Oil Shale Based on Initial Weight (-325 mesh)	A-2
A-3	Heat Capacity of Wyoming Smith-Roland Sub Bituminous Coal Based on Initial Weight (-325 mesh)	A-3
A-4	Heat Capacity of TOSCO II Retorted Shale Based on Initial Sample Weight (-325 mesh)	A-4
A-5	Heat Capacity of Paraho (-325 mesh) Retorted Shale Based on Initial Sample Weight	A-5
A-6	Heat Capacity of Western Kentucky #9 Bituminous Coal Based on Initial Sample Weight (-325 mesh)	A-6
A-7	Heat Capacity of Pocahontas #3 Bituminous Coal Based on Initial Sample Weight (-325 mesh)	A-7
A-8	Heat Capacity of Union Retorted Shale/Raw Shale/Sulfur Mixture at 17% Moisture Based on Initial Sample Weight (-325 mesh)	A-8
A-9	Heat Capacity of Hytort Retorted Shale Based on Initial Sample Weight (-325 mesh)	A-9
A-10	Heat Capacity of Utah Raw Shale (28 Gallon/Ton) Based on Initial Sample Weight (-325 mesh)	A-10
A-11	Heat Capacity of Utah Raw Shale (66 Gallon/Ton) Based on Initial Sample Weight (-325 mesh)	A-11

APPENDIX TABLES (continued)

Number		Page
B-1	Composition of Exit Gas From Nonadiabatic Test Cell at 125° C	A-47
B-2	Composition of Exit Gas From Nonadiabatic Test Cell at 125° C	A-48
B-3	Composition of Exit Gas From Nonadiabatic Test Cell at 150°C	A-49
B-4	Composition of Exit Gas From Nonadiabatic Test Cell at 150°C	A-50
B-5	Composition of Exit Gas From Nonadiabatic Test Cell at 175° C	A-51
B-6	Composition of Exit Gas From Nonadiabatic Test Cell at 175° C	A-52
B-7	Composition of Exit Gas From Nonadiabatic Test Cell at 200° C	A-53
B-8	Composition of Exit Gas From Nonadiabatic Test Cell at 250° C	A-54
B-9	Composition of Exit Gas From Nonadiabatic Test Cell at 300° C	A-55
B-10	Mean Oxygen Concentrations in Effluent Gas at Various Temperatures (Volume %, Dry Basis) Nonadiabatic Test of First Sample Set	A-56
B-11	Mean Oxygen Concentrations in Effluent Gas From Nonadiabatic Test of Second Sample Set	A-57
B-12	Mean Carbon Monoxide Concentrations in Effluent Gas at Various temperatures (Volume %, Dry Basis)	A-58
B-13	Mean Carbon Monoxide Concentrations in Effluent Gas From Nonadiabatic Test of Second Sample Set	A-59
B-14	Mean Carbon Dioxide Concentrations in Effluent Gas at Various Temperatures	A-60
B-15	Mean Carbon Dioxide Concentrations in Effluent Gas From Nonadiabatic Test of Second Sample Set	A-61

APPENDIX FIGURES

Number		Page
B-1	Thermogram of Lurgi retorted shale (-325 mesh), heated at 2° C/minute in dry air	A-12
B-2	Thermogram of TOSCO II retorted shale (-325 mesh), heated at 2° C/minute in dry air	A-13
B-3	Thermogram of Paraho retorted shale (-325 mesh), heated at 2° C/minut in dry air	A-14
B-4	Thermogram of Paraho retorted shale (-48 + 100 mesh), heated at 2° C/minute in dry air	A-15
B-5	Thermogram of C-a raw shale (-325 mesh), heated at 2° C/minute in dry air	A-16
B-6	Thermogram of Wyoming Smith/Roland sub-bituminous coal (-325 mesh), heated at 2° C/minute dry air	A-17
B-7	Thermogram of Western Kentucky No. 9 Bituminous coal (-325 mesh) heated at 2° C/minute in dry air	A-18
B-8	Thermogram of Lurgi retorted shale (-325 mesh), heated at 2° C/minute in humid air	A-19
B-9	Thermogram of TOSCO II retorted shale (-325 mesh), heated at 2° C/minute in humid air	A-20
B-10	Thermogram of Paraho retorted shale (-325 mesh), heated at 2° C/minute in humid air	A-21
B-11	Thermogram of Paraho retorted shale (-48 + 100 mesh), heated at 2° C/minute in humid air	A-22
B-12	Thermogram of C-a raw shale (-325 mesh), hetaed at 2° C/minute in humid air	A-23
B-13	Thermogram of Wyoming Smitn/roland sub bituminous coal	A-24
B-14	Thermogram of Western Kentucky No. 9 bituminous coal	A-25
B-15	Thermogram of Utah (66 GPT) raw shale (first test)	A-26

APPENDIX FIGURES (continued)

Number Page

B-16 Thermogram of Utah (66 GPT) raw shale (second test) A-27
B-17 Thermogram of Utah (66 GPT) raw shale (third test) A-28
B-18 Thermogram of Utah (28 GPT) raw shale (first test) A-29
B-19 Thermogram of Utah (28 GPT) raw shale (second test) A-30
B-20 Thermogram of Utah (28 GPT) raw shale (third test) A-31
B-21 Thermogram of Hytort retorted shale (first test) A-32
B-22 Thermogram of Hytort retorted shale (second test) A-33
B-23 Thermogram of Hytort retorted shale (third test) A-34
B-24 Thermogram of Union shale mixture (first test) A-35
B-25 Thermogram of Union shale mixture (second test) A-36
B-26 Thermogram of Union shale mixture (third test) A-37
B-27 Thermogram of Pocahontas #3 bituminous coal (first test) A-38
B-28 Thermogram of Pocahontas #3 bituminous coal (second test) A-39
B-29 Thermogram of Pocahontas #3 bituminous coal (third test) A-40
B-30 Thermogram of 95% Paraho retorted shale/5% Utah raw shale (28 GPT) mixture A-41
B-31 Thermogram of 90% Paraho retorted shale/10% Utah raw shale (28 GPT) mixture A-42
B-32 Thermogram of 80% Paraho retorted shale/20% Utah raw shale (28 GPT) mixture A-43
B-33 Thermogram of 79% Paraho retorted shale/20% Utah raw shale (28 GPT) mixture/1% sulfur mixture A-44
B-34 Thermogram of 78% Paraho retorted shale/20% Utah raw shale (28 GPT)/12% sulfur mixture A-45
B-35 Thermogram of 755 Paraho retorted shale/20% Utah raw shale (28 GPT)/15% sulfur mixture A-46

APPENDIX FIGURES (continued)

Number		Page
C-1	Thermogravimetric test data, TOSCO II retorted shale, (-325 mesh, 2° C/min heating ramp). Test 1	A-62
C-2	Thermogravimetric test data, TOSCO II retorted shale, (-325 mesh, 2° C/min heating ramp). Test 2	A-63
C-3	Thermogravimetric test data, TOSCO II retorted shale, (-325 mesh, 2° C/min heating ramp). Test 3	A-64
C-4	Thermogravimetric test data, Paraho retorted shale, (-325 mesh, 2° C/min heating ramp). Test 1	A-65
C-5	Thermogravimetric test data, Paraho retorted shale, (-325 mesh, 2° C/min heating ramp). Test 2	A-66
C-6	Thermogravimetric test data, Paraho retorted shale (-325 mesh, 2° C/min heating ramp). Test 3	A-67
C-7	Thermogravimetric test data, Paraho retorted shale (48 x 100 mesh, 2° C/min heating ramp). Test 1	A-68
C-8	Thermogravimetric test data, Paraho retorted shale (-48 + 100 mesh, 2° C/min heating ramp). Test 2	A-69
C-9	Thermogravimetric test data, Paraho retorted shale (-48 + 100 mesh, 2° C/min heating ramp). Test 3	A-70
C-10	Thermogravimetric test data, C-a raw shale (-325 mesh, 2° C/min heating ramp). Test 1	A-71
C-11	Thermogravimetric test data, C-a raw shale (-325 mesh, 2° C/min heating ramp). Test 2	A-72
C-12	Thermogravimetric test data, C-a raw shale (-325 mesh, 2° C/min heating ramp). Test 3	A-73
C-13	Thermogravimetric test data, Western Kentucky #9 bituminous coal (-325 mesh 2° C/min heating ramp). Test 1	A-74
C-14	Thermogravimetric test data, Western Kentucky #9 bituminous coal (-325 mesh 2° C/min heating ramp). Test 2	A-67
C-15	Thermogravimetric test data, Western Kentucky #9 bituminous coal (-325 mesh 2° C/min heating ramp) Test 3	A-76

APPENDIX FIGURES (continued)

Number		Page
C-16	Thermogravimetric test data, Lurgi retorted shale (-325 mesh 2° C/min heating ramp). Test 1	A-77
C-17	Thermogravimetric test data, Lurgi retorted shale (-325 mesh, 2° C/min heating ramp). Test 2	A-78
C-18	Thermogravimetric test data, Lurgi retorted shale (-325 mesh, 2° C/min heating ramp). Test 3	A-79
C-19	Thermogravimetric test data, Wyoming subbituminous coal (-325 mesh 2° C/min heating ramp). Test 1	A-80
C-20	Thermogravimetric test data, Wyoming subbituminous coal (-325 mesh 2° C/min heating ramp). Test 2	A-81
C-21	Thermogravimetric test data, Wyoming subbituminous coal (-325 mesh 2° C/min heating ramp). Test 3	A-82
C-22	Thermogravimetric test data, Pocahontas #3 bituminous coal (-325 mesh 2° C/min heating ramp). Test 1	A-83
C-23	Thermogravimetric test data, Pocahontas #3 bituminous coal (-325 mesh 2° C/min heating ramp). Test 2	A-84
C-24	Thermogravimetric test data, Pocahontas #3 bituminous coal (-325 mesh 2° C/min heating ramp). Test 3	A-85
C-25	Thermogravimetric test data, Hytort retorted shale (-325 mesh, 2° C/min heating ramp). Test 1	A-86
C-26	Thermogravimetric test data, Hytort retorted shale (-325 mesh, 2° C/min heating ramp). Test 2	A-87
C-27	Thermogravimetric test data, Hytort retorted shale (-325 mesh, 2° C/min heating ramp). Test 3	A-88
C-28	Thermogravimetric test data, Utah raw shale (28 GPT) (-325 mesh, 2° C/min heating ramp). Test 1	A-89
C-29	Thermogravimetric test data, Utah raw shale (28 GPT) (-325 mesh, 2° C/min heating ramp). Test 2	A-90
C-30	Thermogravimetric test data, Utah raw shale (28 GPT) (-325 mesh, 2° C/min heating ramp). Test 3	A-91
C-31	Thermogravimetric test data, Union shale mixture (-325 mesh, 2° C/min heating ramp). Test 1	A-92

APPENDIX FIGURES (continued)

Number		Page
C-32	Thermogravimetric test data, Union shale mixture (-325 mesh, 2° C/min heating ramp). Test 2	A-93
C-33	Thermogravimetric test data, Union shale mixture (-325 mesh, 2° C/min heating ramp). Test 3	A-94
C-34	Thermogravimetric test data, Utah raw shale (66 GPT) (-325 mesh, 2° C/min heating ramp). Test 1	A-95
C-35	Thermogravimetric test data, Utah raw shale (66 GPT) (-325 mesh, 2° C/min heating ramp). Test 2	A-96
C-36	Thermogravimetric test data, Utah raw shale (66 GPT) (-325 mesh, 2° C/min heating ramp). Test 3	A-97

SECTION 1

RELATING CHARACTERISTICS OF SOLIDS TO STORAGE PILE BEHAVIOR

1.0 Introduction

The main challenge in determining reactivity of solids is to measure, in the laboratory, properties of the solids which can be used to predict how full-scale storage piles will behave. Factors that influence the tendency of a storage pile to self-heat and eventually ignite can be grouped into two main categories. The first category includes those properties that are peculiar to the solid itself: reactivity toward oxygen, and heat release as a function of temperature. The second group of factors are those relating to the pile and its construction: overall dimensions, particle size, degree of compaction, homogeneity, ambient temperature, temperature of placed material, precipitation, wind speed, etc. It is quickly seen that pile characteristics are going to be more difficult to measure and most likely subject to more variation than the properties of the solid itself.

Unfortunately, few workers have attempted to relate laboratory determinations of reactivity of solids to storage pile behavior. The problem of heat generation and transfer in a large storage pile is very complex and requires several simplifying assumptions to obtain a solvable problem. Perhaps the best attempts to compromise between simplicity and reality have been made by the U.S. Bureau of Mines[1 2] and in a paper by van Doornum.[3]

1.1 Empirical Ranking

In 1945, Elder et al.[1] presented a comparison of the relative tendency of 46 different coals to spontaneously heat. They used a calorimeter with a capacity of 110 lb to measure the temperature vs. time of coals exposed to oxygen under adiabatic conditions. To eliminate temperature gradients within the large solid sample, electrical heaters outside the container wall added heat as necessary to maintain the outer wall temperature equal to that in the center of the sample. They used coal samples predred nitrogen and maintained an upflow of pure oxygen great enough so that the exit gas never dropped below 85 percent oxygen.

The calorimeter was preheated to a starting temperature in nitrogen and allowed to equilibrate. Then oxygen was admitted and the temperature was followed versus time. Figure 1 shows the nature of the curves obtained. Test time varied from three hours to several days. By plot-

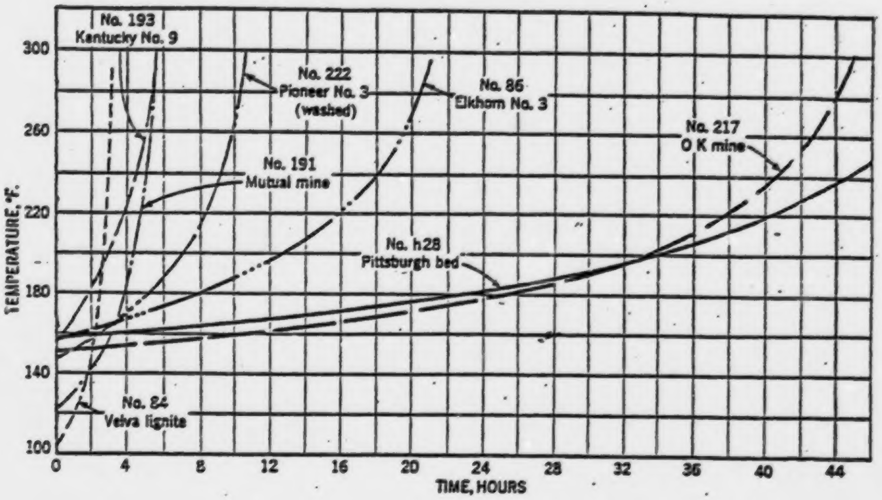

FIGURE 1. Spontaneous heating of dry, stage-crushed, 0 to 1/4 inch coal in an adiabatic calorimeter (Source: Reference 1).

ting the logarithm of the heating rate (°F/hr) versus the reciprocal temperature (°R^{-1}), Arrheius relations were obtained for each coal's reactivity. Each coal's reactivity at 212° F was then expressed relative to a Pittsburgh seam bituminous coal which showed very low reactivity.

The results of Elder et al.[1], cannot be directly related to pile behavior, but are quite useful in that they provide an empirical ranking of a coal's reactivity. The relative ranking of the 46 coals tested are shown in Table 1.

Working with coal dust, Hertzberg et al.[4] found that samples introduced into an oven preheated to 150° C gradually increased in temperature above that of the surroundings. The temperature continued to rise to an "ignition temperature" characterized by an inflection point in the temperature-time curve and then rose rapidly to a maximum. For Pittsburgh (bituminous) coal the ignition temperature varied between 169° C for 2-7 micron particles and 344° C for 147-200 micron particles.

Merrill[5] using differential thermal analysis found that when coal was diluted with inert firebrick material, both the preignition "deflection temperature" (resulting from adsorption of oxygen on the coal surface) and the ignition temperature increased. For a high volatile bituminous coal, "deflection temperatures" increased from 207° to 277° C as coal concentration decreased from 100% to 8.1%. Ignition temperature increased from 346° to 452° C as coal concentration decreased from 51% to 8.1%.

Chamberlain et al.[6] devised an apparatus in which coal was contacted with heated humidified air while being heated at a constant rate. The oxygen consumption and carbon dioxide production in this apparatus were measured at three different temperatures by Schmeling et al.[7] and used to calculate a spontaneous heating liability.

1.2 Analytical Model

Van Doornum[3] devised a calorimeter particularly suitable for self-heating studies. Usually both the rate of heat generation and thermal conductivity of a solid are small. If a large sample is used in a calorimeter, the heat produced may be easily determined, but a significant temperature gradient will occur within the solid sample which is unacceptable because it complicates the interpretation of experimental results. If, on the other hand, a small sample is tested the temperature gradient becomes negligible, but only very little heat is generated and accurate measurements become difficult. Van Doornum overcame these difficulties by using an aluminum block into which 19 holes of 1-inch diameter were drilled. A subdivision of the sample into slender cylinders separated by a material with a high thermal conductivity allowed large samples to be used while maintaining essentially constant temperature throughout the solid. Oxygen was admitted to the calorimeter through a constant flow device, and the resulting he[illegible]nerated versus

TABLE 1. THE RELATIVE TENDENCY OF COALS TO HEAT SPONTANEOUSLY IN STORAGE
(Source: Reference 1)

LOW-VOLATILE BITUMINOUS RANK

Coal No.	Bed or mine	Relative characteristic oxidation rate when X = 1[2]		Adiabatic calorimeter, ratio of self-heating rates at—	
		Basis of dry mineral-matter-free coal	Basis of dry coal	158° F.	212° F.
1	2	3	4	5	6
56	Pocahontas No. 3	0.84	0.82		
73	Pocahontas No. 3	.89	.88		0.52
57	Pocahontas No. 4	1.31	1.27		
Average		1.01	0.99		

MEDIUM-VOLATILE BITUMINOUS RANK

Coal No.	Bed or mine	3	4	5	6
60	Lower Freeport	1.20	1.16		
55	Sewell	1.25	1.26		
58	Lower Banner	1.30	1.24		
64	Bakerstown	1.43	1.43		
80	Stigler	1.92	1.90		
79	Hartshorne	2.52	2.45		
Average		1.61	1.57		

HIGH-VOLATILE A BITUMINOUS RANK

Coal No.	Bed or mine	3	4	5	6
82	Eagle	0.91	0.87		0.61
h28	Pittsburgh, Warden	1.00	1.00	1.00	1.00
67	Taggart	1.26	1.24		
53	Pond Creek	1.41	1.39		
50	Upper Freeport	1.44	1.36		
217	O. K.	1.44	1.39	1.34	1.32
81	Powellton	1.48	1.39		1.91
157	Raton, Van Houten	1.61	1.47		1.30
155	Raton, Koehler	1.64	1.47		1.61
72	Thick Freeport	1.74	1.60		
156	Raton, Brilliant	1.74	1.53		2.02
52	Pittsburgh, Bruceton	1.77	1.68		
102	Raton, Brilliant No. 2	1.80	1.64	1.13	1.21
86	Elkhorn No. 3	2.05	2.07	2.44	2.10
76	Hazard No. 4	2.71	2.71		3.72
71	Bevier	2.77	2.65		
84	High Splint	2.87	2.87		
78	McAlester, Bernardi	3.05	3.01		
73	McAlester, Dow No. 10	3.93	3.91		
b19	Lower Sunnyside	4.66	4.60		
Average		2.07	2.00		

HIGH-VOLATILE B BITUMINOUS RANK

Coal No.	Bed or mine	3	4	5	6
194	Kentucky No. 6	5.59	5.43	9.31	5.57
65	Henryetta	5.66	5.54		
222	Pioneer No. 3 (washed)	5.83	5.33	6.00	5.19
103	Kentucky No. 9	7.02	7.01	13.40	7.65
Average		6.23	5.83		

---

[1] The self-heating tendencies are all expressed as a ratio to Pittsburgh-bed Warden mine (coal h28); e.g. (h28 = 1). The absolute values for h28 are: column 3, 0.133 percent oxygen per day by weight of the dry, mineral-matter-free coal after the dry, mineral-matter-free coal has consumed 1 percent oxygen; column 4, 0.127 percent oxygen per day by weight of dry coal after the dry, mineral-matter-free coal has consumed 1 percent oxygen; column 5, 0.753° F. per hour at 158° F.; and column 6, 1.29° F. per hour at 212° F.

[2] Ratio of the characteristic oxidation rates of 0- to ¼-inch coal at 212° F. in air after the dry, mineral-matter-free coal has consumed 1 percent oxygen.

Reproduced from best available copy.

time was measured. Test time varied from two to eight days, and runs at different temperatures were made by varying the jacket temperature surrounding the calorimeter.

Three coals of widely varying reactivities were measured; Van Doornum found, as would be expected, that:

1. At a constant temperature and rate of oxygen supply, the rate of heat generation decreases in a manner suggesting exponential decay.

2. When oxygen is in excess, the reaction obeys Arrhenius' equation for temperature dependence, $q = A \exp(-E/RT)$ where A and E/R are constants and T is the absolute temperature. (Because the Arrhenius equation is difficult to work with mathematically, van Doornum simplified it over the temperature range of interest by replacing it with a more convenient equation: $q = A \text{ xp } (\alpha T^*)$ where A and α are constants and T^* is the temperature rise of the coal relative to some arbitrary reference temperature.)

3. When oxygen is not present in excess, the sample evolved heat at a slower rate but the period of heat evolution lasted longer. In other words, the oxygen concentration may limit the rate of heat evolution, but the same total amount of heat will eventually be released from the sample.

By using the measured reactivity properties of the solid, van Doornum predicted the behavior of storage piles under several limiting conditions. The case of most practical interest is that which considers both the increased heat generation caused by rising temperatures and the decreasing rate of heat generation caused by the decay in coal reactivity with time. By assuming (1) that oxygen is present in excess throughout the pile, (2) that the entire pile (or subarea within the pile area) is at the same temperature, and (3) that the pile is of uniform construction, van Doornum could solve the resulting equations in terms of two parameters. The first parameter, M, is the ratio of the increase in heat generation due to temperature rise compared to the decrease in heat generation resulting from reactivity decay. For values of M greater than 1, the predicted temperature rises exponentially to infinity. When M = 1, the predicted temperature will rise linearly with time. Finally, for values of M much less than 1, the maximum temperature remains finite.

A second parameter, N, accounts for the loss of heat from a storage pile. The second parameter represents the relative magnitudes of the decrease in heat generation from reactivity decay compared to the decrease in heat generation caused by losses from the exterior of the piles. As N approaches infinity, pile conditions approach adiabatic. For a given value of pile heat loss, there is a maximum reactivity value for material can safely stored in this pile. For values of M higher than this critical value the pile temperature approaches infinity rapidly and spontaneous combustion occurs. As the other parameter, N, becomes lower (that is, as more heat losses occur from the pile) coals of higher reactivity can be safely stored. Figure 2 presents predicted regions of safe storage based on the combination of parameters M and N.

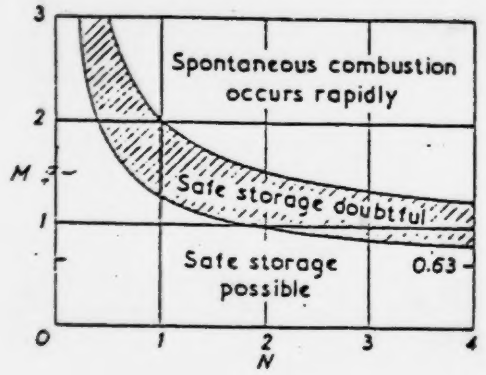

FIGURE 2. Acceptable and unsatisfactory combinations of M and N by van Doornum's model (Source: Reference 3, by permission.

Van Doornum compared results from the theoretical model to large-scale tests on coal bunkers. Qualitatively the model results agreed with observed facts. For instance, some coals under apparently identical conditions may spontaneously combust in one instance while showing no spontaneous combustion in another instance. This can be explained by the model for coals which have large values of M. If M = 5, an increase in N from 0.123 to 0.125 spells the difference between spontaneous combustion and safe storage. Such small variations could easily be accounted for by changes in wind velocity, proportion of coal fines, or a segregation of particle sizes in the pile. Along the same lines, if M is less than 0.63, the coal can be safely stored for any value of N. That means no difficulties would be experienced with coals for which M is less than 0.63 regardless of pile configuration.

A stronger verification was obtained by comparing van Doornum's results with those obtained in large-scale experiments conducted on coal bunkers by the Fuel Research Institute of South Africa. Bunkers 8 ft in diameter and 8 ft high containing approximately 10 tons of coal were insulated and then ventilated with air in the upward direction. The central temperatures of these bunkers could be closely correlated by the model parameters chosen by van Doornum. Bunker tests on coals which had large values of M resulted in spontaneous combustion while those with values of below 0.6 showed a maximum temperature rise of 15° to 20° C.

In summary, van Doornum's approach has the advantages of mathematical simplicity and requires only two experimental parameters. However, it does not account for temperature variations within the storage pile, but treats the entire pile as if it were of one temperature. Nor does it account for the fact that oxygen may be depleted further into the storage pile. This approach does not account for pile compaction which reduces air influx and which has been shown to be the most effective means of controlling spontaneous heating in the storage of reactive lignite coals.[8] [9]

1.3 Computer Simulation

To more fully account for the many factors at play in a storage pile, Sondreal and Ellman[2] carried out detailed computer simulations of storage piles with various dimensions. They also conducted experimental studies to determine values of the factors at work in spontaneous heating. Their work dealt exclusively with North Dakota lignite coals, but is useful as a guide for other carbonaceous materials. A summary of their results follows.

Reaction rates were determined by measuring the decrease in concentrations of oxygen in the void space of a tar filled with lignite. The void space contained a relatively small quantity of oxygen in relation to the weight of lignite. Consequently, the oxygen was nearly depleted in periods lagging from a few minutes to a few hours depending on the temperature level and the lignite reactivity. (In a separate set of experiments the heat of reaction generated by the consumption of oxygen was measured in a calorimeter similar to that used by van Doornum.)

Sample moisture content, particle size, or storage temperature showed no consistent effect on the heat of oxidation. Heat of oxidation varied from approximately 75,000 calories per gram mole adsorbed oxygen at 20° C to almost 90,000 at 90° C. This heat liberation in low temperature oxidation of lignite agrees generally with known values for similar reactions. An upper limit of approximately 90,000 calories per gram mole of adsorbed oxygen was used in all simulations to convert oxygen consumption measured by the closed jar technique into a heat generation rate. It should be noted that reaction rate measurements based on oxygen consumption and the assumption of a constant heat of reaction may not be valid for substances other than the lignite studied.

The influence of sulfur (particularly pyrite) on the oxidation of 56 lignite samples was investigated. After statistical analysis of the resulting data, Sondreal and Ellman[2] found, as did Bacharach et al.[10] that for rate prediction, correlation with sulfur content is of no value.

Sondreal and Ellman[2] used the above and several other experimentally determined values in a computer program to predict temperature distribution in lignite piles. They assumed that heat is transferred within the pile by conduction only and that the boundary temperature of the pile is known. For most of their simulations they assumed that the oxygen concentration was constant throughout the pile although in a special case they considered the effect of oxygen infiltration caused by wind pressure. They found that replenishment of oxygen in the pile is the controlling factor in determining the temperature rise, since at all but the lowest oxygen concentrations, the heat generated cannot be dissipated to the surroundings without an unacceptably large temperature rise. The oxygen concentration or penetration becomes less critical as the reactivity of the lignite decreases with time. They suggested using this phenomenon of decaying reactivity to help in the storage of lignite. Constructing the pile in thin layers, with each layer being allowed to oxidize 1-2 weeks, will reduce the reactivity of the solid. Subsequent compaction of the partially reacted solid is recommended to reduce the air flow into the pile.

In summary, the computer simulations of Sondreal and Ellman were useful to demonstrate general trends and to show that oxygen infiltration may be the controlling factor in the pile heatup. Also, their experimental data on the properties of North Dakota lignites are most helpful in modeling behavior of these coals. However, for a general technique their method is unsuitable because (1) the model is mathematically too complex and contains too many experimental parameters to be readily transferred from one application to another, and (2) the mechanism by which oxygen enters the pile only by wind pressure seems oversimplified and may not account for this most critical of factors.

1.4 Application of Solid-Gas Reaction Models

The reaction of solids and gases has been widely studied in the field of chemical engineering. Many of these results obtained for such reactions may be easily extrapolated to storage pile behavior. Usually the solid under consideration is somewhat porous and the gas combines with the solid not only at the external surface of the particle but also inside the pores which permeate the particle. One method of modeling the behavior of a porous solid is the "grain model" which assumes that each porous particle consists of a large number of equal-sized grains.[11] Both the grains and the particle may assume several shapes--plate-like, needle-like, or spherical. The reaction rate of the solid anywhere inside the particle can then readily be calculated as a function of gas concentration, particle and grain dimensions, temperature, etc.

The above grain model represents the construction of a storage pile if we substitute (a) the overall pile dimensions for the particle size, and (b) the average coal particle diameter for the grain size. Results for temperature and concentration profiles inside a porous pellet may be readily applied to storage pile behavior. This approach has the advantages of (1) separating chemical and diffusional effects; (2) allowing prediction of changing variables, such as particle diameter and pile diffusivity to oxygen; and (3) expressing the relevant variables in only two or three groupings similar to the approach of van Doornum's M and N values. Most importantly, it permits the effect of oxygen infiltration into the pile to be realistically studied.

When oxygen can permeate a pile much more rapidly than it is consumed, its concentration becomes uniform throughout the pile. Each particle then reacts and generates heat at the same rate regardless of its position in the pile. This limiting case is called chemical reaction controlled. If, on the other hand, the infiltrating oxygen reacts as quickly as it can reach unconsumed coal, the reaction will be confined to a narrow zone which will proceed inward as more and more of the pile reacts. This situation is termed diffusion controlled. Figure 3 presents the two limiting cases schematically.

For a pile with constant temperature, the intermediate case that is illustrated in Figure 4 can easily be treated[12] by introducing a single parameter, σ, representing the relative rates of chemical reaction and gas diffusion into the pile. In chemical reaction studies, this parameter is called the Thiele modulus and represents what may be the best means of quantifying air infiltration into compacted storage piles.

Further work is needed to consider models for porous solids that include nonisothermal effects[13-16] and to experimentally determine the effective rate of oxygen diffusion in large piles of varying compaction. Such work is outside the scope of this study which has the more limited goal of comparing the reactivities of various carbonaceous solids, not detailed modeling of pile behavior. It does appear, however, that once solid reactivities (at ambient oxygen levels and known solid surface areas) have been determined, models exist which can be adapted with little effort to predict the effect of storage pile construction.

1.5 Effects of Pore Size and Particle Size Upon Adsorption

In research with coal of various ranks, the size and volume of pores has been found to affect the mechanisms of oxidation. In experiments conducted at 200°-250° C, Avison et al.[17] found two distinct types of oxidation behavior depending on the pore distribution of the coals. Large-pore coals (0.040-0.062 $\mathrm{cm}^2/\mathrm{g} > 300$ Å) showed a long period during which oxidation was limited by oxygen availability. When most of the available oxidation sites were used up diffusional resistance became important and rates fell. In contrast, small-pore coals (0.009-0.022 $\mathrm{cm}^3/\mathrm{g} > 300$ Å) showed oxidation rates which declined monotonically from the very beginning of the test. Kam et al.[18], suggested that low temperature oxidation of bituminous coal takes place solely on external surfaces and macropores. Citing extremely slow oxygen permeation into the micropores, they neglect diffusion into and out of the interior of the coal particle as insignificant.

Several researchers have confirmed the importance of external surface adsorption through studies of the effect of particle size. Working with highly volatile bituminous coal at 135° C, Mahajan et al.[19] found that 40 x 70 mesh particles took 15 times as long as 200 x 250 mesh particles to absorb the same amount of oxygen. For small-pore, low and medium volatility bituminous coal, Avison et al.[17] found oxidation

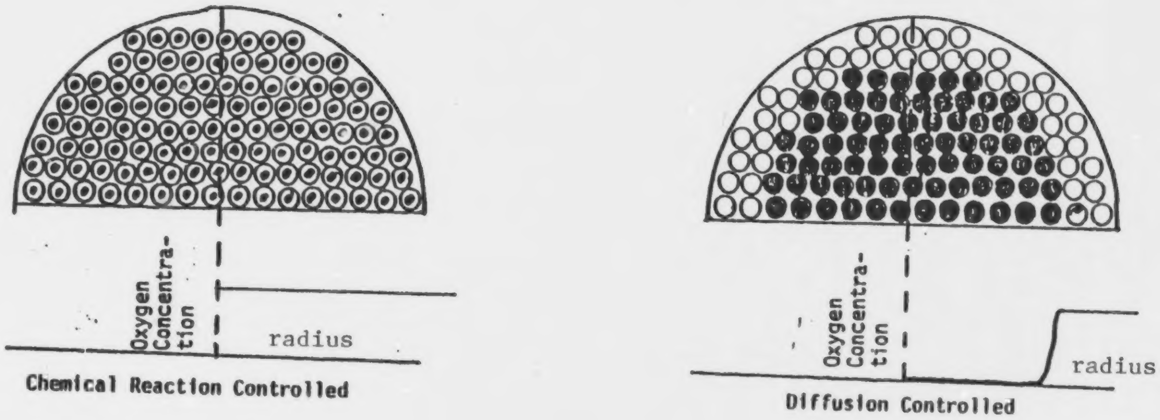

Chemical Reaction Controlled

Diffusion Controlled

FIGURE 3. Limiting cases of the grain model for solid-gas reactions. (Source: Research Triangle Institute)

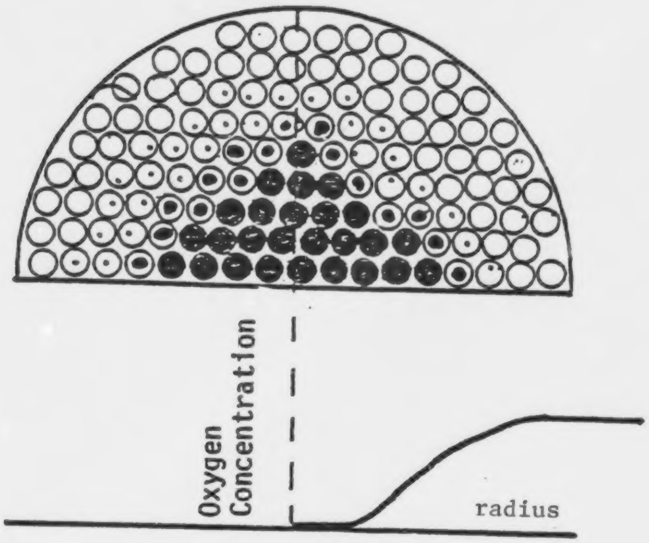

FIGURE 4. Representation of general case of a grain model for a storage pile where both reaction and diffusion control the rate. (Source: Research Triangle Institute)

rates for 18 x 50 mesh coal to be approximately 2½ times higher than those for 6 x 16 mesh coal at 225° C. Bouwman and Freriks[20], in studies of large storage piles (500 metric tons), found that a pile with a maximum particle size of 31.6 mm reached a lower maximum temperature (62° C) than a similar pile with 6.3 mm maximum size (80° C). In addition, the large particle pile which contained a lower proportion of fines, reached its maximum temperature after 62 days while the temperature of the small particle pile continued to increase for approximately 180 days. The authors suggest that removing fines from coal prior to storage may greatly reduce spontaneous heating.

1.6 Chemistry of Low Temperature Oxidation

The physical and chemical reaction of oxygen with coal and char at low temperatures has been the subject of many studies. Uncertainty with respect to the actual chemical reactions involved makes it difficult to generalize the results of auto-oxidation research to other materials such as raw and retorted oil shales. Swann and Evans[21] found that the oxidation of Australian brown coal at low temperatures mainly took place on the aliphatic groups. At 35° C phenolic groups were formed which later broke down to water (most of which remained absorbed on the coal). At 70° C, carboxyl groups were formed which later broke down to carbon dioxide. Aromatic structures were not appreciably oxidized at either temperature. Bouwman and Freriks[20] studied bituminous coal oxidized in a storage pile and found evidence that oxidation at temperatures of approximately 80° C produced arylcarboxylic acids which probably decompose to CO and CO_2.

Painter et al.[22] suggested that oxidation of exposed high volatile bituminous coal in mines resulted in the formation of ester crosslinks, perhaps due to condensation reactions of carboxyl groups which may have been produced initially.

SECTION 2

DESCRIPTION OF SAMPLES

Samples of raw shale, retorted shale and coal were tested in this study. Testing was conducted in two phases; sample handling procedures for the samples obtained in the first and second phase differed slightly.

In the first phase of the study, retorted shale samples from the Lurgi, TOSCO II, and Paraho direct-mode processes were tested in addition to a raw shale sample from Federal lease tract C-a in Colorado, a Wyoming Smith-Roland subbituminous coal, and a Western Kentucky #9 bituminous coal. Samples of raw shale and retorted shale were obtained from Rio Blanco Oil Shale Company (raw C-a shale from R-5 zone, elevation 6141 ft mucked from blast #3 on May 30, 1980), TOSCO, Incorporated (TOSCO II retorted shale, Colony Mine), Development Engineering (Paraho retorted shale, Anvil Points Mine), and Cathedral Bluffs Oil Shale Company (Lurgi retorted shale, C-b tract shale). Coal samples were obtained from the AMAX Coal Company and the Kentucky Center for Energy Research Laboratory. All samples were reduced in size, riffled, ground to final size, and riffled again to select a small subsample for testing. The coal samples were ground and sized under nitrogen.

In the second phase of the study, a mixture of retorted shale, raw shale, and byproduct sulfur from the Union B process was tested in addition to Hytort retorted shale, (Kentucky origin) two raw shale samples of different grades from Federal lease tract Ua/Ub in Utah and Pocahontas #3 bituminous coal. The Union sample was prepared at RTI from separate samples of retorted shale, raw shale fines and byproduct sulfur provided by Union Oil Science and Technology Division. These materials were ground and sized separately and then mixed in the proportion of 5.47 weight-percent raw shale fines to 0.14 weight percent sulfur, with the balance retorted shale. All of these materials had negligible moisture after grinding. The resulting mixture was homogenized and brought to 17 weight percent moisture with distilled, deionized water. The Union oil shale mixture was prepared in this manner per instructions from Union Oil, in order to simulate Union's plans for disposal at their Long Ridge Plant in Colorado.

The Hytort shale was obtained from Phillips Petroleum. The Utah shale was obtained from the U.S. Department of Interior, Bureau of Land Management. Four sections of core were sent from core hole X-13; individual assays were provided for each section. The two leaner samples were composited to make a 28 gallon per ton sample. The two richer samples were composited to make a 66 gallon per ton sample. The Pocahontas #3 coal was obtained from Itmann Coal Company. The samples were handled as above except that the coal sample was not ground and sized under nitrogen. Analyses of these samples for sulfur, higher heating value, and organic carbon are given in Tables 2, 3, and 4.

Heat capacities of materials tested in this study were determined using differential scanning calorimetry. The instrument that was used is described in Section 3. For these determinations, samples were heated at 10° C/minute in dry nitrogen flowing at 50 scc/minute. Aluminum sample pans were used, with empty pans of similar mass and heat capacity used as references. A sapphire disk was tested under identical conditions for use as a heat capacity standard. Calculations were made at 20° C intervals using the formula:

$$C_{sample} = \frac{Q_{sample} \cdot M_{sapphire}}{M_{sample} \cdot Q_{sapphire}} \cdot C_{sapphire}$$

where C_{sample} and $C_{sapphire}$ are heat capacities, J/G

Q_{sample} and $Q_{sapphire}$ are measured heat flows, mW

$M_{sapphire}$ is the mass of the standard sapphire disk,

and M_{sample} is the initial sample mass.

The irregular nature of heat capacity as a function of temperature is due to the endotherms that occur over discrete temperature intervals associated with pyrolysis reactions. In addition, as pyrolysis reactions take place, the actual sample mass being heated decreases.

The heat capacity data have been integrated and tables of the heat required to elevate samples from 25° C to specific temperatures are presented along with the heat capacity data in the appendix. Mean heat capacities based on initial sample weight are given in Table 5. In all cases, except for the Lurgi retorted shale and Union Shale mixture, higher heating values, (given in Appendix A) exceed heat requirements to raise the materials to temperature above 600° C. This comparison does not take into account the severe nature of the reaction in the higher heating value determinations or the energy required to heat the gases produced in combustion.

The generally lower exotherms observed during the differential scanning calorimetry testing described in section three also exceed the energy requirements to raise the materials to 600° C with the exception of the Lurgi retorted shale and Union shale mixture. (The Union shale mixture has a high apparent heat capacity due to the energy required to evaporate the 17% moisture content as tested. This material dries rapidly at ambient temperatures). As a result, even the retorted oil shale could burn if ignited; this is an unlikely source to bring these retorted shale materials to the point where they would produce a net energy release.

TABLE 2. TOTAL SULFUR CONTENT OF SAMPLES (WEIGHT %)

	As received	Dry
Western Kentucky #9 Bituminous Coal (-325 mesh)	3.65	3.73
Hytort Retorted Shale (-325 mesh)	2.39	2.40
Utah Raw Shale (66 GPT) (-325 mesh)	1.84	1.85
C-a Raw Shale (-325 mesh)	0.97	0.98
Lurgi Retorted Shale (-325 mesh)	0.86	0.86
Utah Raw Shale (28 GPT) (-325 mesh)	0.75	0.75
Union Shale Mixture* (-325 mesh)	0.68	0.68
Pocahontas #3 Bituminous Coal (-325 mesh)	0.64	0.65
Wyoming Sub-Bituminous Coal (-325 mesh)	0.60	0.63
TOSCO II Retorted Shale (-325 mesh)	0.58	0.58
Paraho Retorted Shale (-325 mesh)	0.57	0.57
Paraho Retorted Shale (-48 + 100 mesh)	0.57	0.57

*If brought to 17% moisture, sulfur content would be 0.56%.

TABLE 3. HIGHER HEATING VALUES OF SAMPLES (-325 mesh)

	J/g	(BTU/LB)	J/g	(BTU/LB)
W. Kentucky #9 Bituminous Coal	28210	(12130)	30350	(13050)
Pocahontas #3 Bituminous Coal	27870	(11980)	28190	(12120)
Wyoming Sub-Bituminous Coal	20600	(8860)	26890	(11560)
Utah Raw Shale (66 GPT)	14400	(6200)	14500	(6240)
Utah Raw Shale (28 GPT)	4840	(2080)	4860	(2090)
C-a Raw Shale	2030	(871)	2040	(878)
TOSCO II Retorted Shale	1000	(430)	1010	(433)
Hytort Retorted Shale	972	(418)	977	(420)
Paraho Retorted Shale (-48 + 100 mesh)	686	(295)	688	(296)
Union Shale Mixture*	483	(208)	486	(209)
Paraho Retorted Shale	434	(187)	437	(188)
Lurgi Retorted Shale	100	(44)	100	(44)

*If brought to 17% moisture, the heating value would be 173 Btu/lb.

TABLE 4. ORGANIC CARBON CONTENT OF MATERIALS TESTED
(WEIGHT-PERCENT ON DRY BASIS, -325 mesh)

Pocahontas #3 Bituminous Coal	69
Wyoming Subbituminous Coal	64
Western Kentucky #9 Bituminous Coal	61
Raw Utah Shale (66 GPT)	28
Raw Utah Shale (28 GPT)	11
C-a Raw Shale	5.2
Union Shale Mixture	4.1
Hytort Retorted Shale	3.8
TOSCO II Retorted Shale	3.5
Paraho Retorted Shale	3.1
Paraho Retorted Shale (-48 + 100 mesh)	1.3
Lurgi Retorted Shale	0.13

*Reflects the organic carbon content of the bulk sample. The lower organic carbon content for the -48 + 100 fraction may be due to composition differences among the different particle sizes produced in the grinding process.

TABLE 5. MEAN HEAT CAPACITY OF COAL AND SHALE MATERIALS
BASED ON INITIAL SAMPLE WEIGHT (J/g, -325 mesh)

	TEMPERATURE RANGE (°C)		
MATERIAL	25-200	25-400	25-600
C-a Raw Shale	0.76	0.72	0.73
Utah Raw Shale (66 GPT)	2.18	2.13	2.56
Utah Raw Shale (28 GPT)	1.17	1.15	1.23
Hytort Retorted Shale	1.08	1.03	1.17
Pocahontas #3 Bituminous Coal	1.19	1.28	1.40
Western Kentucky #9 Bituminous Coal	0.69	0.47	0.44
Wyoming Subbituminous Coal	1.28	0.67	0.63
Lurgi Retorted Shale	0.82	0.87	0.92
TOSCO II Retorted Shale	0.39	0.89	0.86
Paraho Retorted Shale	0.73	0.71	0.66
Union Shale Mixture	2.57	1.75	1.60

SECTION 3

DIFFERENTIAL SCANNING CALORIMETRY TESTING AND NONADIABATIC OXYGEN ABSORPTION TESTING

3.1 Differential Scanning Calorimetry

Differential scanning calorimetry (DSC) involves the measurement of heat evolved or absorbed by a sample at a given temperature relative to a known reference material at the same temperature. When the temperature is increased or decreased, heat effects arise from differences in specific heats, phase changes and chemical reactions. Low temperature oxidation is an exothermic reaction. When spontaneous heating occurs, the heat produced by this reaction (and other exothermic reactions including the heat of wetting) is greater than the heat that is rejected to the surroundings, and the temperature of the material which is oxidizing increases. As the temperature of the material increases, the rate of oxidation increases and, in some cases, an even more rapid temperature increase then occurs.

DSC data, obtained while the temperature of the sample and reference are increased at a slow constant rate, indicate the difference in heat flow between sample and reference as a function of temperature. When the reference is an empty sample pan of equal mass and specific heat to the pan in which the sample is held, the net heat effect is that produced by the sample. When the temperature of the apparatus is controlled to eliminate the possibility of phase changes in the sample, endothermic effects are associated with the heat capacity of the sample, and with some materials, such effects as drying, desorption of gases, and volatilization. Exothermic effects in excess of the sample heat capacity are associated with exothermic chemical reactions.

Several previously described approaches[4,5] characterized the self-heating tendency of materials by promoting low temperature oxidation by heating samples in the presence of air or oxygen and noting the point at which the sample temperature began to rise above that of its surroundings. This approach has been followed in this study using DSC to detect the onset temperature of this exothermic reaction and the extent of heat released when samples were slowly heated in the presence of air.

All samples were tested at a particle size of -325 U.S. mesh. The Paraho retorted shale sample was also tested at -48 + 100 U.S. mesh. The set of samples obtained in the first phase was tested in both dry and humid air (0.016 g H_2O per liter dry air). As only minor differences in response were observed due to humidity, the samples obtained in the second phase were tested in dry air only. Samples were tested in a duPont Instruments Model 951 differential scanning calorimeter equipped with a standard low pressure cell. The calorimeter was connected to a duPont Instruments Model 1090/1092 thermal analyzer which permitted temperature programming and data acquisition/playback using magnetic disk storage. Samples of between 17 and 54 mg were used. Variations in sample mass for the different materials tested were primarily due to differences in bulk density. Samples were loaded into open aluminum pans; the pans were completely filled to the top edge and excess material was removed so that the sample surface was level. An empty pan of comparable mass (and heat capacity) was used as a reference in all tests.

An air flow rate of 50 cc/min was maintained during all tests. Air was supplied from compressed gas cylinders (breathing grade, U.S.P) and flow rates were determined with a rotameter. The dryness of the air was insured by passing the air through a desiccant trap. For tests in which humid air was used, metered air was passed through a bubbler system filled with deionized water. The inlet line was constructed of a 1/8-inch O.D. stainless steel tubing (0.028-inch wall) which was crimped at the bottom. Two 1/64-inch holes were bored through the wall of the tube near the bottom. The tube was inserted into a stainless steel reservoir using a bored-through compression fitting. The air was humidified as it bubbled to the top of the reservoir where it exited to the DSC. The reservoir was maintained at 20°-25° C. A check of the humidity of the air that was produced by this system was conducted gravimetrically using predried silica gel and found to be 0.016 g/L dry air.

With air flowing through the cell, a preweighed sample in a tared aluminum pan was placed on the sample thermocouple disk, and an empty sample pan was placed on the reference thermocouple disk. The lid, cover, and bell jar were then replaced. A diagram of the cell is shown in Figure 5.

The test was conducted by programming the heater to increase the temperature of the thermoelectric disk to which sample and reference thermocouples are attached. A precisely controlled heating ramp of 2° C per minute was followed from slightly above ambient temperatures (25°-30° C). Different samples were heated to different final temperatures (380°-550° C) but in all cases the test was continued to the end of the exotherm.

Exothermic reactions were sensed by a slight lead in temperature of the sample thermocouple over the reference thermocouple. The instrument was calibrated to convert this lead into an actual heat effect. Indium metal and its melting point was used as a standard for both sample temperature (mp = 157° C) and heat effect (heat of fusion = 28.4 J/g).

As the tests proceeded, sample temperature, differential heat flow and time were recorded at 1 second intervals on a magnetic disk. Following the test, heat flow data could be plotted against either time or temperature. As a constant rate temperature ramp was used, these curves have the same shape. Heat flow versus temperature curves are included in Appendix B. Actual heat data reported on these curves were obtained from integration of the corresponding heat flow versus time data.

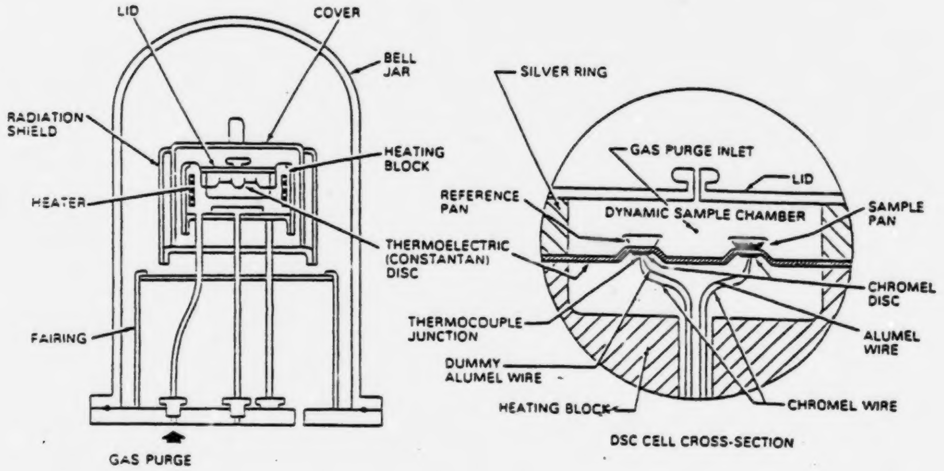

FIGURE 5. DSC cell cross section.
(Source: duPont Instruments)
by permission

The most important measurement relating DSC data to spontaneous heating behavior is the onset temperature of the exothermic oxidation reaction. When an exotherm is observed while a sample is being heated, this temperature is characterized by extrapolating the slope of the leading edge of the exothermic peak to the baseline. It is assumed that the lower this temperature is, the greater is the tendency of the material to spontaneously heat. This provides a means for empirically ranking materials of unknown self-heating potential by comparison to materials of known heating potential. The plot of heat flow versus temperature characterizes the distribution of reactivites associated with oxidation of the complex chemical structure of fossil fuels. In some cases, the thermogram include more than one broad peak. This results from a reactivity distribution which includes some oxidation reactions of low activation energy and high activation energy with relatively few reactions of intermediate reactivity. Since the low temperature (i.e., low activation energy) reactions are most important from the standpoint of spontaneous heating, the lowest temperature peak has been used to determine the exothermic onset temperature where more than one peak was observed. A ranking of the materials by exothermic onset temperature is given in Table 6. The Wyoming subbituminous and Western Kentucky bituminous coals exhibited the earliest exothermic onset temperatures followed by the 66 gallon/ton raw Utah shale. The low volatility bituminous Pocahontas #3 coal was less reactive than any of the raw western shales that were tested. The carbonaceous retorted shale samples exhibited considerably higher exothermic onset temperatures than the raw shale indicating that they present less of a spontaneous heating hazard than the raw shale and much less than the coal. Decarbonized shale from the Lurgi process was also tested but absolutely no exothermic reaction was observed at temperatures up to 550° C. This response by Lurgi shale was expected since the carbon is oxidized (burned off) during the retorting process. The Hytort retorted shale was extremely unreactive, exhibiting an exothermic onset temperature higher than that of any of the retorted shale samples except for the Lurgi retorted shale.

The magnitude of the exothermic reaction was calculated for each test. These values are ranked in Table 7. No exothermic reaction was observed in the test of Lurgi decarbonized retorted shale. As would be expected, the coal produced the highest heat of reaction, followed by the raw shale and then the retorted shale. The data presented in this table do not represent heats of combustion or heating values as commonly measured using bomb calorimeters. Heating value determinations made in bomb calorimeters involve ignition of the sample under a high pressure of oxygen. Data obtained by a bomb calorimeter method are used to estimate the amount of energy available under relatively severe combustion conditions.

Heats reported in Table 7 have been obtained by integrating the heat flow versus time data which correspond to the heat flow vs. temperature data given in the Appendix. These data can be used to conservatively estimate the potential temperature elevation of a material undergoing spontaneous heating. The temperature ranges given in the table correspond to the limits over which the exotherm was integrated. Samples obtained in the first phase of testing were tested in both dry and humid air.

TABLE 6. EXOTHERMIC ONSET TEMPERATURE OBSERVED IN OXIDATION OF COAL, OIL SHALE, AND RETORTED OIL SHALE (2° C/MINUTE HEATING RAMP, -325 mesh, except where noted)

MATERIAL	ATMOSPHERE	TEMPERATURE
Wyoming Subbituminous Coal	Humid Air	190 ° C
Wyoming Subbituminous Coal	Dry air	190
Western Kentucky #9 Bituminous Coal	Humid air	190
Western Kentucky #9 Bituminous Coal	Dry air	193
Utah Raw Shale (66 GPT)	Dry air	211
C-a Raw Shale	Humid air	225
C-a Raw Shale	Dry air	226
Utah Raw Shale (28 GPT)	Dry air	227
Pocahontas #3 Bituminous Coal	Dry air	230
TOSCO II Retorted Shale	Humid air	296
Paraho Retorted Shale	Dry air	300
Paraho Retorted Shale	Humid air	300
Paraho Retorted Shale (-48 + 100)	Humid air	300
Paraho Retorted Shale (-48 + 100)	Dry air	302
TOSCO II Retorted Shale	Dry air	306
Union Shale Mixture	Dry air	331
Hytort Retorted Shale	Dry air	357
Lurgi Retorted Shale	Dry air	*
Lurgi Retorted Shale	Humid air	*

*No exotherm observed up to 550° C.

TABLE 7. MAGNITUDE OF EXOTHERMIC REACTION OF COAL, OIL SHALE, AND RETORTED OIL SHALE
(2° C/MINUTE HEATING RAMP, -325 mesh, except where noted)

MATERIAL	ATMOSPHERE	EXOTHERM	TEMPERATURE RANGE
Bituminous Coal (Pocahontas #3)	Dry air	15,700	150-575° C
Bituminous Coal (W. Kentucky #9)	Dry air	13,800	90-550
Bituminous Coal (W. Kentucky #9)	Humid air	13,800	120-550
Subbituminous Coal (Wyoming)	Humid air	11,200	50-440
Subbituminous Coal (Wyoming)	Dry air	10,900	50-550
Utah (66 GPT) Raw Shale	Dry air	8,320	125-420
Utah (28 GPT) Raw Shale	Dry air	2,990	125-420
Hytort Retorted Shale	Dry air	1,340	175-575
Raw Shale (C-a)	Humid air	1,050	125-550
Raw Shale (C-a)	Dry air	920	160-480
TOSCO II Retorted Shale	Humid air	880	125-550
Union Shale Mixture	Dry air	860	200-575
TOSCO II Retorted Shale	Dry air	560	160-410
Paraho Retorted Shale (-325)	Humid air	490	175-410
Paraho Retorted Shale (-325)	Dry air	480	150-550
Paraho Retorted Shale (-48 + 100 mesh)	Humid air	470	175-550
Paraho Retorted Shale (-48 + 100 mesh)	Dry air	430	175-550
Lurgi Retorted Shale	Dry air	0	30-550
Lurgi Retorted Shale	Humid air	0	30-550

The effect of humidity on exothermic onset temperature was most noticeable for the TOSCO II retorted shale in which a 10° C reduction was observed for the test conducted with humid air. A slight decrease in exothermic onset temperature was observed for the bituminous coal. Reports of adiabatic experiments by Guney[23] have demonstrated an extremely significant effect of humidity on low temperature (<100° C) spontaneous heating of coal. Much less dramatic effects were noted upon the measured exothermic onset temperature in this study because the parameter measured for ranking purposes was consistently above the normal boiling point of water. The reason why humidity did not produce a more significant effect in this study may lie in the rapid "forcing" of the reaction (2° C/min heating ramp) in the nonadiabatic DSC testing. Additionally, the equilibrium moisture content of the shale and shale refuse at the test conditions is unknown. The role of the heat of wetting of coal in raising its temperature is well known; at higher temperatures the rate of atmospheric oxidation is accelerated and temperature increases to the point of spontaneous ignition may result. In all cases except for the Western Kentucky bituminous coal, the tests conducted humidified air produced slightly greater exotherms. The ranking of the sample was however, unaffected by the difference in atmosphere.

Varying particle size had a negligible effect upon the exothermic onset temperature of Paraho retorted shale. It is uncertain whether this is because intraparticle diffusion effects are unimportant in the reaction or because the heating ramp obscures differences in heat release once the reaction has been initiated.

Based on exothermic onset temperatures, none of the raw shale samples are as susceptible to spontaneous combustion as the Wyoming subbituminous and Western Kentucky (high volatility) bituminous coals. The western shales are more susceptible to spontaneous combustion than the Pocahontas #3 low volatility bituminous coal which is considered to present a low hazard relative to most other coals. None of the retorted shale samples exhibited exothermic onset temperatures lower than the Pocahontas #3 coal, and these are therefore even less likely to spontaneously combust.

An additional series of tests was conducted to determine the effect of codisposal of raw shale fines and elemental sulfur with retorted oil shale. In some cases, retorting processes are designed to accept material of a certain minimum size. In grinding and preparation of the raw shale, fines (i.e., particles below the minimum size) are produced. As raw shale has been found to pose a greater hazard of spontaneous combustion than retorted shale, the effects of adding up to 20% raw shale to retorted shale was investigated. A similar situation exists with respect to sulfur removed from retort effluents. In some cases this sulfur may be disposed of together with retorted shale and/or raw shale fines. A series of tests was conducted to determine the effect of codisposal of elemental sulfur on spontaneous combustion potential of retorted shale.

In order to investigate the effects that adding raw shale fines might have on retorted oil shale self heating properties, raw shale was mixed with Paraho retorted shale (note that the Paraho project proposes separate disposal as opposed to mixing of these wastes). Thermograms for three tests conducted with 5, 10, and 20% raw Utah (28 GPT) shale added to Paraho retorted shale are shown in Figure 6. These tests were conducted by using the same procedure described previously in dry air with a -325 mesh particle size. Individual test data are given in Appendix B. The test results show that adding raw shale decreases the exothermic onset temperature and superimposes an additional exotherm on the thermogram of the retorted shale. The superimposition of the raw shale exotherm on the retorted shale thermogram lowers the exotherm onset temperature of the mixture to the range (225°-230° C) of the raw shale. The retorted shale, by itself, has an exothermic onset temperature of approximately 300° C. Increasing the raw shale fraction between 5 and 20 percent increased the magnitude of the raw shale exotherm (as would be expected) but had no significant effect on the exothermic onset temperature.

Thermograms for the three tests conducted with elemental sulfur added to the mixture of raw and retorted shale are shown in Figure 7. Individual test data are given in Appendix B. Samples of raw Utah (28 GPT) shale, Paraho retorted shale and elemental sulfur were prepared. In each case, 20% of the mixture was made up of raw shale. Sulfur contents of 1, 2, and 5 percent were tested. The balance, in each case, was made up of Paraho retorted shale.

The effect of the sulfur addition was to add an endotherm at the sulfur melting point, and to generally increase the heat capacity of the mixture. Sulfur, in the form added, is not particularly liable to spontaneous combustion and may have a slight inhibiting effect by providing an additional heat sink if codisposed with retorted shale. However, this observation should not be extrapolated to sulfur compounds which may behave very differently.

Based on these tests, it is recommended that raw shale be segregated to the greatest extent possible from retorted shale when these materials are ultimately returned to the land. Alternatives for processing of raw shale fines include combustion and retorting in a separate process capable of handling fines. If no market can be found for byproduct elemental sulfur, it can probably be codisposed with retorted shale without increasing the risk of spontaneous combustion. However, impure forms of sulfur, sulfur compounds, or disposal in higher concentrations should be tested and evaluated to determine potential impacts on auto oxidation properties of the mixture. Other potential environmental problems such as increased impacts or leachates on surface and groundwater quality may be of concern when sulfur is codisposed with retorted shale.

3.2 Nonadiabatic Oxygen Absorption Testing

3.2.1 Introduction

The samples described in Section 2 were subjected to a nonadiabatic oxygen absorption test that had been developed for coal testing. The samples obtained during the first phase of the study were tested at Denver Research Institute (DRI) under a subcontract. These were the Western Kentucky #9 bituminous coal, the Wyoming subbituminous coal, the C-a raw shale and

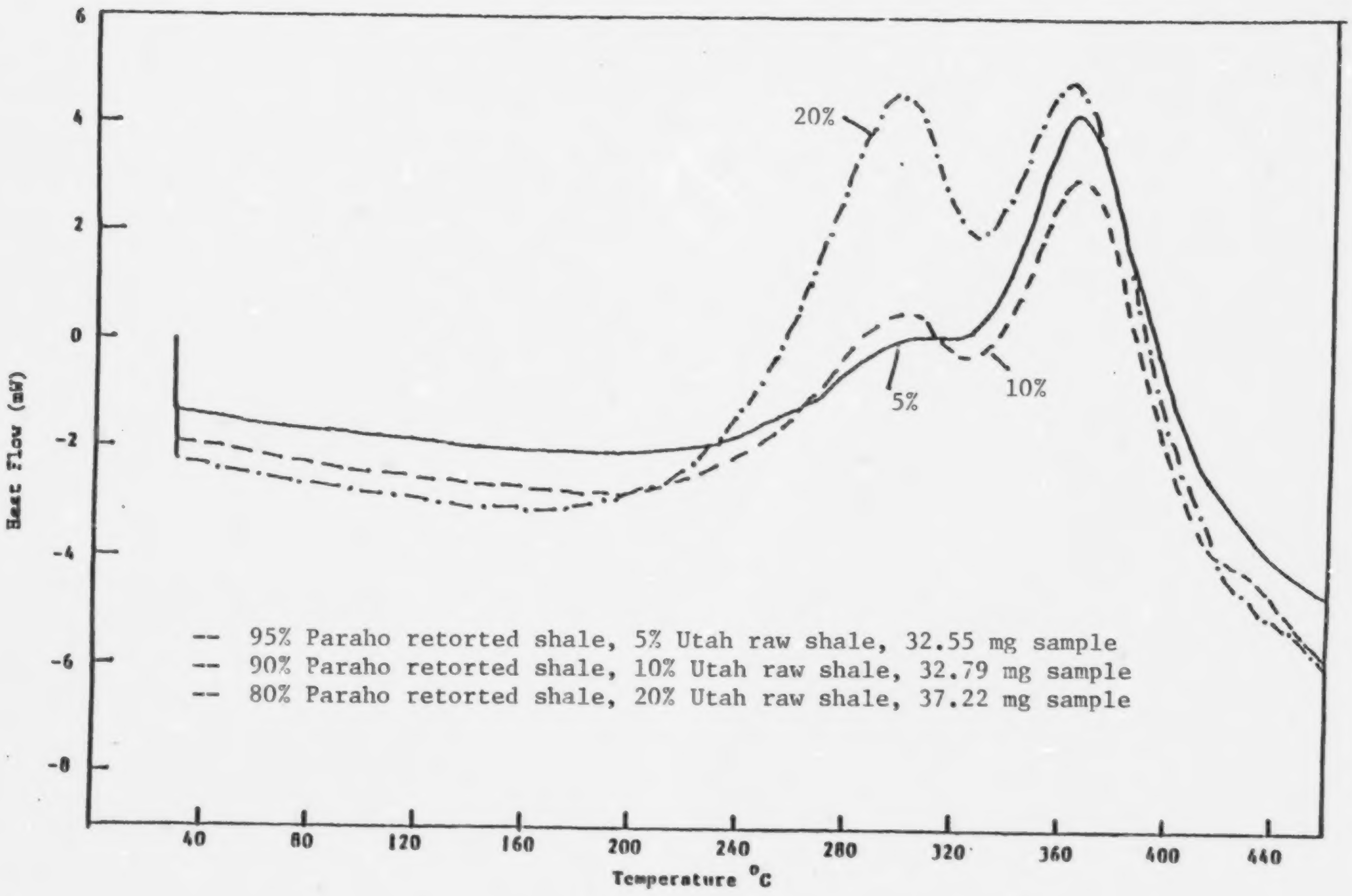

FIGURE 6. Effect of adding raw Utah (28 GPT) shale to Paraho retorted shale (2°C/min heating ramp, dry air -325 mesh)

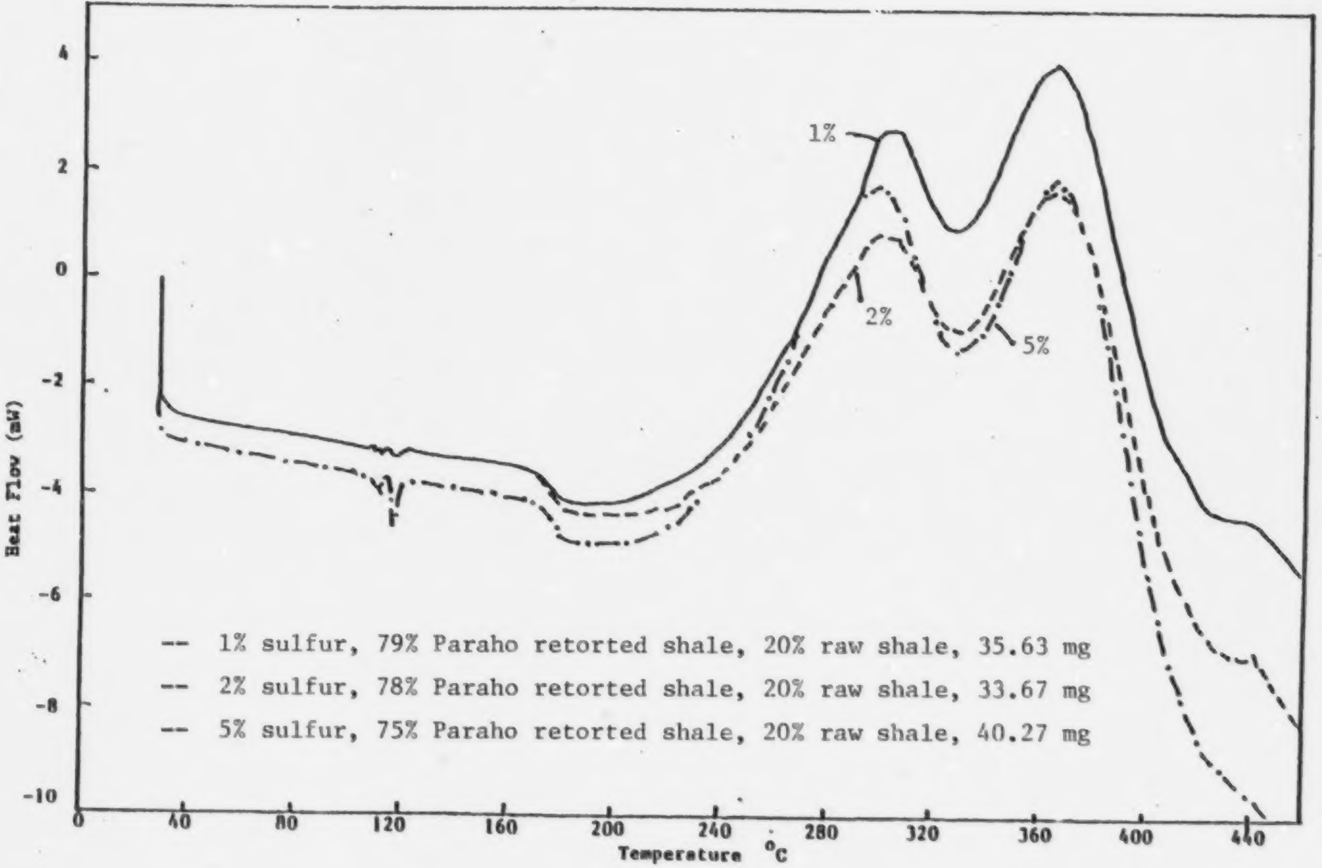

FIGURE 7. Effect of adding sulfur to raw/retorted shale mixture (2°C/min heating ramp, dry air, -325 mesh)

retorted shale from the Paraho, TOSCO, and Lurgi processes. This work was supervised by Mr. Charles Habernicht of the DRI Chemical Division. The samples obtained during the second phase of the study were tested at Research Triangle Institute (RTI) via an equivalent procedure using a different apparatus and instrumentation setup. One sample from the first sample group was also tested at RTI to confirm the comparability (±4%) of the two apparatus.

3.2.2 Method: Phase I Samples

The test apparatus and procedure were based on those of Schmeling et al.[7]. This procedure was modified to reduce operator time and improve precision. A mass flow controller was used instead of needle valves for inlet gas control and a temperature controlled oven was used instead of an oil bath to maintain apparatus temperature. Chromatographic data acquisition and reduction was done electronically rather than by use of strip chart recorders.

The standard testing sequence consisted of placing 100 g of -48 + 100 mesh (150 to 300 μm) sample into a glass sample cell (see Figure 8) where it was equilibrated at ambient temperature with humidified (ambient temperature saturation) air flowing through the sample at 60 mL/min. This required about two hours if the sample had been stored under nitrogen. When the inlet and outlet oxygen concentrations equalized, the oven was closed and the run started. The sample temperature was elevated at a rate of 25° C/hr up to a final temperature of 300° C. The effluent gas stream was analyzed every 12 minutes for oxygen, carbon monoxide, carbon dioxide, and methane. After reaching 300 ° C, the oven was shut off and allowed to cool. Occasionally, a sample continued to oxidize in the cell and was extinguished by purging with nitrogen.

For this program, two size ranges of each of six available sample materials were analyzed. The -48 + 100 size (150 to 300 μm) is the specified size range (Schmeling, et al.[7]) for this test and all samples tested with the exception of the Lurgi retorted shale were tested in this size range. In addition, -325 mesh (< 45μm) cuts from each sample were tested in an attempt to simulate processing fines such as those collected from baghouses, etc. The Lurgi material was tested in the -200 + 325 (45 to 75 μm and -325 (45 μm) size ranges (no appreciable Lurgi material existed in the original sample in larger size ranges). Triplicate determinations were made for each sample type and size range.

3.2.3 Apparatus: Phase I Samples

The gas introduction system consists of a nitrogen and air supply, a humidifier and a flow measurement and control assembly. The gas supplies consist of bottled dry nitrogen and manufactured air containing 21 percent oxygen and 79 percent nitrogen by volume. Standard two-stage pressure regulators reduce tank pressures to 2.0 atm (30 psi). A manually operated switching valve allows the operator to select either the nitrogen or air stream. A temperature controlled bubbler-type humidifier controls the water

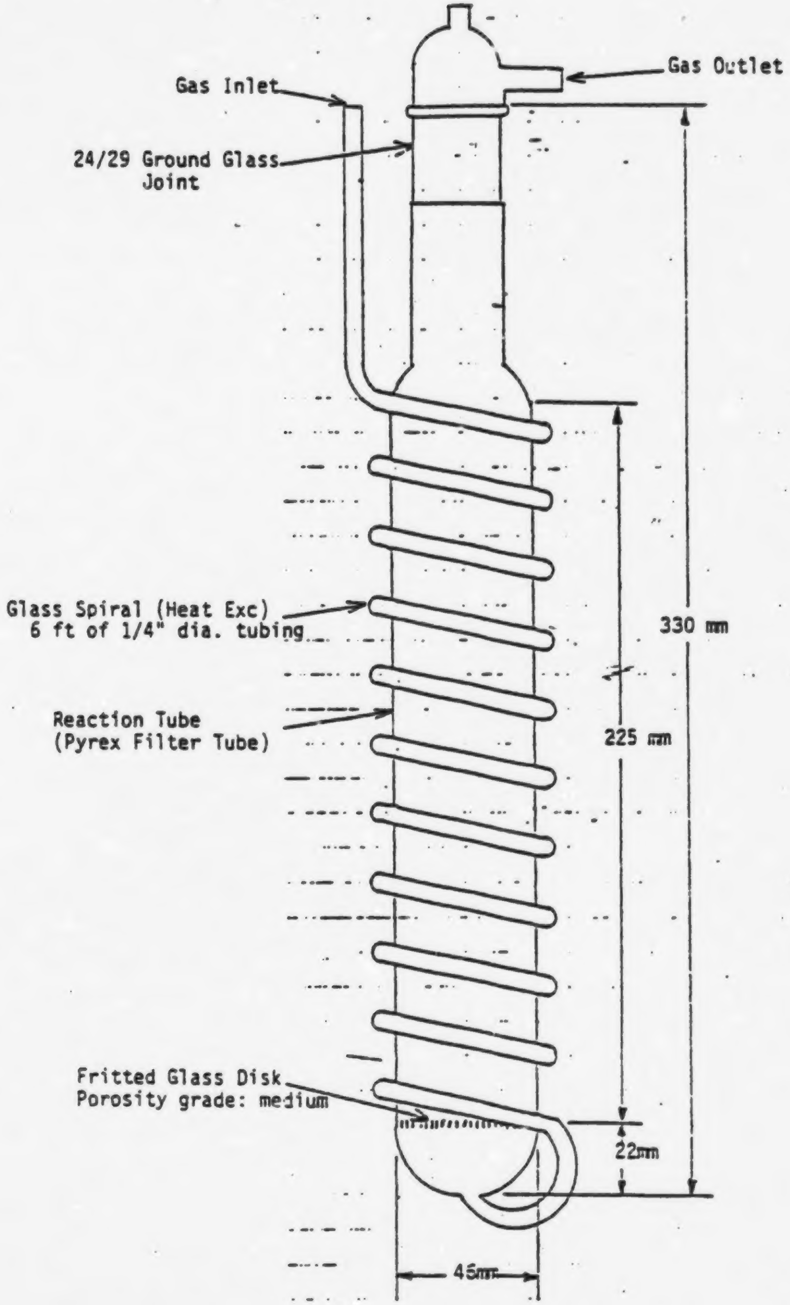

FIGURE 8. Nonadiabatic test apparatus
(Source: Research Triangle Institute)

content of the gas stream. Finally, a mass flow controller maintains a steady flow of 60 mL/min (air adjusted) to the cell.

A temperature-controlled oven is used to adjust the sample temperature. Thermocouples inside and outside of the sample cell have verified that all sample types will track the oven temperature to within ±3° C throughout the temperature range. A blower located within the oven assures uniform temperatures throughout. Oven temperature is controlled by a West Model 270-A temperature programmer which ramps the temperature in response to a clock-driven cam. The cam is cut to adjust the temperature from 25° C to 300° C at a rate of 25° C/hr. A preheater heats the incoming gas stream to oven temperature prior to its entry to the test cell. The preheater has the capacity to handle a 400 mL/min gas stream to a 300° C oven temperature at its exit. This insures that at only 60 mL/min, a thermally equilibrated gas stream enters the cell.

The all-glass cell has a 40 mm inside diameter and a 150 mm nominal height and is fitted with a bottom gas entry through a glass frit and a wide-mouthed spherical glass joint top for sample loading. Three glass sidearms have been added for thermocouple probes at 40, 80, and 120 mm from the cell bottom. These allow separate temperature measurements of incoming, central, and exiting gas/sample regions to be made.

The gas stream exits the sample cell through a glass frit for filtering and immediately upon exiting passes through a condenser and liquid trap. This trap is cooled by an ice bath and removes all condensable water and higher molecular weight hydrocarbons from the gas stream.

The principal method of gas analysis is a dedicated gas chromatographic system consisting of three automated switching valves, two columns, and a thermal conductivity bridge detector. In series with this system, continuous real-time carbon monoxide and oxygen detectors are used to supplement the analyses.

An automated stream selector valve can be switched between the sample line, a zero gas nitrogen supply or a calibration standard gas. The gas stream is sampled by a 0.5 mL loop sampling valve. At regular predetermined intervals the sampling loop is rotated to the "inject" position where a helium carrier gas loads the sample into a 1.6 mm x 50 cm packed Chromosorb 102 column which is used only to separate carbon dioxide from the effluent gas stream. All other gases are allowed to pass through the first column and are collected on a molecular sieve column for temporary storage and separation. Just prior to the time when the carbon dioxide is eluted from the Chromosorb column, a series-bypass valve switched to allow the gas to be bypassed to the thermal conductivity detector, where it is quantitatively measured. After the carbon dioxide peak has passed the detector, the series-bypass valve again switches to allow the remainder of the gases stored on the molecular sieve to be separated and quantitatively detected. The molecular sieve column is a 1.6 mm by 120 mm column packed with molecular sieve 5A and has the ability to separate hydrogen, oxygen, nitrogen, carbon monoxide and hydrocarbons (methane in this program) from the sample stream, but irreversibly absorbs carbon dioxide.

A Beckman Model F-3 oxygen analyzer equipped with an activated carbon filter to remove sulfur-containing gases and Ecolyzer Model 2000 carbon monoxide detector were used to confirm chromatographic results.

Chromatographic output data were stored and reduced with a Hewlett-Packard 9825T computer equipped with an HP digital multimeter and HP 3494 scanner. Long-term replicate determinations of multicomponent mixtures show typical accuracies of ±2 percent for all components, except for high concentrations (>10 percent) of oxygen which show a deviation of ±5 percent.

3.2.4 Method and Apparatus: Phase II Samples

Samples that were obtained during the second phase of the study were tested in a different apparatus, more closely related to that described by Schmeling et al.[7]. Gas flow was adjusted with needle valves and metered with rotameters. The sample cell was immersed in an oil bath; the oil was heated by an electric resistance element and agitated to maintain a uniform temperature. The bath temperature was increased using an R I. Controls model 5500 Data Trak programmer coupled to an Omega Model 22-M-9389 proportional controller. Separate type K thermocouples were used to measure samples and bath temperatures.

A Carle Model 111H gas chromatograph was used to measure concentrations of oxygen, nitrogen, carbon monoxide, carbon dioxide, and methane. This chromatograph has a Poropak T column in place of the Chromosorb 102 column. The effluent gas stream was sampled once every 15 minutes; gas analysis data were automatically integrated with a Spectra-Physica Minigrator.

In the second phase of the study, all samples tested had a particle size of -325 U.S. mesh. The Union raw shale/retorted shale/sulfur mixture was tested dry as uniform gas flow could not be maintained through a sample containing 17 weight percent moisture. Tests were terminated at a temperature of 175° C.

3.2.5 Results

Based on the gas analysis, a spontaneous combustion liability index (the S index) was calculated. The formula for this index was devised by Schmeling et al.[7] and is based on the conversion of oxygen in the inlet gas to CO and CO_2.

$$S = \frac{h_1 + h_2}{2} (x_1) + \frac{h_2 + h_3}{2} (x_2)$$

where S = the spontaneous combustion index

h_1 = 21 - oxygen concentration at 125° C

h_2 = 21 - oxygen concentration at 150° C

h_3 = 21 - oxygen concentration at 175° C

x_1 = carbon dioxide concentration at 150° C - carbon dioxide concentration at 125° C

x_2 = carbon dioxide concentration at 175° C - carbon dioxide concentration at 150° C

All concentrations are expressed in volume percent.

Although carbon monoxide concentration is not explicitly included in the above forumla, the reaction of oxygen to form carbon monoxide increase the parameters h_1, h_2, and h_3 which contributes to an increased S index. The total measured carbon dioxide concentration does not necessarily result from oxidation only but may also result from pyrolysis and desorption reactions. The potential contribution of these mechanisms is extremely low at the conditions employed in the nonadiabatic tests. Cummins and Robinson[23] found that after 90 days in an inert helium atmosphere at 150° C only 20% of the kerogen in Green River shale was converted, and, this material was converted mostly to bitumen and oil "as evidenced by little or no formation of gas ....." At 200° C, the corresponding conversion was 3.0%. Arnold[24] found that mineral decomposition, i.e., the calcining of calcium carbonate and magnesium carbonate was negligibly slow up to about 600° C. For these reasons, no attempt was made to correct the gas analyses for the effects of pyrolysis (i.e., for CO_2 which might have evolved even in the absence of oxygen).

Using data averaged from triplicate tests, S indices were determined for the materials tested. The samples are ranked in order of decreasing spontaneous combustion hazard in Table 8. The parameters used in calculation of the S index are also given. Gas concentration data from which these parameters have been obtained are given in Appendix B. Tables B-1 through B-9 give mean gas compositions at specific temperatures for each sample type. Tables B-10 through B-16 given mean concentrations of oxygen, carbon monoxide, and carbon dioxide as a function of temperature.

Samples tested in the first phase of the study were tested in two different particle sizes. The difference in particle size produced a considerable but inconsistent difference in S index. The C-a raw shale and TOSCO retorted shale produced higher S indices when tested in the larger particle size. The remaining samples produced higher S indices when tested in the finer particle size. The difference in results due to particle size did not affect relative rankings of samples tested in the first phase of the study. In the second phase, samples were tested at -325 mesh only.

Decreasing solid particle sizes would be expected to increase the rate of gas/solid reactions (due to increased surface area) and thus increase the S index. The C-a raw shale and Tosco retorted shale did not exhibit this behavior. One explanation for this observation would be channeling of the gas flow through clumps of finely divided material in the sample cell. This would decrease gas/solid contact and effectively decrease the surface area of the smaller particles.

3.2.6 Interpretation

The nonadiabatic test indicated that the Wyoming subbituminous coal was by far the most reactive material with an S index of 108 in the -48 + 100 size and an S index of 165 when tested in the -325 particle size. This is consistent with the generally observed phenomena of spontaneous heating in low rank coals. The criterion, adopted by Schmeling[7], that materials with S indices greater than 30 (for the -48 + 100 mesh test) are dangerous, also puts the Western Kentucky #9 bituminous coal (S = 37.5) in this category. As would be expected from historical observations of spontaneous combustion, the bituminous coals are much less dangerous than the subbituminous coal.

The ranking of Table 8 indicates, as expected, that the retorted shales are less likely to spontaneously combust than any of the coals or raw shales. The three coals rank in the order expected from past experience and larger scale testing.[1] The raw shales exhibit oxygen absorption behavior which ranks with their energy content. (The richer Utah shale has a higher S index than the leaner Utah shale and the three western shales follow the same order in S index as in ASTM higher heating value.)

While none of the raw shales rank as high as the subbituminous coal, the richer (66 GPT) Utah shale ranks intermediate between it and the high volatility Western Kentucky #9 bituminous coal and the leaner (28 GPT) Utah shale ranks intermediate between the Western Kentucky #9 bituminous coal and the low volatility Pocahontas #3 bituminous coal. On the basis of this test, the raw shales present a hazard of spontaneous combustion on the order of bituminous coals, and the greater the energy content of the shale is, the greater is the tendency for spontaneous combustion. The low ranking of the retorted shales is due both to low levels of oxygen consumption and correspondingly low levels of carbon dioxide generation. All of the retorted shales tested rank well below the bituminous coals in spontaneous combustion risk based on Schmeling's index.

TABLE 8. SPONTANEOUS COMBUSTION INDEX AND CALCULATION PARAMETERS OF MATERIALS SUBJECTED TO NONADIABATIC TEST (Tested dry)

MATERIAL (-325 mesh unless stated)	S	h_1	h_2	h_3	x_1	x_2
Wyoming Subbituminous Coal*	165.75	9.44	17.42	20.97	4.48	5.48
Wyoming Subbituminous Coal* (-48 + 100 mesh)	108.00	3.55	17.60	20.88	2.80	4.10
Raw Utah Shale (66 GPT)	86	7.41	19.7	20.8	3.56	1.86
Western Kentucky #9 Bituminous Coal*	60.00	2.97	12.59	20.87	1.16	3.05
Raw Utah Shale (28 GPT)	44	1.55	8.49	18.2	1.10	2.88
Pocahontas #3 Bituminous Coal	42	3.43	11.2	21.0	1.03	2.13
Western Kentucky #9 Bituminous Coal* (-48 + 100 mesh)	37.50	4.85	12.34	20.35	1.13	1.70
Raw Shale C-a (-48 + 100 mesh)	6.89	0.45	2.60	6.55	0.23	1.43
Raw shale C-a	5.59	1.12	2.50	6.09	0.17	1.23
Union Shale Mixture	4.6	0.41	3.00	6.37	0.61	0.76
Hytort Retorted Shale	3.3	0.90	3.14	5.26	0.43	0.68
TOSCO II Retorted Shale* (-48 + 100 mesh)	3.60	1.10	1.44	2.79	0.22	1.57
TOSCO II Retorted Shale*	1.38	0.57	1.28	2.02	0.08	0.79
Paraho Retorted Shale*	0.27	0.10	0.47	0.78	0.01	0.42
Paraho Retorted Shale* (-48 + 100 mesh)	0.21	0.68	0.84	1.04	0.02	0.21
Lurgi Retorted Shale*	0.00	0.38	(-)0.04	0.00	0.00	0.00
Lurgi Retorted Shale* (-200 + 325 mesh)	0.00	0.32	0.14	0.15	0.00	0.01

where S = the spontaneous combustion index

h_1 = 21 - oxygen concentration at 125° C

h_2 = 21 - oxygen concentration at 150° C

h_3 = 21 - oxygen concentration at 175° C

x_1 = carbon dioxide concentration at 150° C
carbon dioxide concentration at 125° C

x_2 = carbon dioxide concentration at 175° C
carbon dioxide concentration at 150° C

*Source: Denver Research Institute

SECTION 4

OTHER EXPERIMENTAL METHODS

4.1 Thermogravimetric Analysis

4.1.1 Introduction

The samples described in Section 2 were subjected to thermogravimetric analysis. In this technique, the weight of a sample is continuously recorded while the sample is heated using a specific temperature program. The rate and extent of physical and chemical changes that are accompanied by an increase or decrease in mass can be determined in this manner. Weight losses can be ascribed to drying, volatilization, or combustion (desorption of carbon monoxide or carbon dioxide). Weight losses occurring below 100° C are assumed to be due to drying. With increasing temperatures the effects of combustion, volatilization and eventually mineral carbonate decomposition occur but cannot be distinguished by this method. Comparison of TGA data with DSC data however can be used to distinguish exothermic (combustion reactions from endothermic volatilization) reactions where these effects do not occur simultaneously.

Thus, a weight loss occurring at a specific temperature can be correlated to the same temperature on a DSC thermogram conducted at the same heating rate. The endothermicity or exothermicity can be used to distinguish between pyrolysis or drying and combustion.

4.1.2 Experimental

Samples of 20 to 50 mg were heated from ambient temperatures at 2° C per minute to approximately 600° C at atmospheric pressure. A duPont Instruments Model 951 thermogravimetric analyzer coupled to a duPont Instruments model 1090/1092 data analyzer was used. A diagram of the thermogravimetric analyzer is shown in Figure 9. The sample is loaded into a platinum pan which is suspended horizontally from a quartz balance beam in a quartz tube. A thermocouple is located next to the sample pan. The reaction tube can be moved into an electric resistance heater, capable of operation at up to 1200° C.

The quartz balance beam is attached to a precision meter movement outside the reaction tube. Deflections of this movement are automatically corrected by a voltage proportional to the sample mass. A flow of 50 cc per minute of dry air was maintained through the quartz tube surrounding the sample for the duration of the test. Temperature programming of the furnace

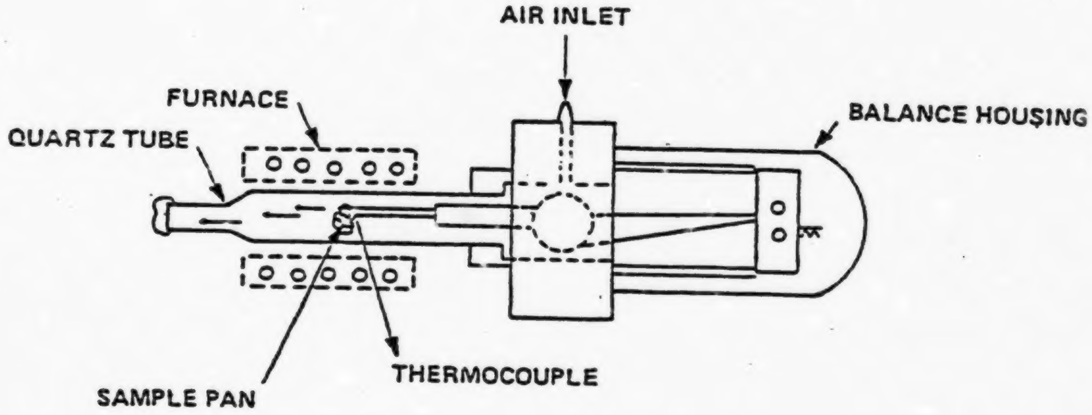

FIGURE 9. TGA Diagram

was automatically controlled by a separate furnace thermocouple. The thermal analyzer, in addition to controlling furnace temperature automatically records sample mass and sample temperature on a magnetic disk at two second intervals.

All samples tested had a particle size of -325 mesh. In addition, a Paraho retorted shale sample of -48 + 100 mesh was tested. All tests were conducted in triplicate. Test data are given in the appendix. The instrument was calibrated for temperature against Permanorm 3 obtained from the National Bureau of Standards, and for mass against reagent grade calcium oxalate monohydrate.

4.1.3 Results

Minor weight losses due to drying were observed in the Wyoming and Western Kentucky coal samples. The shale and retorted shale samples were all very dry (<0.6% weight loss on heating to 120° C) with the exception of Union shale mixture which was tested after addition of 17% moisture to simulate disposal conditions. Taking the dry weight as the weight at 120° C, none of the samples showed much additional weight loss (<1% of dry weight) upon heating to 200° C.

Most samples showed a slow decline in weight up to a point where weight decreased rapidly; for the coal samples this point was very distinct as a rapid combustion reaction was initiated. For the shale and retorted shale samples, the weight loss was more gradual with increasing temperature.

Several different approaches were taken with respect to ranking materials on the basis of TGA data. While it is impossible to separate weight losses due to combustion (i.e., desorption of carbon monoxide and carbon dioxide) from those due to pyrolysis, low temperature pyrolysis losses are also indicative of the volatility and tendency to auto-ignition. The first two rankings are based on sample weight losses normalized for drying. In Table 9 materials are ranked on the basis of the ratio of sample mass at 300° C and 500° C to sample mass at 120° C.

The data based on sample mass at 300° C are probably a better indicator of auto-oxidation tendency because lower temperature reactions are most important. None of the retorted shale materials show any appreciable weight loss up to 300° C, so that no distinction can be drawn between these materials. The most reactive materials are the Wyoming subbituminous and Pocahontas #3 bituminous coals being substantially combusted at 300° C. The richer Utah shale shows a weight loss of 14% at this temperature which is greater than that of the Western Kentucky bituminous coal. The three raw shale samples, considered by themselves rank in order of richer Utah shale, leaner Utah shale, and C-a shale.

The weight loss data obtained at 500° C reflect the obvious effects of combustion of the coal samples. The raw shales rank below the coal samples in the same order as above. Two of the retorted shale samples showed significant weight losses at 500° C. These materials, TOSCO retorted shale, and the Union shale mixture showed no weight loss at 300° C.

TABLE 9. WEIGHT LOSSES OBSERVED AT 300° C AND 500° C DURING THERMOGRAVIMETRIC ANALYSIS (2°/MIN HEATING RAMP, DRY AIR, -325 mesh)

MATERIAL	$\text{Weight}_{300}/\text{Weight}_{120}$	$\text{Weight}_{500}/\text{Weight}_{120}$
Wyoming Subbituminous Coal	0.25	0.07
Pocahontas #3 Bituminous Coal	0.52	0.23
Utah Raw Shale (66 GPT)	0.86	0.62
Western Kentucky #9 Bituminous Coal	0.94	0.09
Utah Raw Shale (28 GPT)	0.94	0.86
C-a Raw Shale	0.95	0.92
TOSCO II Retorted Shale	~ 1.0	0.95
Union Shale Mixture	~ 1.0	0.95

The above methods of ranking have the advantage of being numerically unambiguous. They do not reveal much information about the nature of the weight loss or the potential for a self-sustaining reaction to occur. A procedure was employed involving an attempt to determine the temperature at which the weight loss increases rapidly. All of the materials with the exception of the Lurgi retorted shale showed a gradual weight loss on heating which began to accelerate at a particular point. An attempt was made to characterize the point at which the rate of weight loss began to increase by extrapolating the portions of the weight temperature curves representing the first two linear weight loss periods to an intersection. This method did not yield a valid indicator temperature, however, as it did not rank the three coals in the known order of auto oxidation potential.

Another procedure was attempted involving ranking of materials on the basis of the temperature at which the maximum rate of weight loss occurred. This approach did not appear to be suitable because the temperature at which the maximum weight loss occurred for the Western Kentucky coal was greater than that for three of the retorted oil shale samples. A third unsuccessful approach involved ranking by the temperature at which the sample temperature outran the heating ramp (due to combustion). This method proved unsuitable because this phenomenon was only observed with the three coals. In addition, for these materials, the order was inconsistent with expected behavior, as the Pocahontas #3 coal ignited and outran the temperature program at 295° C, well ahead of the Western Kentucky coal which ignited at 385° C. It was concluded therefore that thermogravimetric analysis is not very useful in determining auto oxidation potential. Data plots for the TGA tests are given in Appendix C.

4.2 Peroxide Test

A method based on thermal measurements of oxidation by hydrogen peroxide[26] was investigated at the Denver Research Institute. Samples obtained during the first phase of the study were tested by this method in which adiabatic temperature increases due to hydrogen peroxide oxidation were determined as a function of time. The procedure was developed for coal testing, and the application of this test to raw oil shale samples was reported by Atwood et al.[27]

In work with samples obtained in the first phase of the study, anomalous results were obtained. Specifically, Western Kentucky coal proved extremely reactive relative to Wyoming coal, and the Lurgi retorted shale proved more reactive than the C-a raw shale. Further considerations of the test procedure revealed that the exothermic decomposition of hydrogen peroxide was great enough to produce large temperature increases without any contribution from exothermic oxidation reactions involving coal or shale. To confirm this, an additional test was conducted at RTI using silica sand as an inert test material. This material produced a temperature rise indicating that it was more reactive than subbituminous coal and raw shale. The results from this test were deemed unreliable.

4.3 Adiabatic Oxygen Absorption Test

The method of Guney[25] involves a procedure similar to the nonadiabatic test method described in Section 4. Theoretically, Guney's method should be much better than the nonadiabatic method because it is conducted under adiabatic conditions and auto-oxidation potential is indicated by temperature increase. In this method, the reaction is not forced by external heating. Dried sample material, originally under nitrogen at 40° C, is contacted with humidified air at the same temperature. The temperature is permitted to rise and the incoming air is adjusted to sample temperature. Rate of temperature rise and final sample temperatures are used as indicators.

This technique was attempted with Wyoming subbituminous and Western Kentucky bituminous coals, Utah (66 GPT) and C-a raw shales and Paraho retorted shale. In four replicate tests with the Wyoming subbituminous coal, a temperature increase of 65° C after eight hours was observed in one test. In two tests, no appreciable temperature increase (i.e., $\leq$ 3° C) was observed and in the fourth test a 7° temperature rise was observed. In testing, the raw shale (66 GPT Utah) no temperature rise was observed in one case and a 6° C rise was observed in a second test. No appreciable temperature rise was observed with the Western Kentucky coal and Paraho retorted shale samples.

One possible reason for nonreproducibility in this test is inconsistent contact between air and sample material. The incoming air may have passed through the sample in channels, and the contact area may have varied from test to test. A second possibility is that the sample thermocouple, located in the center of the reaction cell, may not have accurately measured the maximum temperature in the cell. Thus, the incoming air could be at a lower temperature than any particular "hot spot" and could possibly quench the reaction.

4.4 Pressure Differential Scanning Calorimetry

An attempt was made to develop an isothermal DSC test in which a sample is held at a constant temperature in an oxygen atmosphere until a spontaneous temperature rise is observed. Similar tests are used to characterize the degradation of polymers.[28] To reduce the test time, a high pressure of oxygen was used. The apparatus was identical to that described in Section 3 except that a high pressure DSC cell was used. In successive 16-hour tests, oxygen pressure was increased from 35 to 69 atmospheres at temperatures up to 150 ° C. Even at the most severe conditions of 69 atmospheres oxygen pressure and 150° C, no exotherm was observed within 16 hours. Wyoming subbituminous coals, C-a raw shale, and Paraho retorted shale were tested in this manner.

SECTION 5

QUALITY ASSURANCE

5.0 Introduction

The measurements that were made in the course of this study were directed toward developing quantitative indicators of auto-oxidation potential. No reference standards for these indicator parameters are available, thus accuracy cannot be discussed quantitatively. In terms of ranking, the three coals that were tested conformed in DSC and nonadiabatic oxygen absorption testing to rankins developed in the past by other methods.[1] In addition, the raw Utah oil shale samples ranked in order of their Fischer assays (i.e., the richer the shale the greater the tendency to auto-oxidation) as expected from past work.[27]

5.1 DSC Testing

DSC testing of samples that were obtained in the second phase of the study was done in triplicate. Exothermic onset temperatures were within 0.5° C of the mean value for the three tests with each sample. The magnitude of the exotherm observed in these tests was not as precise, due in part to the effect of slight changes in baseline. The greatest deviation of one replicate from the mean was 15% for the Utah (66 GPT) raw shale. Individual measurements of the exotherm from the other materials were ±3% of the mean value.

The DSC instrument was calibrated for temperatures against the melting point of indium once per week, during the period when samples were being tested. The onset of the melting point was always within 0.5° C of the true melting point. No adjustment was made for this. The DSC was calibrated for heat effect at the same time against the heat of fusion of indium. The cell constant was automatically calculated and used until the next calibration. In the course of the study, the cell calibration constant varied between 1.107 and 1.122.

5.2 Nonadiabatic Oxygen Absorption Testing

Nonadiabatic oxygen absorption testing was based on chromatographic analysis of off-gases from a heated sample. Chromatographs were calibrated against a (secondary) standard gas mixture. The chromatographic equipment at DRI produced long term replicate analyses of ±2% except for oxygen (±5%). Chromatographic calibration factors, obtained from analyses of standards, at RTI drifted by as much as 9% but the data reduction procedure was adjusted to account for these changes.

All tests were run in triplicate. Tests conducted at DRI on replicate samples yielded S (Schemling[7]) indices within 5% of the mean. Tests conducted at RTI on coal and raw shale samples yielded S indices within 5% of the mean; tests conducted at RTI on retorted shale samples yielded S indices within 20% of the mean.

Samples obtained in the first phase of the study were ground and split at DRI with a portion forwarded for testing at RTI. To evaluate representativeness of splits, subsplits from each portion were analyzed for total sulfur. Comparative data are given in Table 10.

To confirm comparability of data from the nonadiabatic oxygen absorption apparatus at RTI and DRI, one sample was tested in both apparatus. C-a raw shale produced an S index of 5.59 at DRI and 5.1 at RTI.

5.3 Specific Heat Determination

Specific heat determinations were based on sample heat flows relative to heat flows observed with a standard reference disk of sapphire. DSC tests were conducted under identical conditions of temperature ramp and gas flow rate for sample and standard. An empty sample pan was used as a reference for both the sapphire standard tests and the sample tests. Any effects due to changing cell calibration or baseline would be identical in the two tests and exert no influence on the result. The tests were conducted in triplicate. Heat flows varied among tests of the same material due to slightly different sample masses but calculated specific heats were consistently within 0.1 J/g for replicates. The values that were reported are given in two significant figures as integration was carried out at 20° C intervals and precise average values over these intervals were difficult to obtain from the complex thermograms.

5.4 Heating Value, Sulfur, and Organic Carbon Determination

Determinations of higher heating value[29], sulfur[30] and organic carbon were done in duplicate. Organic carbon was determined by removing carbonate from the samples with boiling HCl, followed by analysis for carbon.[31] Reported values are based on original sample weight. Heating value determinations were ±15% of the mean for the retorted shales (which is to be expected as these have very low values) and ±4% for the coal and raw shale samples. Duplicate total sulfur analyses varied by a maximum of 0.05% from each other. Duplicate organic carbon analyses varied by a maximum of 7% from the mean.

TABLE 10. SULFUR CONTENTS OF TEST MATERIALS

	Total Sulfur (%)		
	RTI Sample Split*		DRI Sample Split
Material (-325 mesh unless stated)	As Tested	Dry	Dry
Lurgi Retorted Shale	0.86	0.86	0.80
Paraho Retorted Shale	0.57	0.57	0.69
Paraho Retorted Shale (-48 + 100 mesh)	0.57	0.57	0.55
TOSCO II Retorted Shale	0.58	0.58	0.61
C-a Raw Shale	0.97	0.98	0.95
Wyoming Subbituminous Coal	0.60	0.63	0.69
Western Kentucky #9 Bituminous Coal	3.65	3.73	3.72

*Used for DSC Testing.

**Used for nonadiabatic testing.

SECTION 6

CONCLUSIONS

It must be noted that the results reported here are based on a very limited number of samples of raw and retorted shale. Substantial variations in composition of raw shales occur with geographic and stratigraphic location. The retorted shale samples came from pilot plant operations which may not be completely representative of commercial operations. Hence, it is strongly recommended that actual samples of waste materials proposed for field disposal be tested to determine their actual spontaneous combustion hazard.

Retorted shales that were investigated in this study are unlikely to present a spontaneous combustion hazard. These include retorted shales from the Paraho direct, TOSCO II, Hytort, and Lurgi processes and a mixture of retorted shale, raw shale "fines," and sulfur from the Union B process. These materials proved to be far less reactive than Pocahontas #3 low-volatility bituminous coal which is generally regarded at the low end of the spectrum of coals susceptible to spontaneous heating. This conclusion was reached on the basis of both the exothermic onset temperature, as determined by differential scanning calorimetry, and the nonadiabatic oxygen absorption test, and supported by TGA weight loss data. The Lurgi retorted shale is non-combustible and could not burn even if an attempt was made to ignite it.

The raw western shales, while not as liable to ignite as the Wyoming Smith-Roland subbituminous coal (which is generally placed at the higher end of the spectrum of coals susceptible to spontaneous heating) present a potential hazard. The richer of the Utah shale samples (66 GPT) is particularly reactive, falling between the Wyoming subbituminous and the Western Kentucky high volatile bituminous coal (of intermediate reactivity with regard to coal) in the nonadiabatic oxygen absorption test. In the DSC test, it falls below the Western Kentucky coal but above the relatively unreactive Pocahontas #3 coal. In the TGA weight loss test (based on mass remaining after heating to 300° C), a greater weight loss is observed with this sample than with the Western Kentucky bituminous coal.

The leaner Utah shale (28 GPT) is intermediate in tendency to auto-ignite between the Western Kentucky coal and the Pocahontas #3 coal in both the nonadiabatic oxygen absorption test and the DSC test (ranked by exothermic onset temperature). This material falls below the coal samples in the TGA weight loss tests. By Schmeling's criteria (S index > 30), this is also a potential hazard. The C-a shale has about the same exothermic onset temperature as the leaner Utah shale (i.e., intermediate between the Western Kentucky and Pocahontas bituminous coals, but considerably ranks lower than the Pocahontas coal in the nonadiabatic oxygen absorption test with an S index of about 6.) This is probably the least reactive of the three western raw shales tested but should still be regarded as posing potential problems.

The results of the study suggest that carbonaceous retorted oil shale poses less hazard of spontaneous combustion than bituminous coal and it is logical that the more severe the retorting process and the more complete the removal of the organic matter, the less reactive the resulting waste product will be. This does not imply that the risk of spontaneous combustion can be ignored but rather that the risk should be low if proper disposal practices are followed. Good practices would likely include cooling before disposal, compaction in lifts, and excluding air flow into the pile. Decarbonized shales, such as the Lurgi decarbonized retorted shale, are essentially inert since substantially all of the energy content has been removed. Such shales should present no hazard of spontaneous combustion.

On the basis of differential scanning calorimetry (DSC) testing, codisposal of byproduct elemental sulfur with retorted oil shale will not increase the hazard of spontaneous combustion of the mixture. The mixing of raw shale fines with retorted oil shale prior to disposal should be approached very cautiously and preferably be avoided. The addition of as little as 5% raw shale fines, appears to lower the exothermic onset temperature of the mixture to approximately that of the fines themselves. Although the energy available in the mixture is much less than that of the raw shale fines, the potential for spontaneous combustion may be significantly increased as compared to the retorted shale alone and may in fact be as great as that of the raw shale fines alone. For example, the addition of as little as 5 percent raw shale fines (Utah 28 GPT) lowered the exothermic onset temperature to that of the raw shale fines alone. However, it must be emphasized that the data on this point are somewhat conflicting. The Union B shale mixture which contained 5.47 weight percent raw shale fines behaved in a manner similar to other carbonaceous retorted oil shales which did not include admixture of raw shale fines. Hence, it is recommended that particular mixtures of raw and retorted shales proposed for disposal be individually evaluated. It is considered likely that for each specific retorted/raw shale mixture, there is a unique value of raw to retorted shale ratio which, if exceeded, will cause the mixture to assume the properties of the raw shale.

The raw western shales present a potential hazard, but if stored and disposed of under conditions suitable for long term storage of reactive coals, then they should pose no greater risk than such coals. Ideally, however, raw shales should be processed for energy recovery to the greatest extent possible. Material produced during crushing operations that is too small for retorting would be preferably subjected to combustion for production of process heat, or if feasible, agglomerated with a binder to a size where it could be retorted for maximum energy recovery.

Of the test methods used in this study, the DSC test and the nonadiabatic oxygen absorption test appear to be the most meaningful. These tests were reproducible and, when the tests were applied to coal samples, the results conformed to generally observed rankings of spontaneous combustion potential. Of the other tests considered, the peroxide test was technically unsound; pressure differential scanning calorimetry and adiabatic oxygen absorption tests did not produce useful, reproducible results in the course of this particular study. These methods may, however, after further development, be made useful. The thermogravimetric analysis weight loss test, while potentially useful in characterizing samples, was found unsuitable as results for coal samples did not conform to generally accepted spontaneous combustion rankings, and the retorted shale samples produced an insufficient response to evaluate.

A summary of results obtained in the differential scanning calorimetry and nonadiabatic oxygen absorption testing is given in Table 11. As no reference standards are available for the test parameters which were determined, the accuracy of these tests cannot be determined. However, the ranking of the materials can be used as an indicator of relative spontaneous combustion hazard.

TABLE 11. SUMMARY OF RESULTS FROM DIFFERENTIAL SCANNING CALORIMETRY AND NONADIABATIC OXYGEN ABSORPTION TESTING

Material	DSC* onset °C	exotherm J/g	Nonadiabatic test S index
Wyoming Subbituminous Coal	190	10,900	165
Western Kentucky #9 Bituminous Coal	193	13,800	60
Utah Raw Shale (66 GPT)	211	8,320	86
C-a Raw Shale	226	920	5.6
Utah Raw Shale (28 GPT)	227	2,990	44
Pocahontas #3 Bituminous Coal	230	15,700	42
Paraho Retorted Shale	300	480	0.27
TOSCO II Retorted Shale	306	560	1.4
Union Shale Mixture	331	860	4.6
Hytort Retorted Shale	357	1,340	3.8
Lurgi Retorted Shale	***	~0	0.00

*tested in dry air, particle size: -325 mesh

**no exotherm observed to 550° C

REFERENCES

1. Elder, J.L., L.D. Schmidt, W.A. Steiner, and J.D. Davis, "Relative Spontaneous Heating Tendencies of Coals," Bureau of Mines Technical Paper 681, 1945.

2. Sondreal, E.A., and R.C. Ellman, "Laboratory Determination of Factors Affecting Storage of North Dakota Lignite - Computer Simulation of Spontaneous Heating," Bureau of Mines Report of Investigations 7887, 1974.

3. van Doornum, G.A.W., "The Spontaneous Heating of Coal," Journal of the Institute of Fuel, 482-495, October 1954.

4. Hertzberg, M., et al., "Studies of Incipient Combustion and Its Detection," Bureau of Mines Report of Investigation 8206, 1977.

5. Merrill, L.S., "The Coal-Oxygen Reaction Near the Ignition Temperature," Fuel, 52: 61-65, January 1973.

6. Chamberlain, E.A.C., et al., "The Ambient Temperature Oxidation of Coal in Relation to the Early Detection of Spontaneous Heating," The Mining Engineer, 130, 1970.

7. Schmeling, W.A., et al., "Spontaneous Combustion Liability of Subbituminous Coals: Development a Simplified Test Method For Field Lab/Mine Application," In: Analytical Chemistry of Liquid Fuel Sources, P.C. Uden et al., eds., ACS, 1978.

8. Allen, R.R., and V.F. Parry, "Storage of Low-Rank Coals," Bureau of Mines Report Investigations 5034, 1954.

9. Ellman, R.C., J.W. Belter, and L. Docketer, "Long-term Storage of Lignite at Garrison Dam Riverdale, North Dakota," Bureau of Mines Report Investigations 7037, 1967.

10. Bacharach, J.P.L., E.A.C. Chamberlain, D.A. Hall, S.B. Lord, and D.J. Steel, "Review of Spontaneous Combustion Problems and Controls With Application to U.S. Coal Mines," NTIS No. TID-28879, 1978.

11. Sohn, H.Y., and J. Szekely, Chemical Engineering Science, 27:763, 1972.

12. Szekely, J., J.W. Evans, and H.Y. Sohnm, Gas-Solid Reactions, Academic Press, New York, 1976.

13. Wen, C.Y., and S.C. Wang, Industrial Engineering Chemistry, 62:8-30, 1969.

14. Luss, D., and N.R. Amundson, AIChE Journal, 15:194, 1969.

15. Sohn, H.Y., AIChE Journal, 19:191, 1973; 20:416, 1974.

16. Amundson, N.R., and L.R. Raymond, AIChE Journal, 11:339, 1965.

17. Avison, N.L., R.M. Winters, and D.D. Perlmutter, "On the Kinetics of Coal Oxidation," AIChE Journal, 25(5):773-781, 1979.

18. Kam, A.Y., A.N. Hixson, and D.D. Perlmutter, "The Oxidation of Bituminous Coal-I, Development of a Mathematical Model," Chemical Engineering Science, 31:815-819, 1976.

19. Mahajan, O.P., M. Komatsu, and P.L. Walker, Jr., "Low-Temperature Air Oxidation of Caking Coals. 1: Effect on Subsequent Reactivity of Chars Produced," Fuel, 59:3-10, January 1980.

20. Bouwman, R., and I.L.C. Freriks, "Low-Temperature Oxidation of a Bituminous Coal. Infrared Spectroscopic Study of Samples from a Coal Pile," Fuel, 59:315-322, May 1980.

21. Swann, P.D., and D.G. Evans, "Low-Temperature Oxidation of Brown Coal. 3: Reaction with Molecular Oxygen at Temperatures Close to Ambient," Fuel, 58:276-280, April 1979.

22. Painter, P.C., R.W. Snyder, D.E. Pearson, and J. Kwong, "Fourier Transform Infrared Study of the Variation in the Oxidation of a Coking Coal," Fuel, 59:282-286, May 1980.

23. Cummins, J.J., and W.E. Robinson, "Thermal Degradation of Green River Kerogen at 150° to 350° C, "Bureau of Mines Report of Investigation 7620," 1972.

24. Arnold, Jr. C., "Effect of Heating Rate on Pyrolysis of Oil Shale," In: Industrial and Laboratory Pyrolysis, L. F. Albright and B. L. Crynes, eds., ACS, 1978.

25. Guney, M., "Oxidation and Spontaneous Heating of Coal." METU Journal of Pure and Applied Sciences, 5(1): 109-155, April 1972.

26. Maciejasz, Z., Archiwum Gornictwa, 4(1): Plka. Akad. Nauk. 1959.

27. Atwood, M.T., L. Goodfellow, and R.K. Kauffman, Proc. 12th Oil Shale Symposium, Golden, Colorado (April 1979).

28. A.S.T.M., Standard D-20.30. Proposed Method on Oxidative Degradation of Polyolefins.

29. A.S.T.M., Standard D2015-77. Test Method for Gross Calorific Value of Solid Fuel by the Adiabatic Bomb Calorimeter.

30. A.S.T.M., Standard D3177-82. Test Methods for Total Sulfur in the Analysis of Coal and Coke.

31. A.S.T.M., Standard D3178-73(1979). Test Methods for Carbon and Hydrogen in the Analysis Sample of Coal and Coke.

APPENDIX

TABLE A-1. HEAT CAPACITY OF C-a RAW SHALE BASED ON INITIAL SAMPLE WEIGHT (-325 mesh)

T °C	Cp J/g°C	$\int_{25}^{T}$ Cp dt J/g
40	0.66	9.9
60	0.72	24
80	.73	38
100	.74	53
120	.93	70
140	.70	86
160	.70	100
180	.87	116
200	.91	133
220	.94	152
240	.90	170
260	.82	188
280	.75	203
300	.63	217
320	.56	229
340	.56	240
360	.56	251
380	.48	262
400	.52	272
420	.58	283
440	.69	295
460	.77	310
480	1.11	329
500	1.03	350
520	.71	367
540	.60	381
560	.63	393
580	.68	406
600	.77	421

TABLE A-2. HEAT CAPACITY OF LURGI RETORTED OIL SHALE BASED ON INITIAL WEIGHT (-325 mesh)

T °C	Cp J/g°C	$\int_{25}^{T}$ Cp dt J/g
40	.73	11
60	.78	26
80	.81	42
100	.81	58
120	.83	75
140	.85	91
160	.83	108
180	.88	125
200	.87	143
220	.94	161
240	.93	180
260	.87	198
280	.92	216
300	.92	234
320	.92	253
340	.94	271
360	.93	290
380	.94	309
400	.95	327
420	.96	347
440	.96	366
460	.96	385
480	.97	404
500	.98	424
520	1.00	443
540	1.02	464
560	1.04	484
580	1.09	505
600	1.13	528

TABLE A-3. HEAT CAPACITY OF WYOMING SMITH-ROLAND SUB BITUMINOUS COAL BASED ON INITIAL WEIGHT (-325 mesh)

T °C	Cp J/g°C	$\int_{25}^{T}$ Cp dt J/g
40	1.24	19
60	2.58	56
80	2.91	110
100	1.99	159
120	1.10	190
140	0.57	207
160	.32	216
180	.18	221
200	.13	224
220	.10	226
240	.076	228
260	.075	230
280	.10	231
300	.16	234
320	.18	237
340	.18	241
360	.16	244
380	.23	248
400	.26	253
420	.31	259
440	.37	266
460	.42	274
480	.44	282
500	.52	292
520	.60	303
540	.66	316
560	.72	329
580	.79	344
600	.87	361

TABLE A-4. HEAT CAPACITY OF TOSCO II RETORTED SHALE BASED ON INITIAL SAMPLE WEIGHT (-325 mesh)

T °C	Cp J/g°C	$\int_{25}^{T}$ Cp dt J/g
40	.86	13
60	.93	31
80	.94	49
100	.95	68
120	.93	87
140	.95	106
160	.93	124
180	.95	143
200	.94	162
220	.98	181
240	.98	201
260	.90	220
280	.91	238
300	.84	255
320	.81	272
340	.76	288
360	.74	303
380	.74	317
400	.73	332
420	.73	347
440	.75	361
460	.74	376
480	.76	391
500	.80	407
520	.82	423
540	.84	440
560	.92	457
580	.98	476
600	1.07	497

TABLE A-5. HEAT CAPACITY OF PARAHO (-325 MESH) RETORTED SHALE BASED ON INITIAL SAMPLE WEIGHT

T °C	Cp J/g°C	$\int_{25}^{T}$ Cp dt J/g
40	.69	9.9
60	.73	24
80	.74	39
100	.75	54
120	.74	69
140	.74	83
160	.72	98
180	.75	113
200	.74	128
220	.76	143
240	.75	158
260	.73	173
280	.74	187
300	.71	202
320	.68	216
340	.65	229
360	.63	242
380	.58	254
400	.57	265
420	.55	277
440	.55	288
460	.57	299
480	.56	310
500	.55	321
520	.57	332
540	.55	343
560	.61	355
580	.64	368
600	.70	381

TABLE A-6. HEAT CAPACITY OF WESTERN KENTUCKY #9 BITUMINOUS COAL BASED ON INITIAL SAMPLE WEIGHT (-325 mesh)

T °C	Cp J/g°C	$\int_{25}^{T}$ Cp dt J/g
40	1.01	15
60	1.23	38
80	.99	60
100	1.13	81
120	.64	99
140	.34	109
160	.26	115
180	.24	120
200	.24	125
220	.16	129
240	.24	133
260	.27	138
280	.25	143
300	.25	148
320	.25	153
340	.25	158
360	.27	163
380	.28	168
400	.33	175
420	.44	182
440	.47	191
460	.44	201
480	.44	209
500	.44	218
520	.55	228
540	.17	235
560	.28	240
580	.56	248
600	.14	255

TABLE A-7. HEAT CAPACITY OF POCAHONTAS #3 BITUMINOUS COAL BASED ON INITIAL SAMPLE WEIGHT (-325 mesh)

T °C	Cp J/g°C	$\int_{25}^{T}$ Cp dt J/g
40	1.11	17
60	1.19	40
80	1.11	63
100	1.19	86
120	1.16	109
140	1.19	133
160	1.22	157
180	1.30	182
200	1.27	208
220	1.34	234
240	1.33	260
260	1.32	287
280	1.38	314
300	1.34	341
320	1.35	368
340	1.34	395
360	1.36	422
380	1.40	450
400	1.59	480
420	1.55	511
440	1.60	542
460	1.66	575
480	1.66	608
500	1.62	641
520	1.61	674
540	1.59	706
560	1.65	738
580	1.67	771
600	1.68	805

TABLE A-8. HEAT CAPACITY OF UNION RETORTED SHALE/RAW SHALE/SULFUR MIXTURE AT 17% MOISTURE BASED ON INITIAL SAMPLE WEIGHT (-325 mesh)

T °C	Cp J/g°C	$\int_{25}^{T}$ Cp dt J/g
40	6.1	92
60	7.6	229
80	1.5	320
100	1.0	346
120	1.2	368
140	1.0	390
160	.98	410
180	1.0	430
200	1.0	450
220	1.0	470
240	1.0	491
260	.99	511
280	1.0	532
300	1.0	552
320	1.0	572
340	1.0	594
360	1.0	614
380	1.0	635
400	1.1	657
420	1.1	679
440	1.1	701
460	1.2	724
480	1.3	750
500	1.3	776
520	1.4	803
540	1.4	832
560	1.5	860
580	1.5	890
600	1.5	920

TABLE A-9. HEAT CAPACITY OF HYTORT RETORTED SHALE BASED ON INITIAL SAMPLE WEIGHT (-325 mesh)

T °C	Cp J/g°C	$\int_{25}^{T}$ Cp dt J/g
40	.99	15
60	1.1	36
80	1.0	57
100	1.1	78
120	1.1	101
140	1.1	123
160	1.1	146
180	1.1	168
200	1.1	189
220	1.1	212
240	1.0	233
260	1.0	254
280	1.0	274
300	0.96	294
320	0.92	312
340	0.87	330
360	0.90	348
380	0.97	367
400	1.1	388
420	1.1	411
440	1.2	435
460	1.3	460
480	1.4	488
500	1.6	518
520	1.5	548
540	1.5	579
560	1.6	610
580	1.6	642
600	1.6	674

TABLE A-10. HEAT CAPACITY OF UTAH RAW SHALE (28 GALLON/TON) BASED ON INITIAL SAMPLE WEIGHT (-325 mesh)

T °C	Cp J/g°C	$\int_{25}^{T}$ Cp dt J/g
40	1.0	16
60	1.1	37
80	1.1	60
100	1.2	82
120	1.2	106
140	1.2	129
160	1.2	153
180	1.3	179
200	1.3	204
220	1.3	229
240	1.2	254
260	1.2	277
280	1.1	300
300	1.1	323
320	1.1	344
340	1.0	365
360	1.0	385
380	1.1	407
400	1.3	431
420	1.3	457
440	1.4	484
460	1.5	513
480	1.5	543
500	1.5	572
520	1.6	604
540	1.6	636
560	1.7	669
580	1.7	702
600	1.8	738

TABLE A-11. HEAT CAPACITY OF UTAH RAW SHALE (66 GALLON/TON) BASED ON INITIAL SAMPLE WEIGHT (-325 mesh)

T °C	Cp J/g°C	$\int_{25}^{T} Cp\ dt$ J/g
40	1.4	21
60	1.4	63
80	1.4	105
100	1.5	148
120	1.5	192
140	1.6	238
160	1.6	285
180	1.6	334
200	1.6	382
220	1.6	431
240	1.5	476
260	1.4	519
280	1.3	560
300	1.3	599
320	1.2	636
340	1.2	673
360	1.3	711
380	1.4	751
400	1.7	799
420	1.8	852
440	2.1	911
460	2.7	986
480	2.6	1066
500	1.8	1128
520	2.0	1186
540	2.3	1251
560	2.4	1322
580	2.5	1395
600	2.7	1473

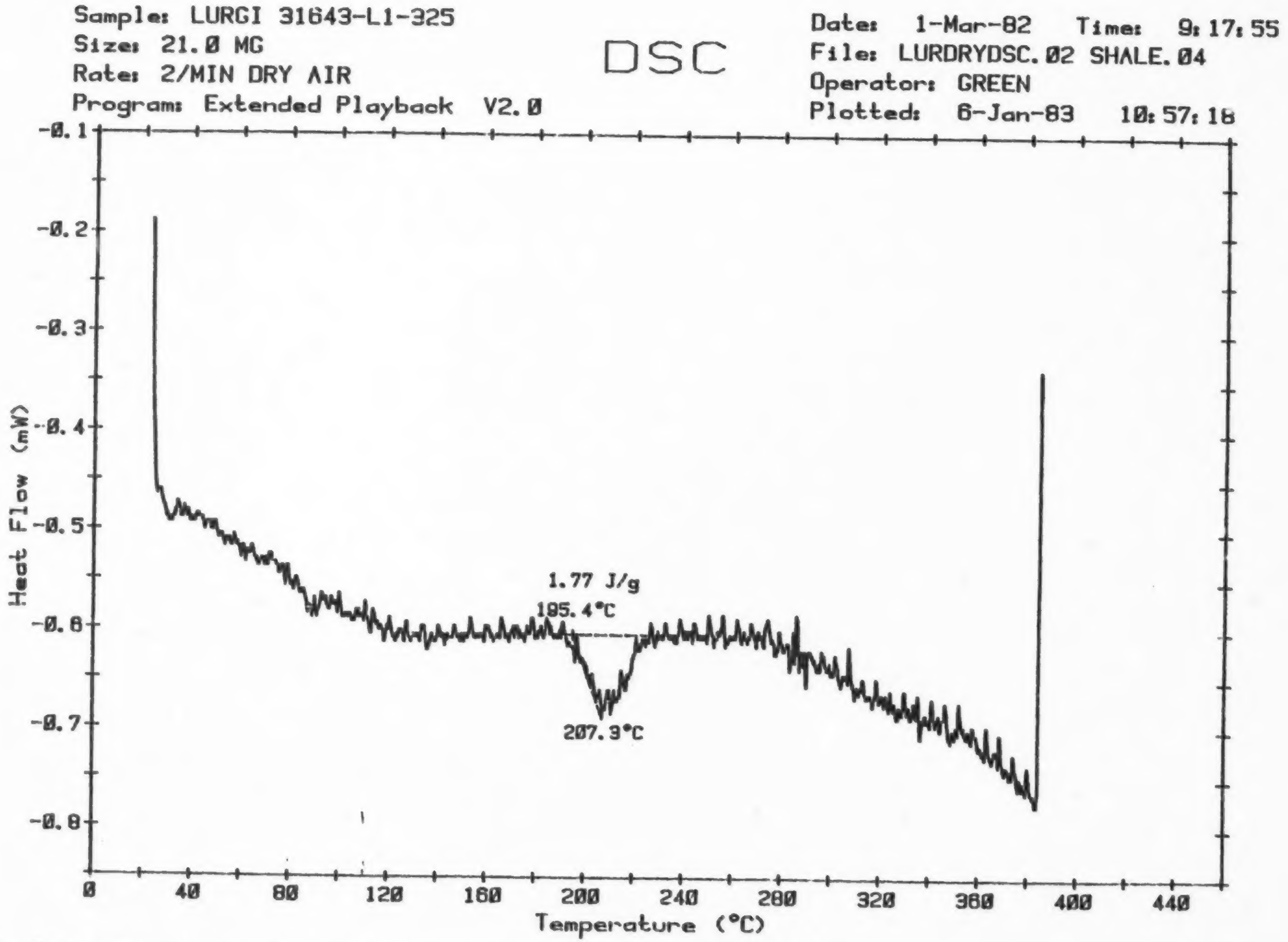

Figure B-1. Thermogram of Lurgi retorted shale (-325 mesh), heated at 2°C/minute in dry air.

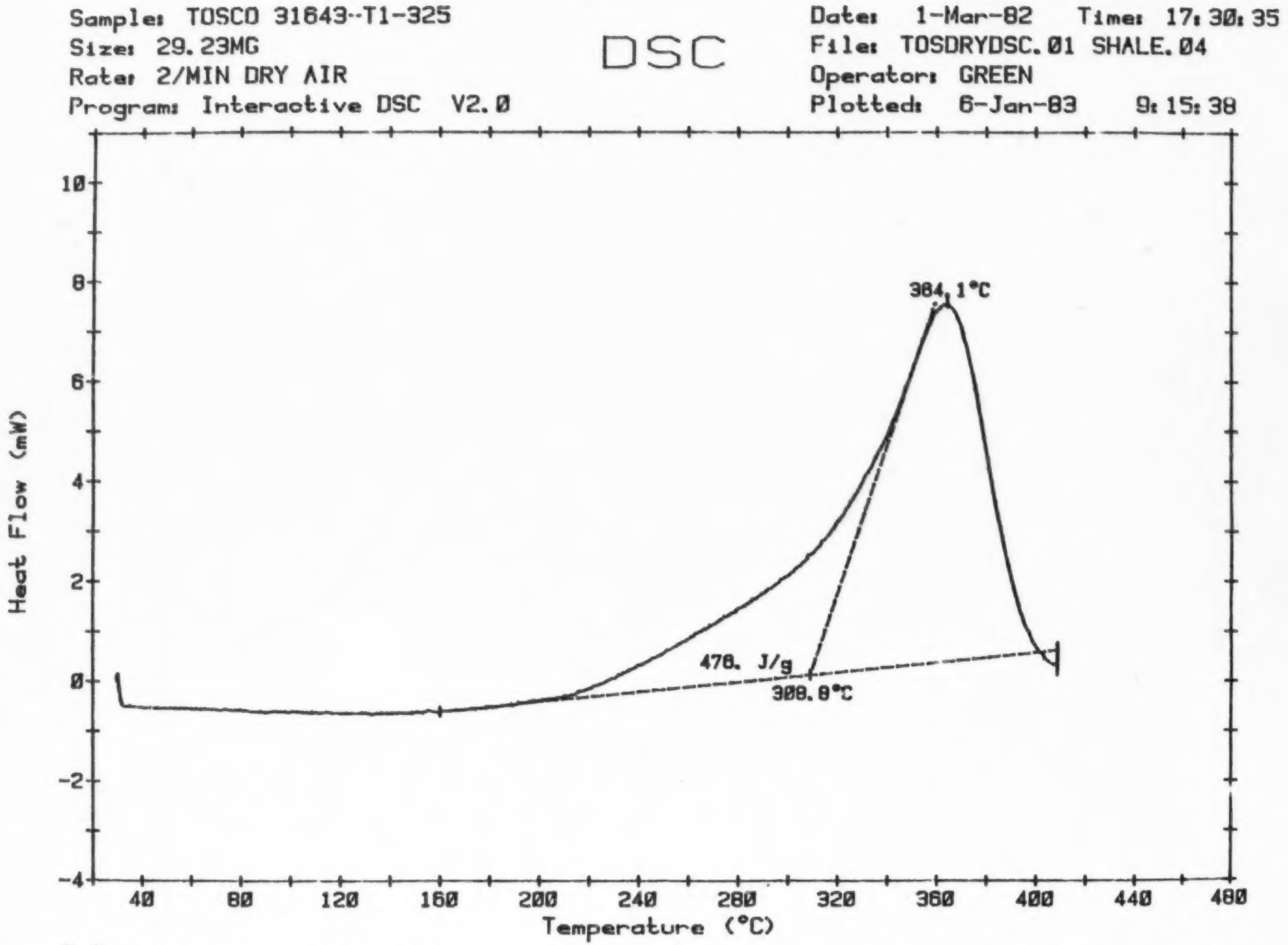

Figure B-2. Thermogram of Tosco II retorted shale (-325 mesh), heated at 2^{0}C/minute in dry air

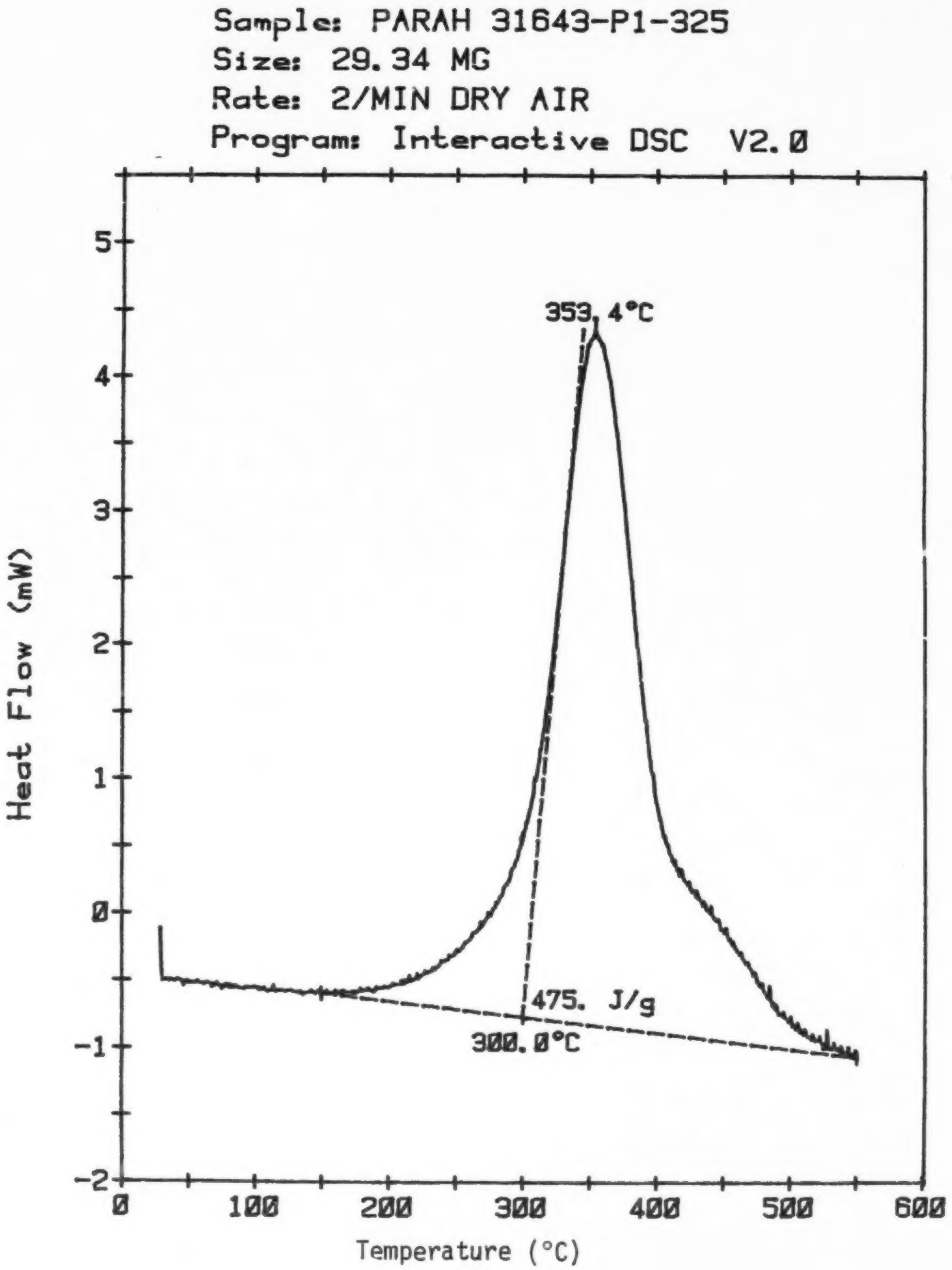

Figure B-3. Thermogram of Paraho retorted shale (-325 mesh), heated at 2°C/minute in dry air.

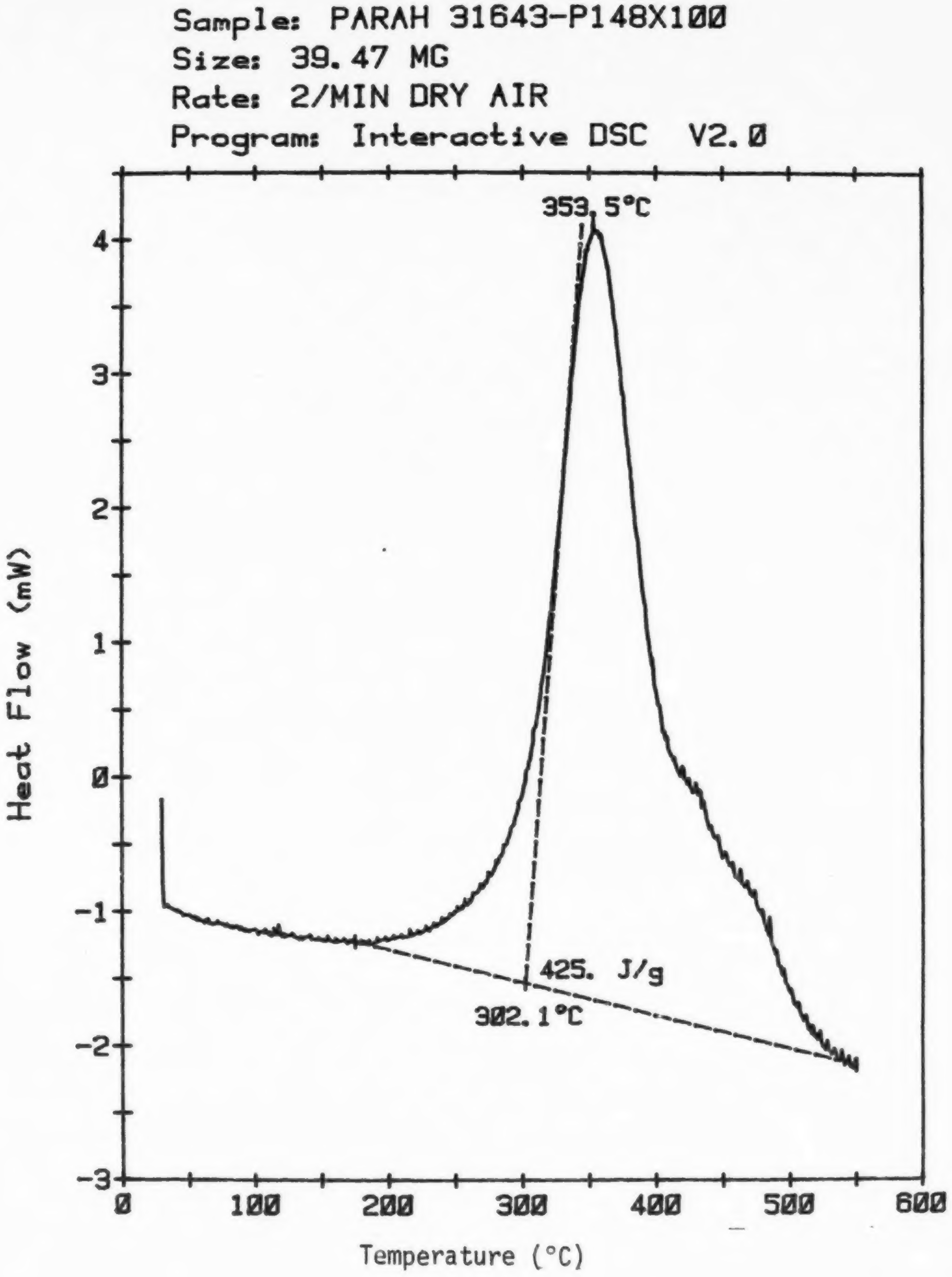

Figure B-4. Thermogram of Paraho retorted shale (-48 + 100 mesh), heated at 2°C/minute in dry air.

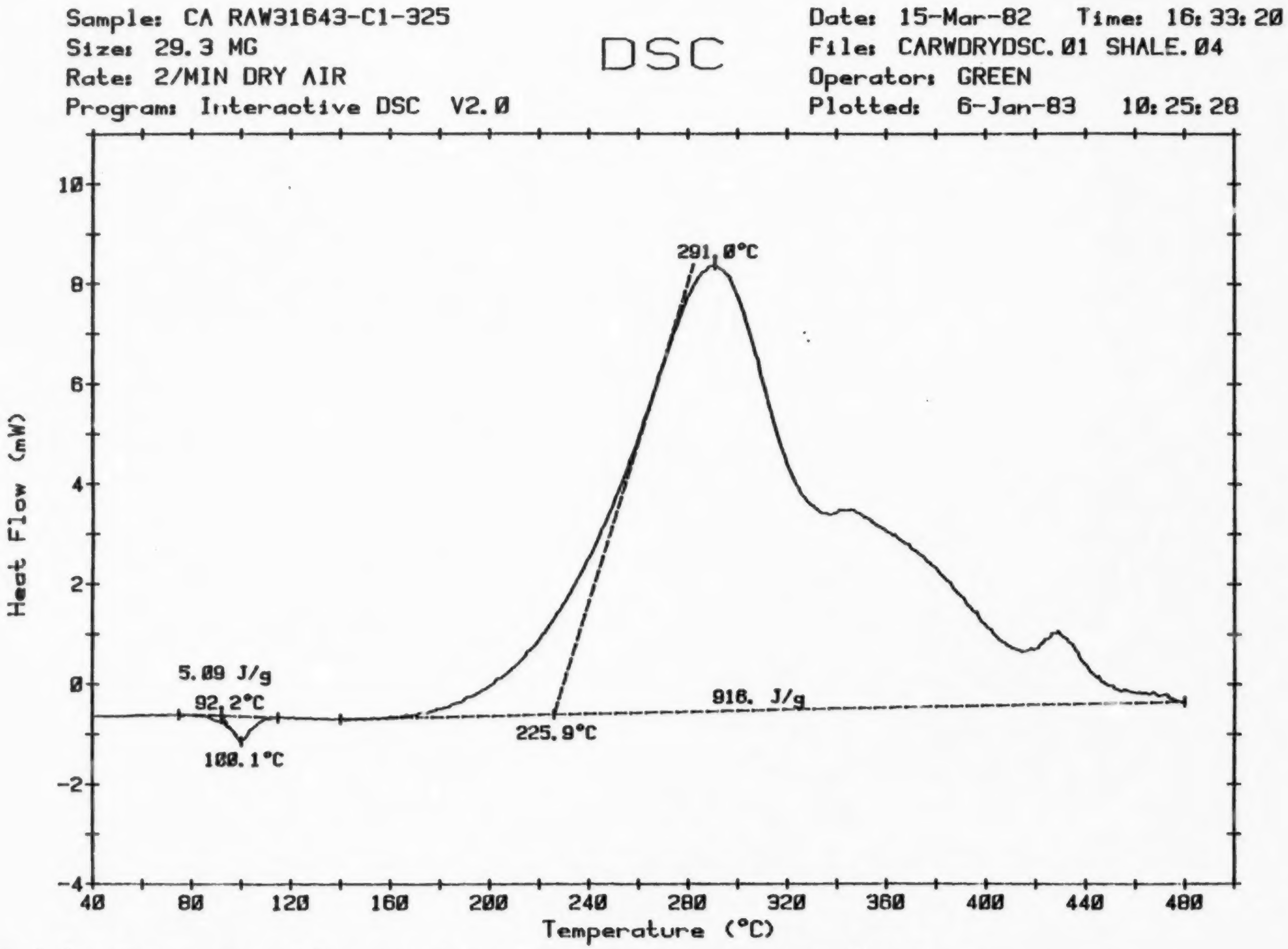

Figure B-5. Thermogram of C-a raw shale (-325 mesh), heated at 2°C/minute in dry air.

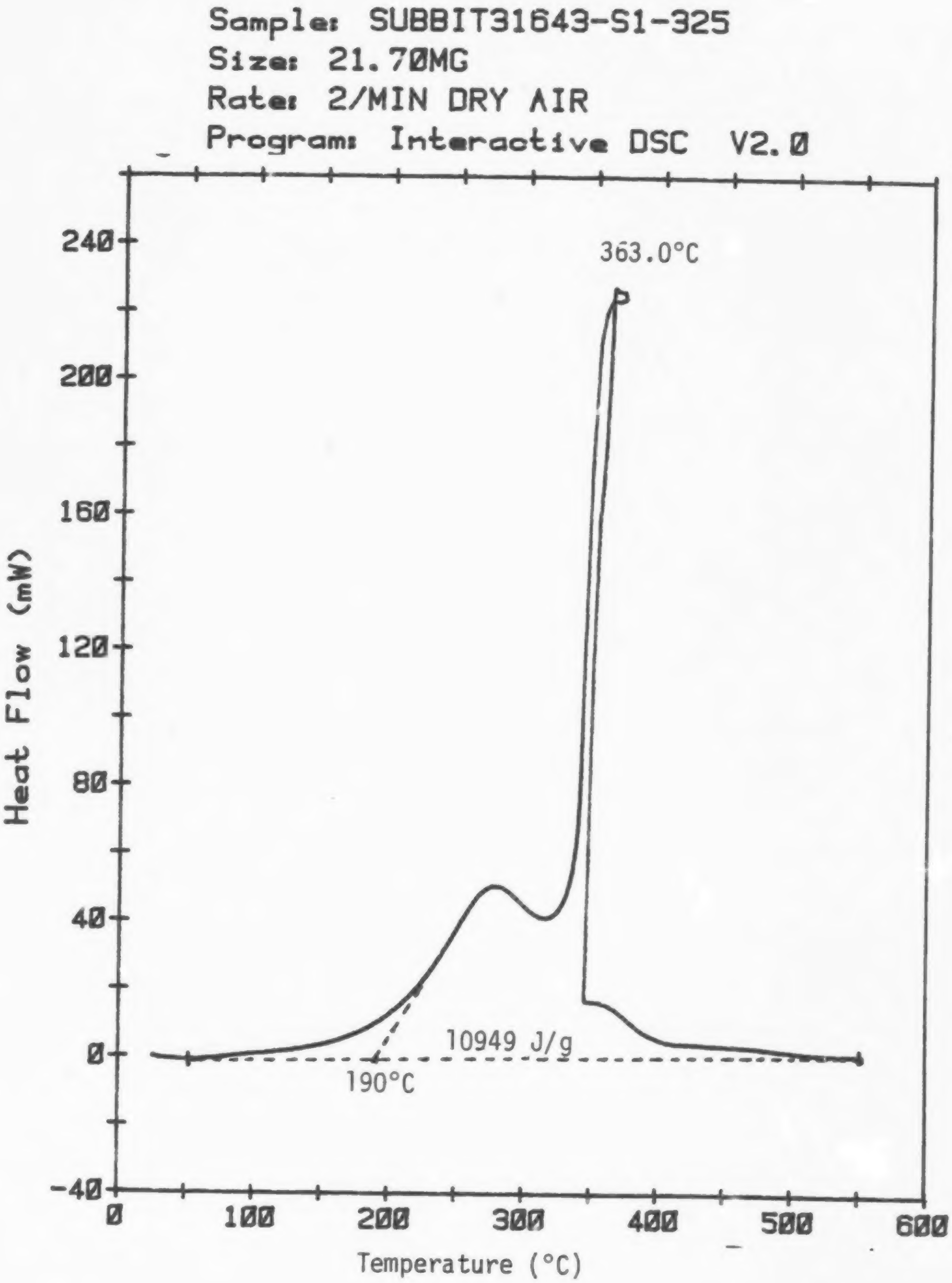

Figure B-6. Thermogram of Wyoming Smith/Roland sub-bituminous coal (-325 mesh), heated at 2°C/minute dry air.

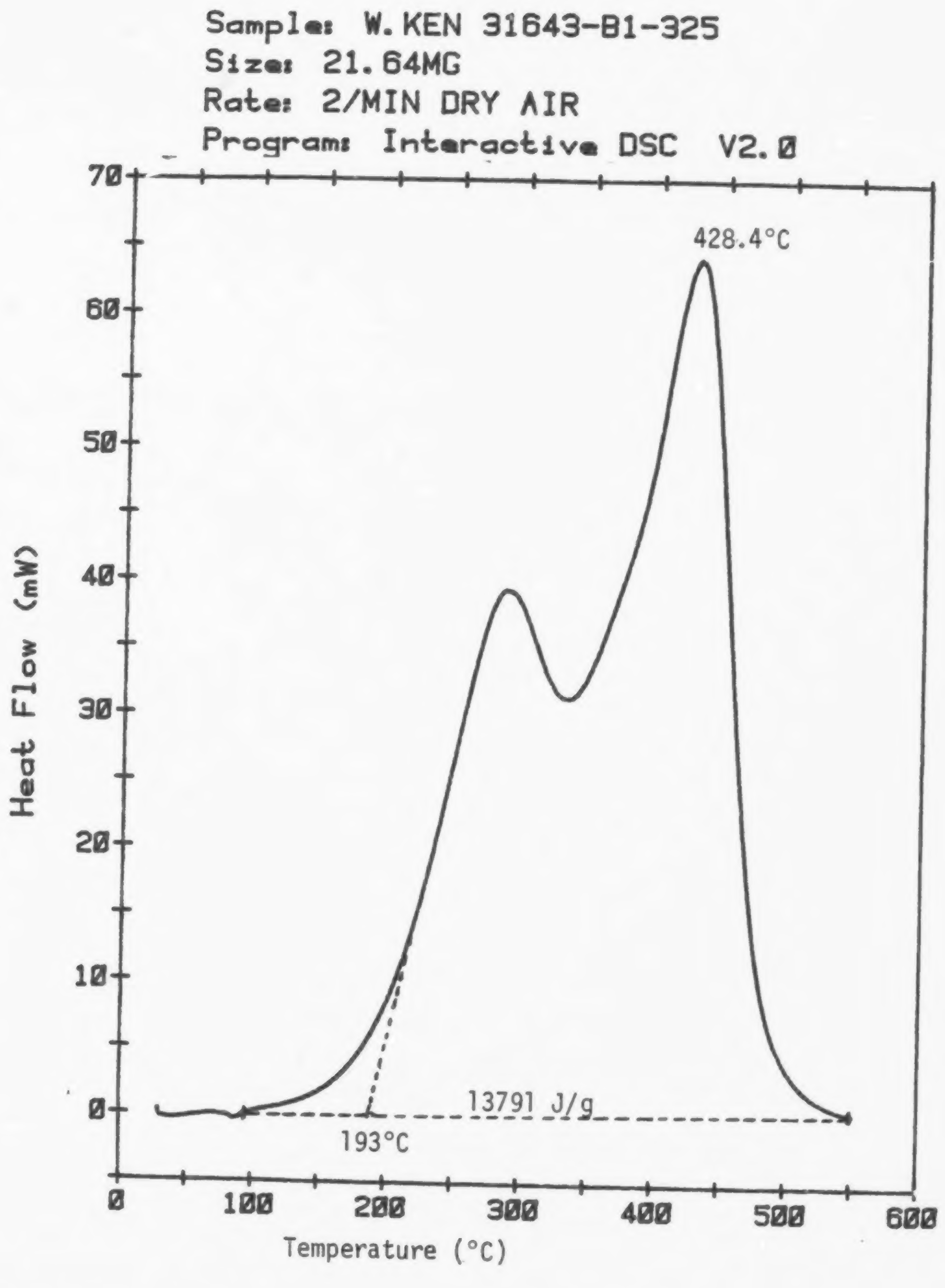

Figure B-7. Thermogram of Western Kentucky No. 9 Bituminous coal (-325 mesh), heated at 2°C/minute in dry air.

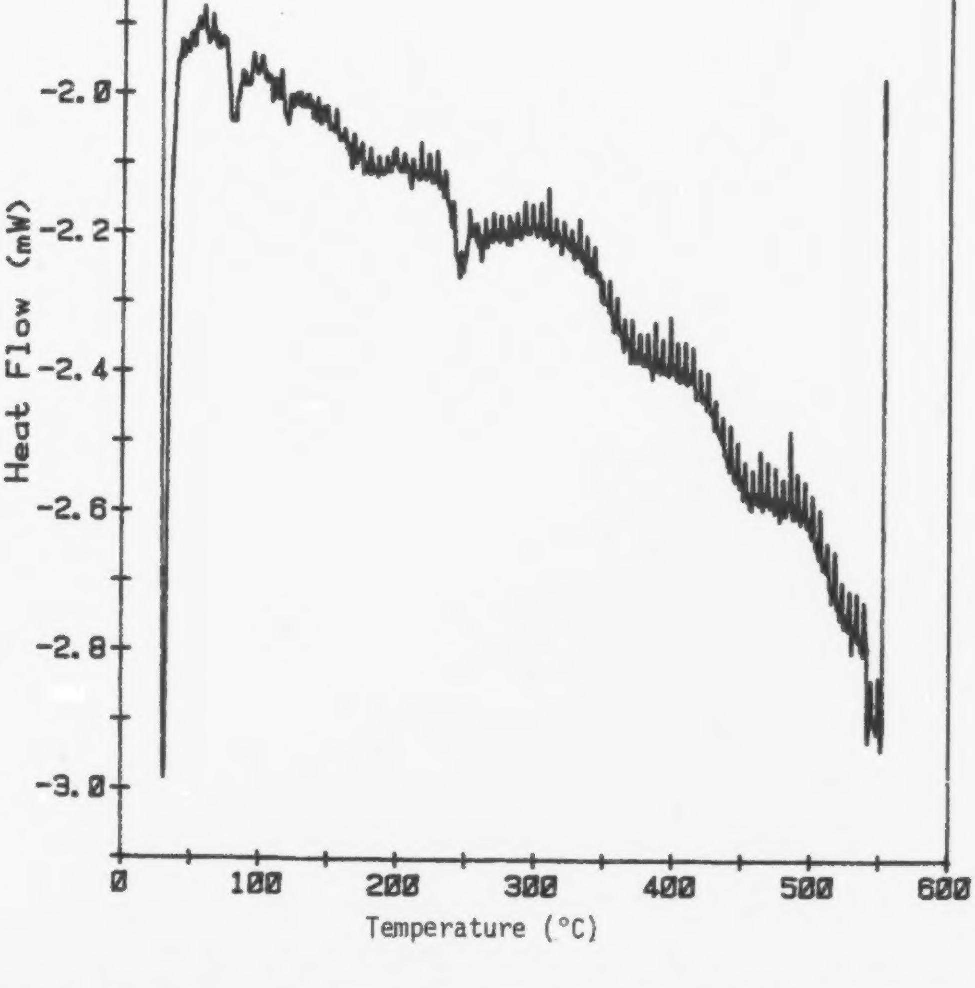

Figure B-8. Thermogram of Lurgi retorted shale (-325 mesh), heated at 2°C/minute in humid air.

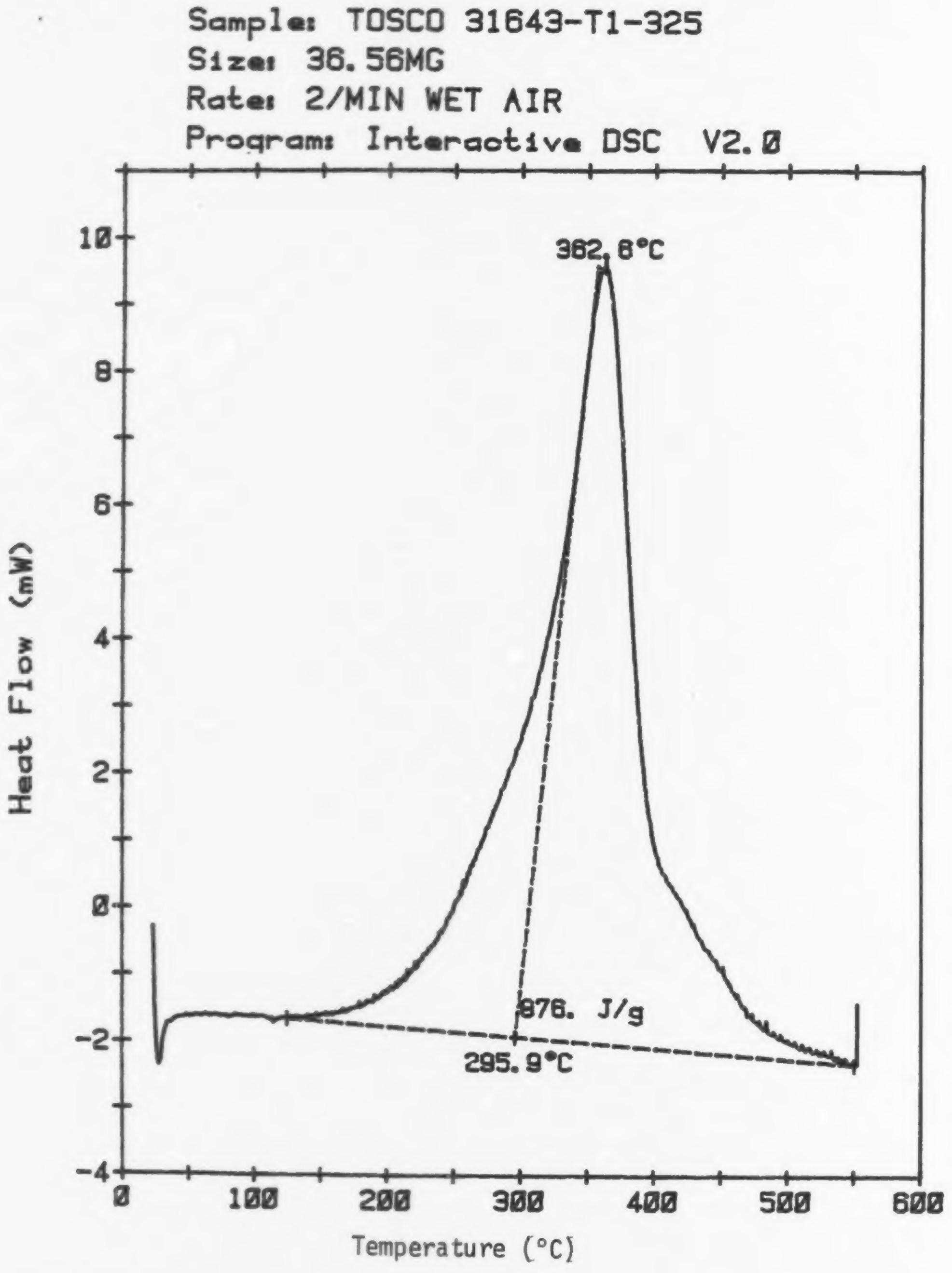

Figure B-9. Thermogram of Tosco II retorted shale (-325 mesh), heated at 2°C/minute in humid air.

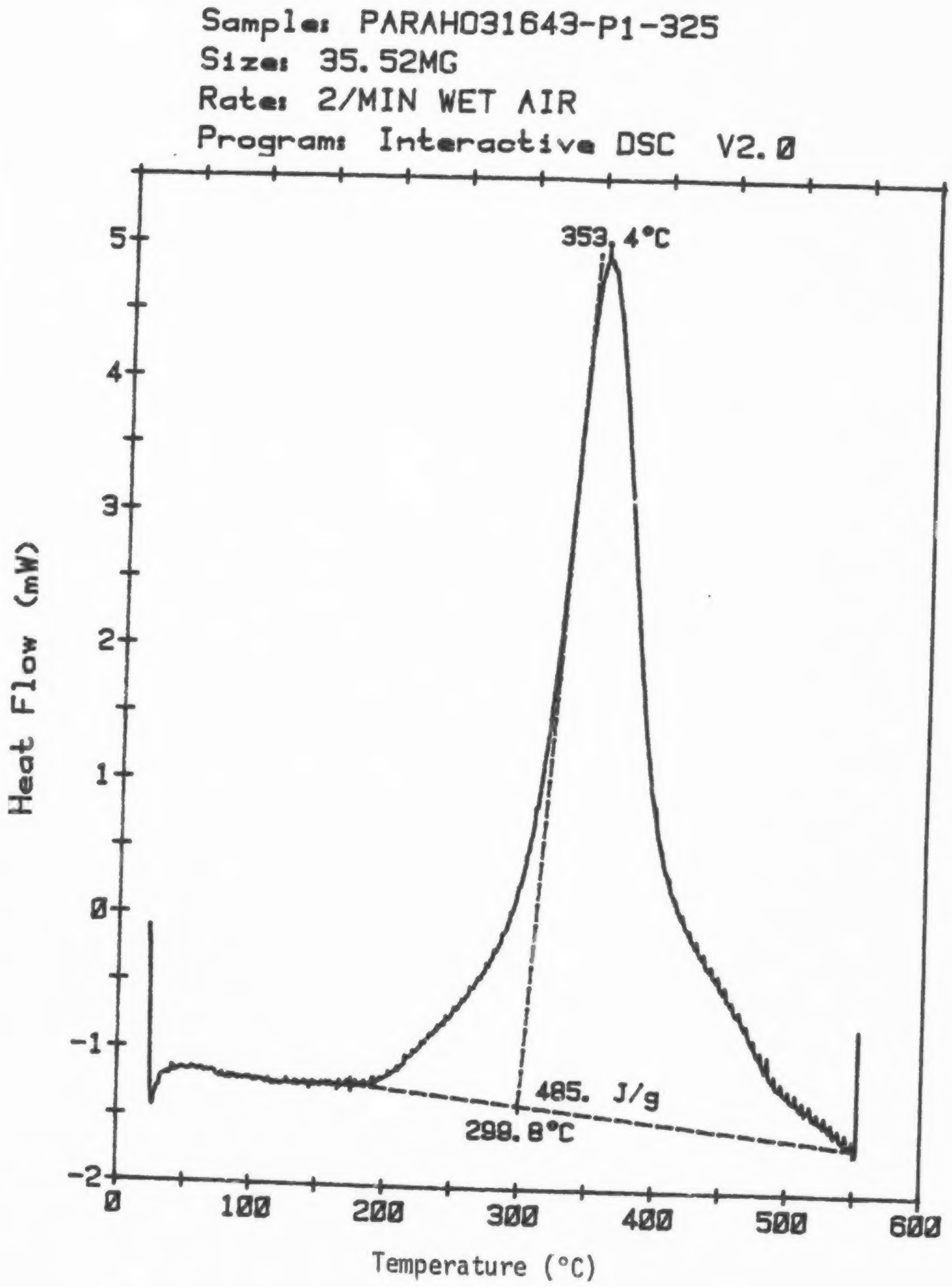

Figure B-10. Thermogram of Paraho retorted shale (-325 mesh), heated at 2°C/minute in humid air.

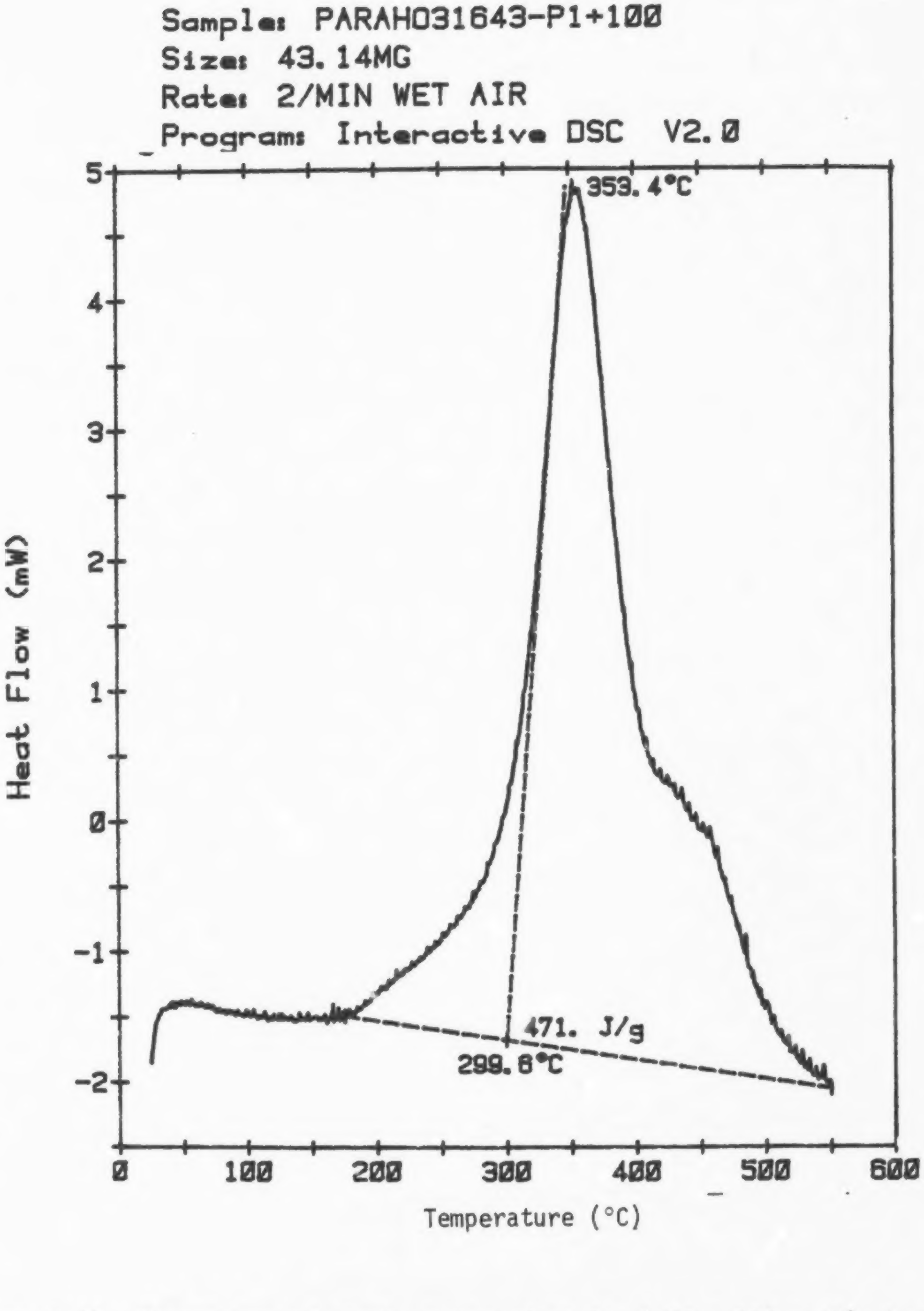

Figure B-11. Thermogram of Paraho retorted shale (-48 + 100 mesh), heated at 2°C/minute in humid air.

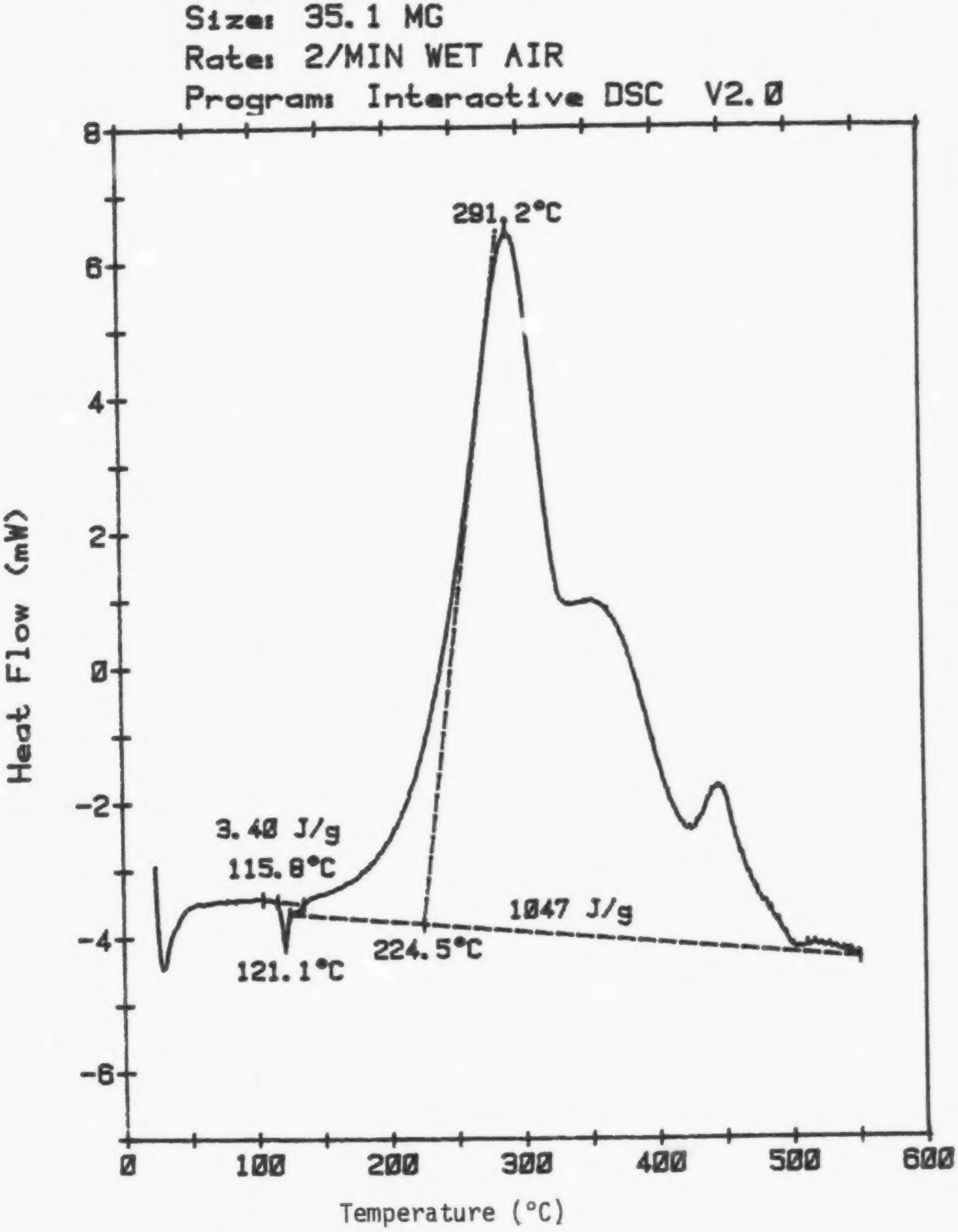

Figure B-12. Thermogram of C-a raw shale (-325 mesh), heated at 2^{o}C/minute in humid air.

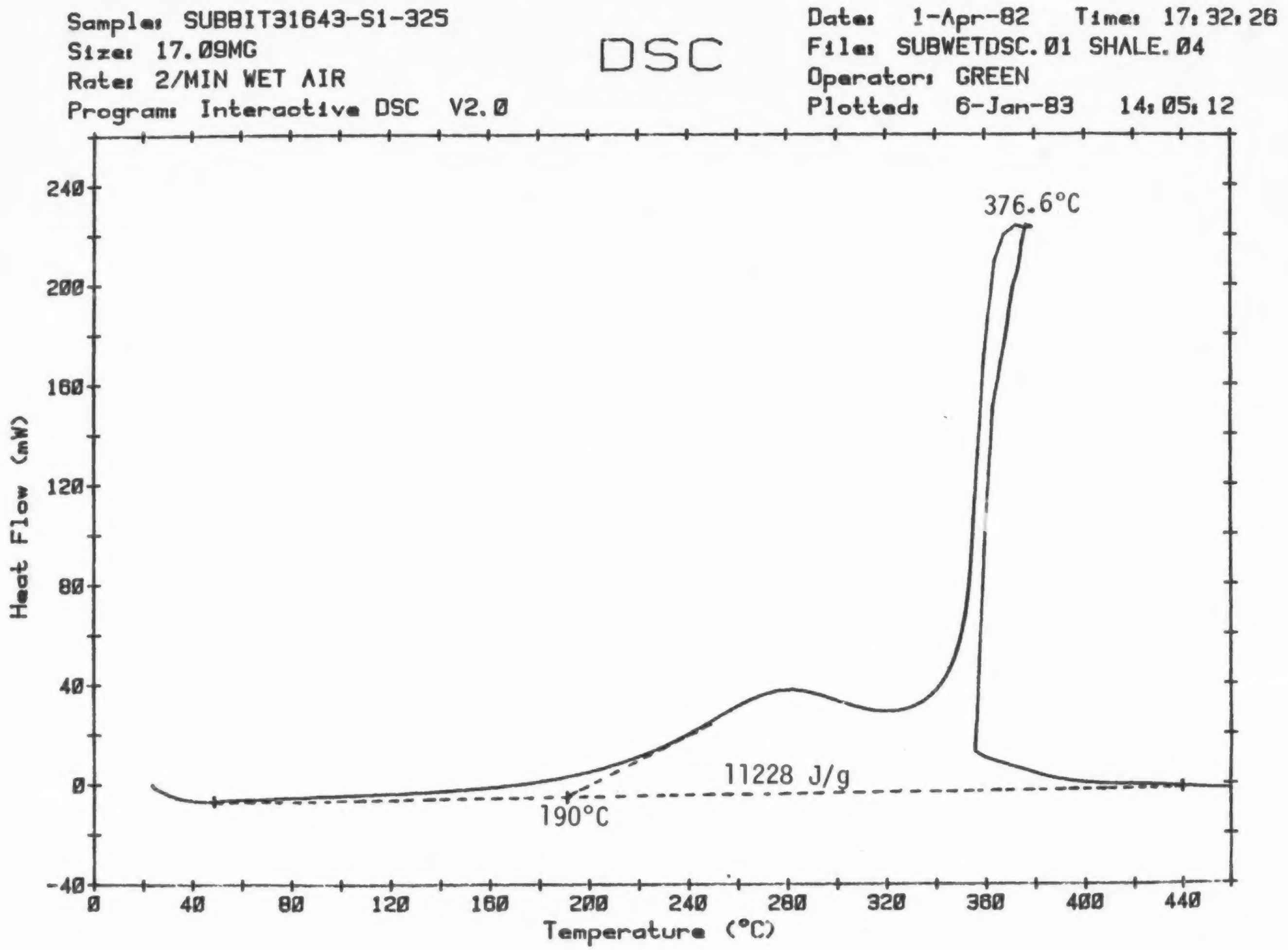

Figure B-13. Thermogram of Wyoming Smith/Roland subbituminous coal (-325 mesh), heated at 2°C/minute in humid air.

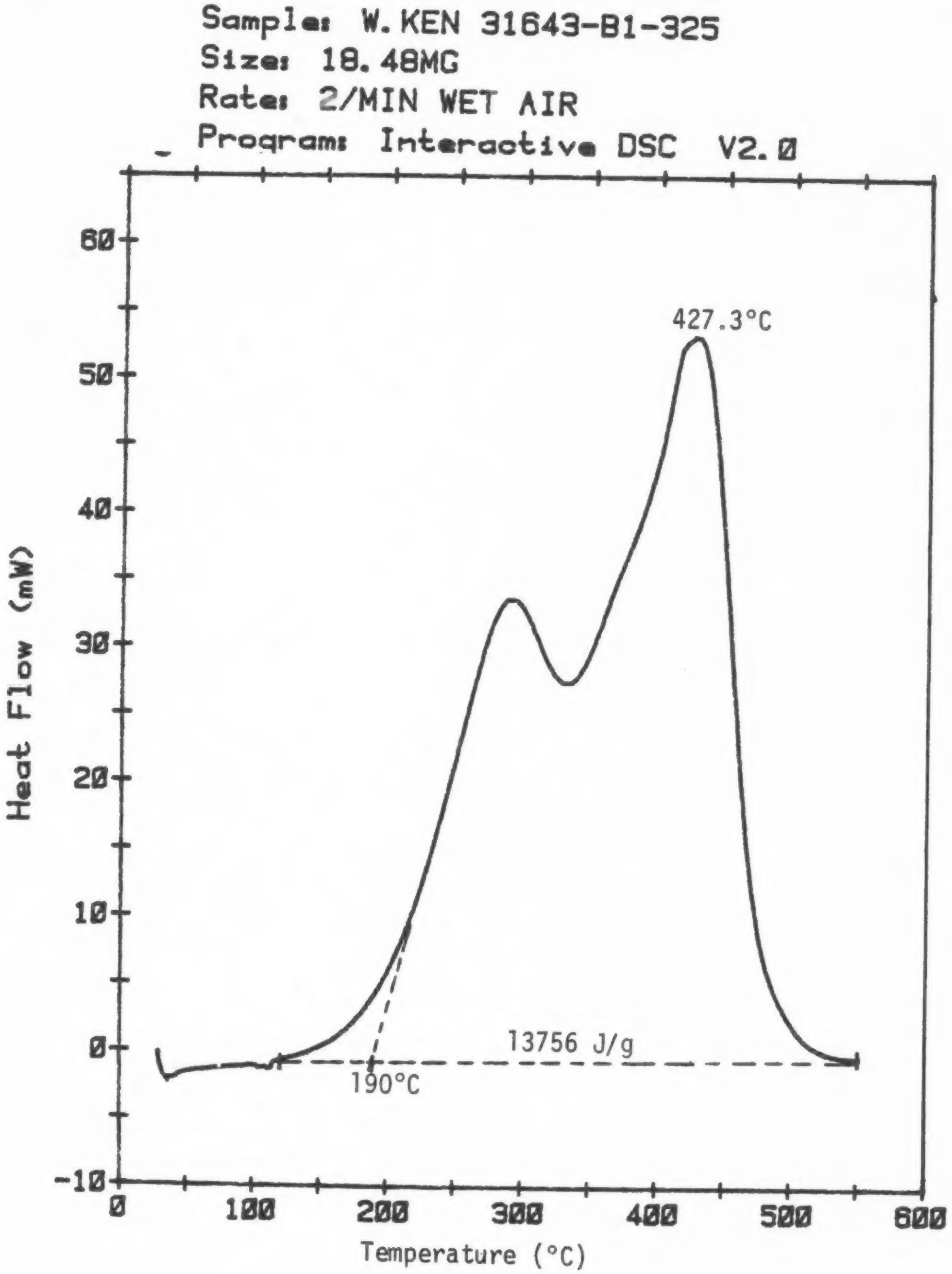

Figure B-14. Thermogram of Western Kentucky No. 9 bituminous coal (-325 mesh), heated at 2°C/minute in humid air.

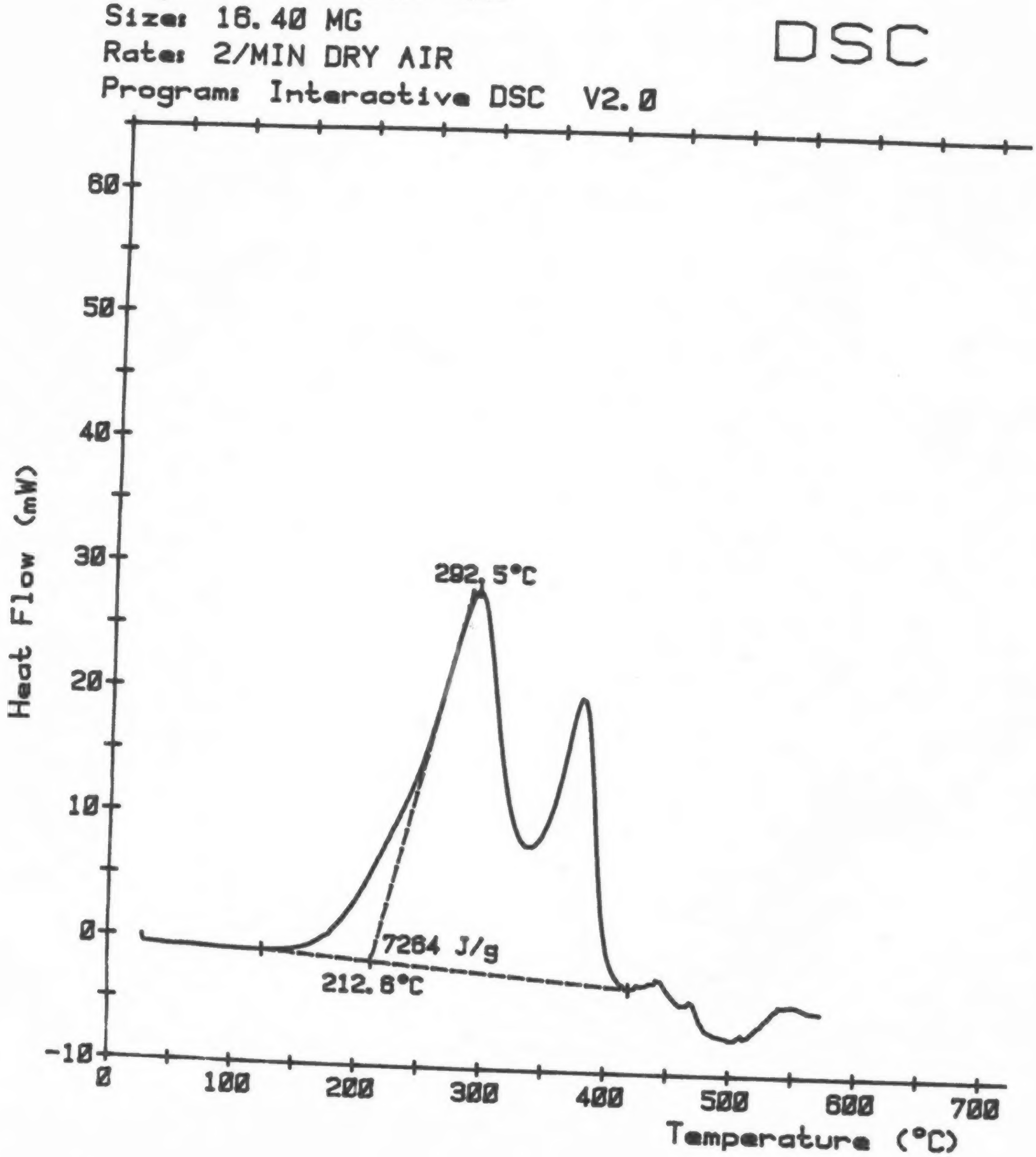

Figure B-15. Thermogram of Utah (66 GPT) raw shale (-325 mesh), heated at 2°C/min in dry air. First test.

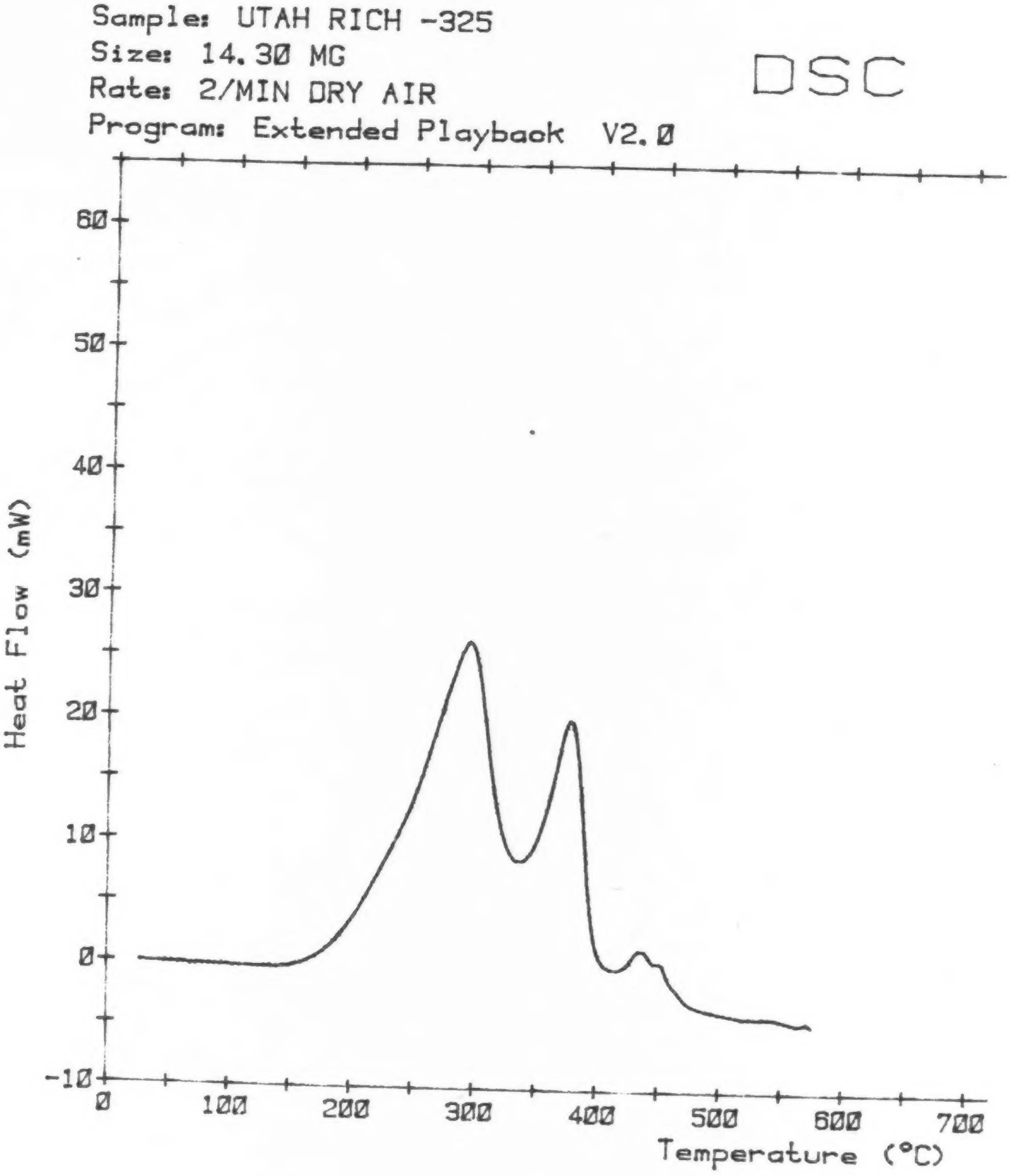

Figure B-16. Thermogram of Utah (66 GPT) raw shale (-325 mesh), heated at 2°C/min in dry air. Second test.

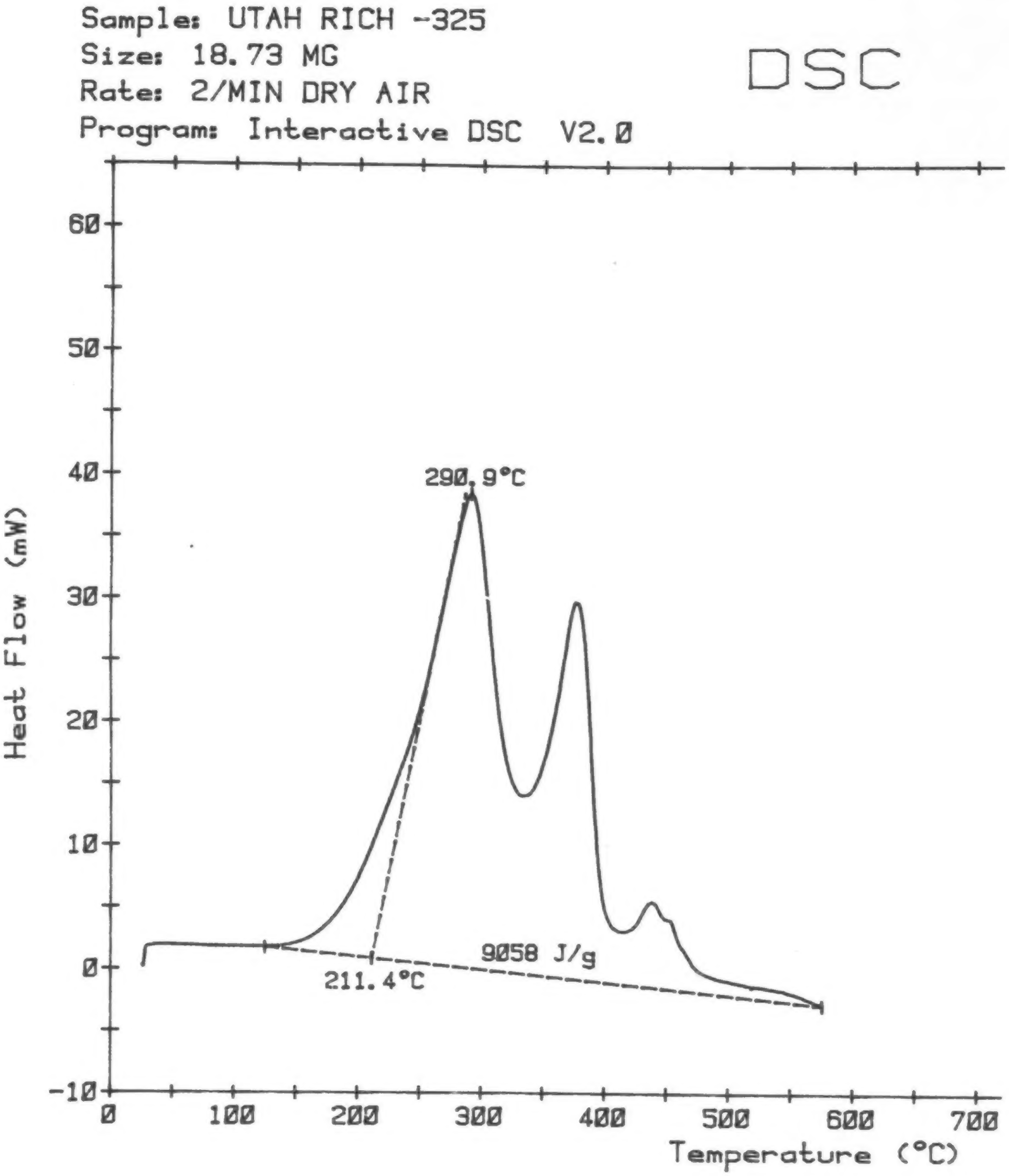

Figure B-17. Thermogram of Utah (66 GPT) raw shale (-325 mesh), heated at 2°C/min in dry air. Third test.

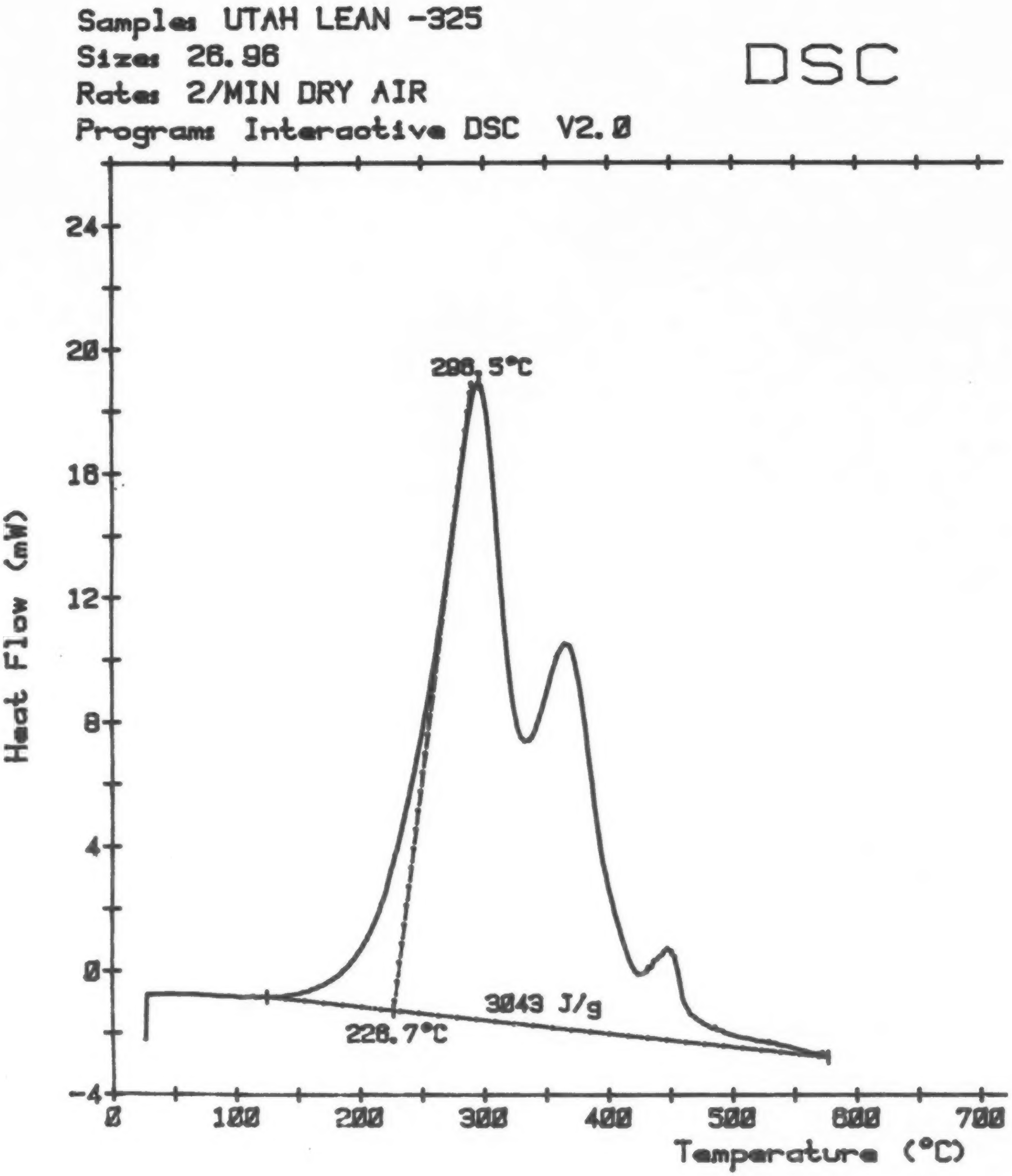

Figure B-18. Thermogram of Utah (28 GPT) raw shale (-325 mesh), heated at 2°C/min in dry air. First test.

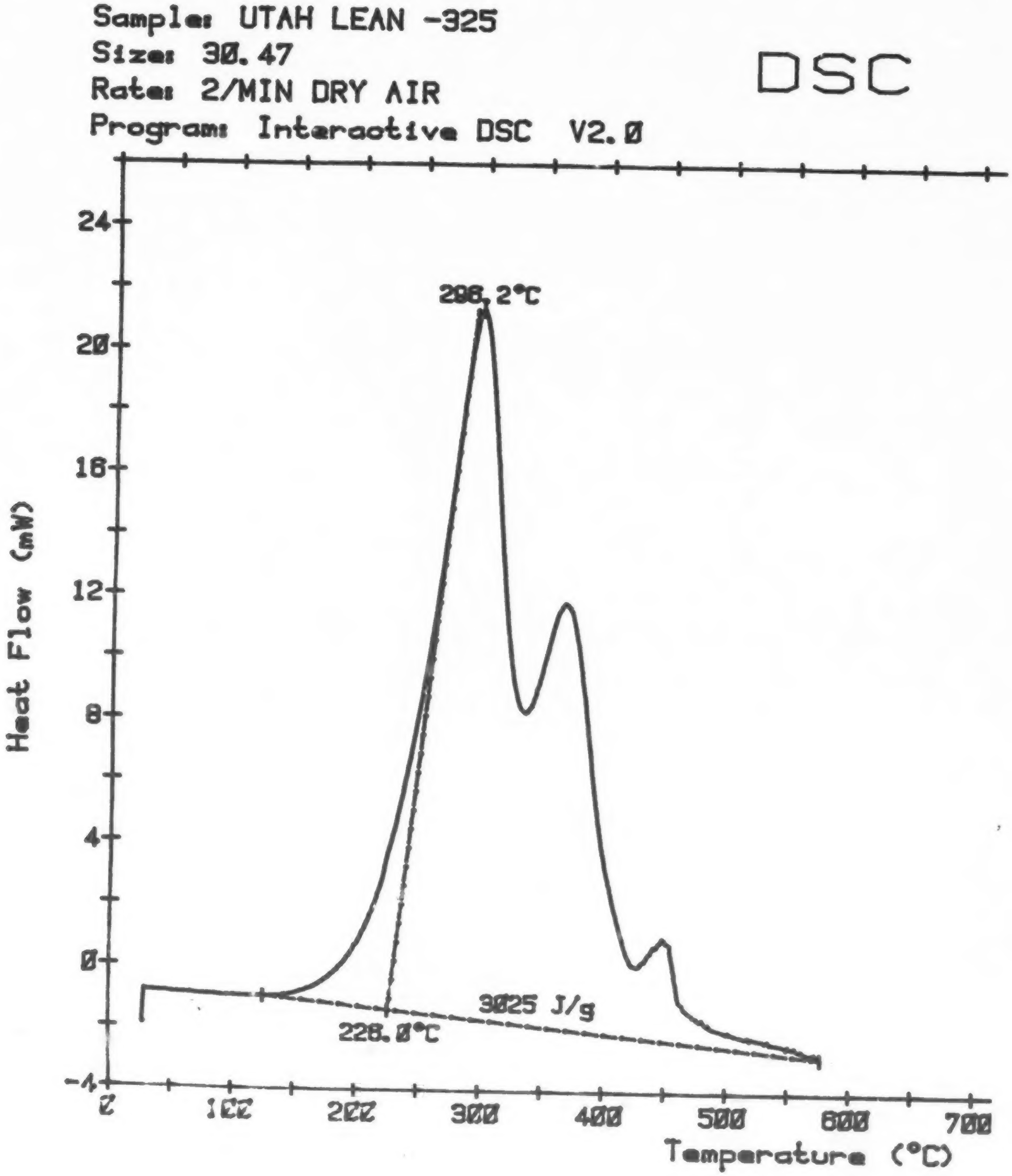

Figure B-19. Thermogram of Utah (28 GPT) raw shale (-325 mesh), heated at 2°C/min in dry air. Second test.

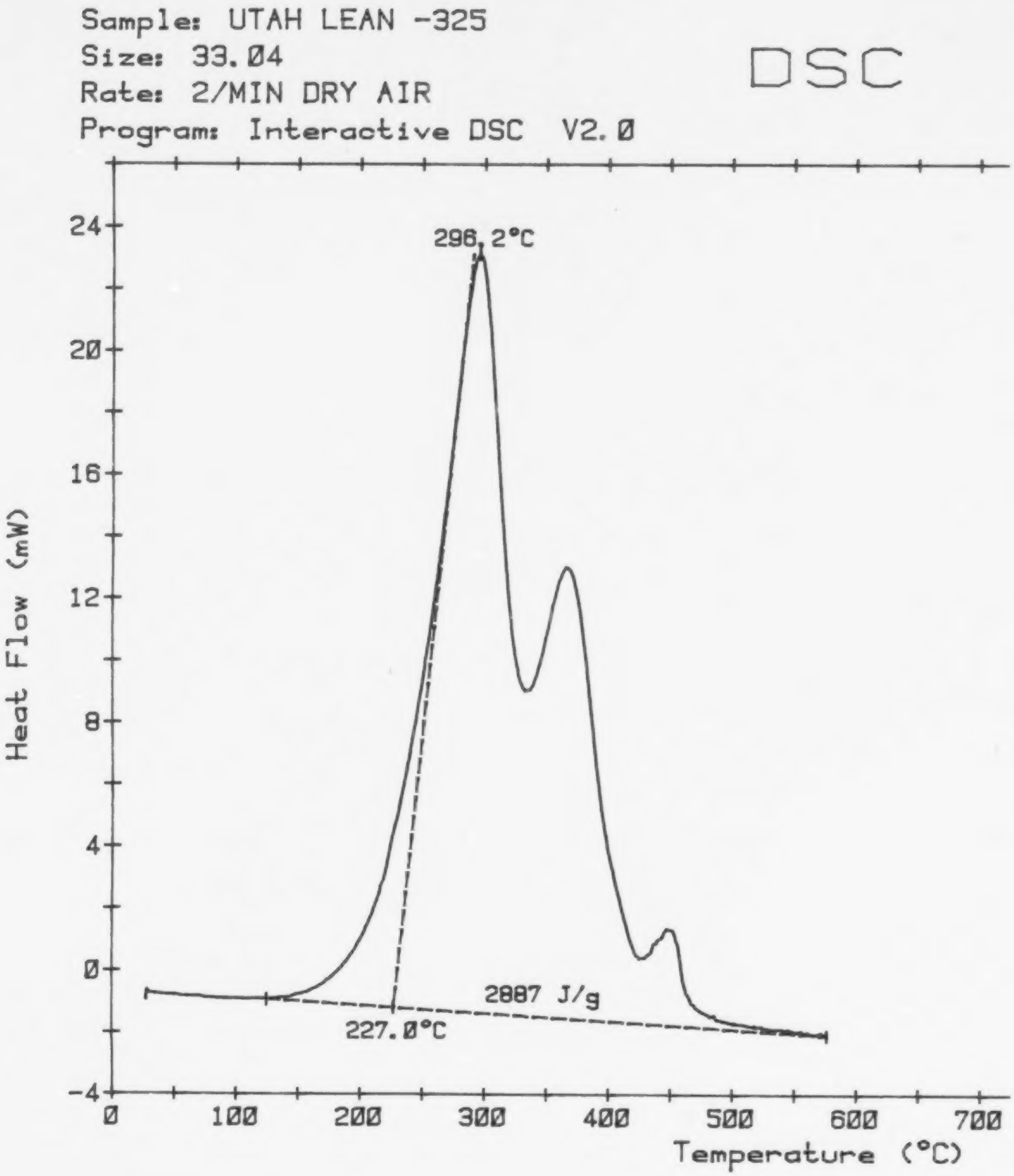

Figure B-20. Thermogram of Utah (28 GPT) raw shale (-325 mesh), heated at 2°C/min in dry air. Third test.

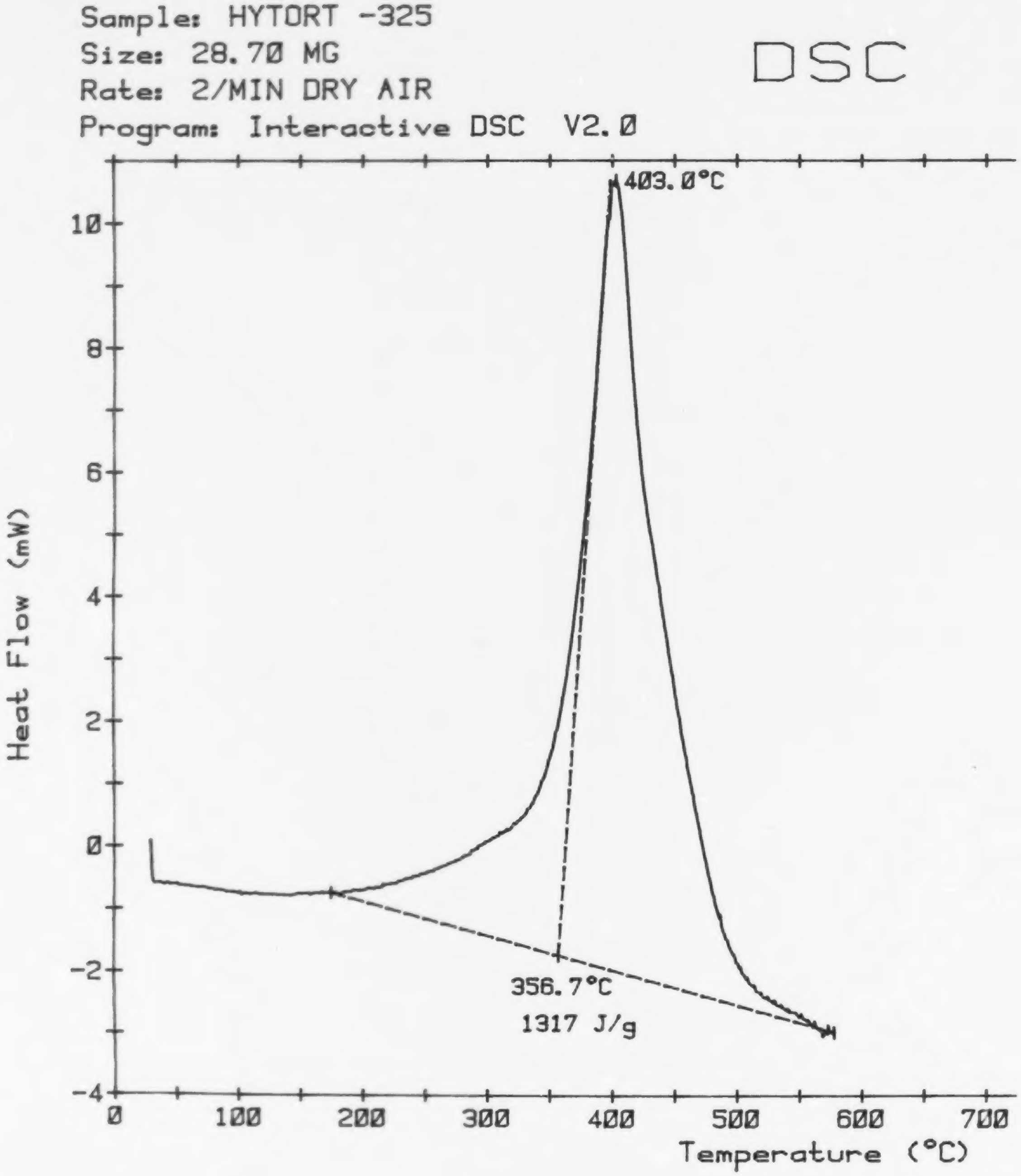

Sample: HYTORT -325
Size: 28.70 MG
Rate: 2/MIN DRY AIR
Program: Interactive DSC V2.0

Figure B-21. Thermogram of Hytort retorted shale (-325 mesh), heated at 2°C/min in dry air. First test.

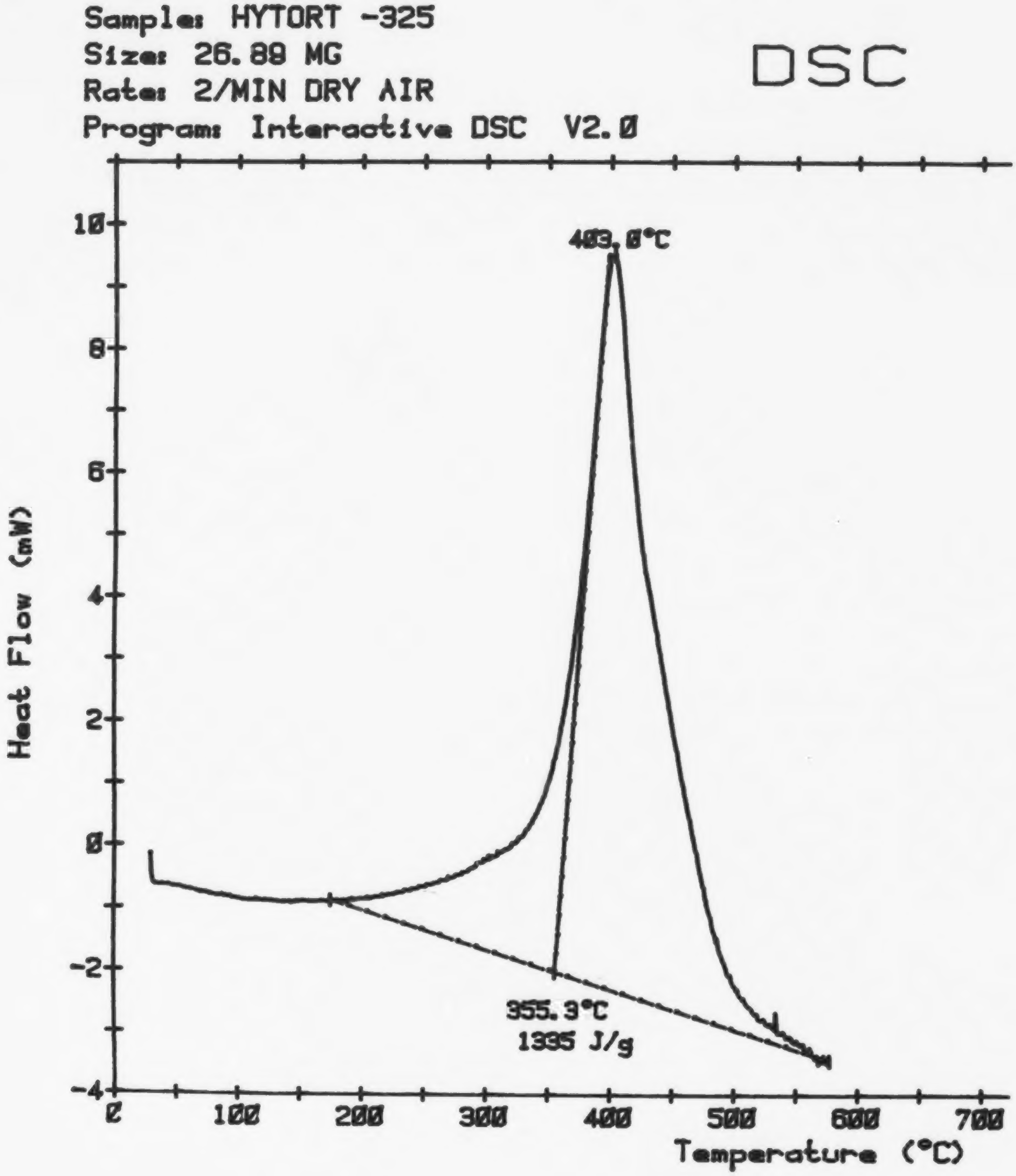

Figure B-22. Thermogram of Hytort retorted shale (-325 mesh), heated at 2°C/min in dry air. Second test.

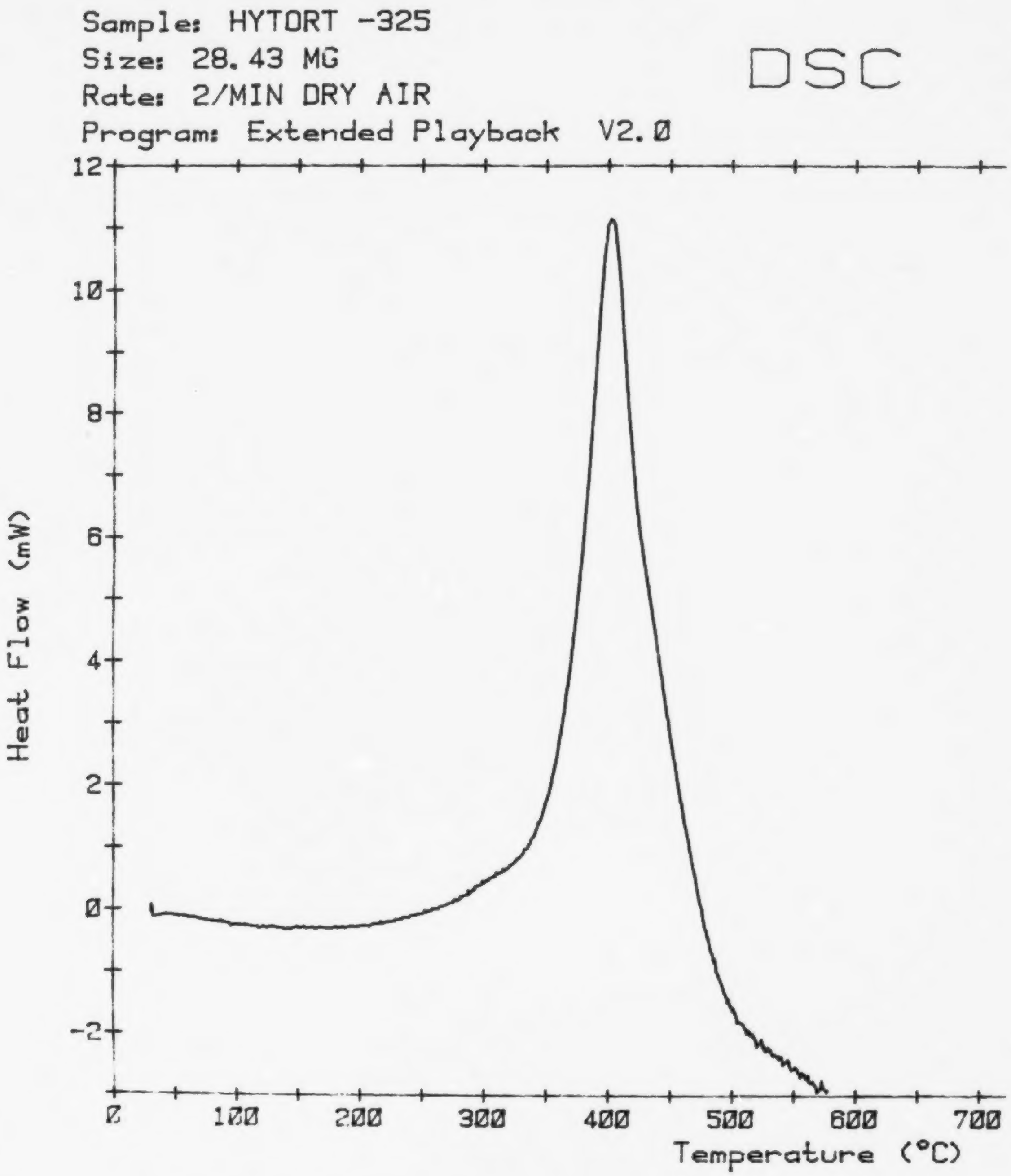

Figure B-23. Thermogram of Hytort retorted shale (-325 mesh), heated at 2°C/min in dry air. Third test.

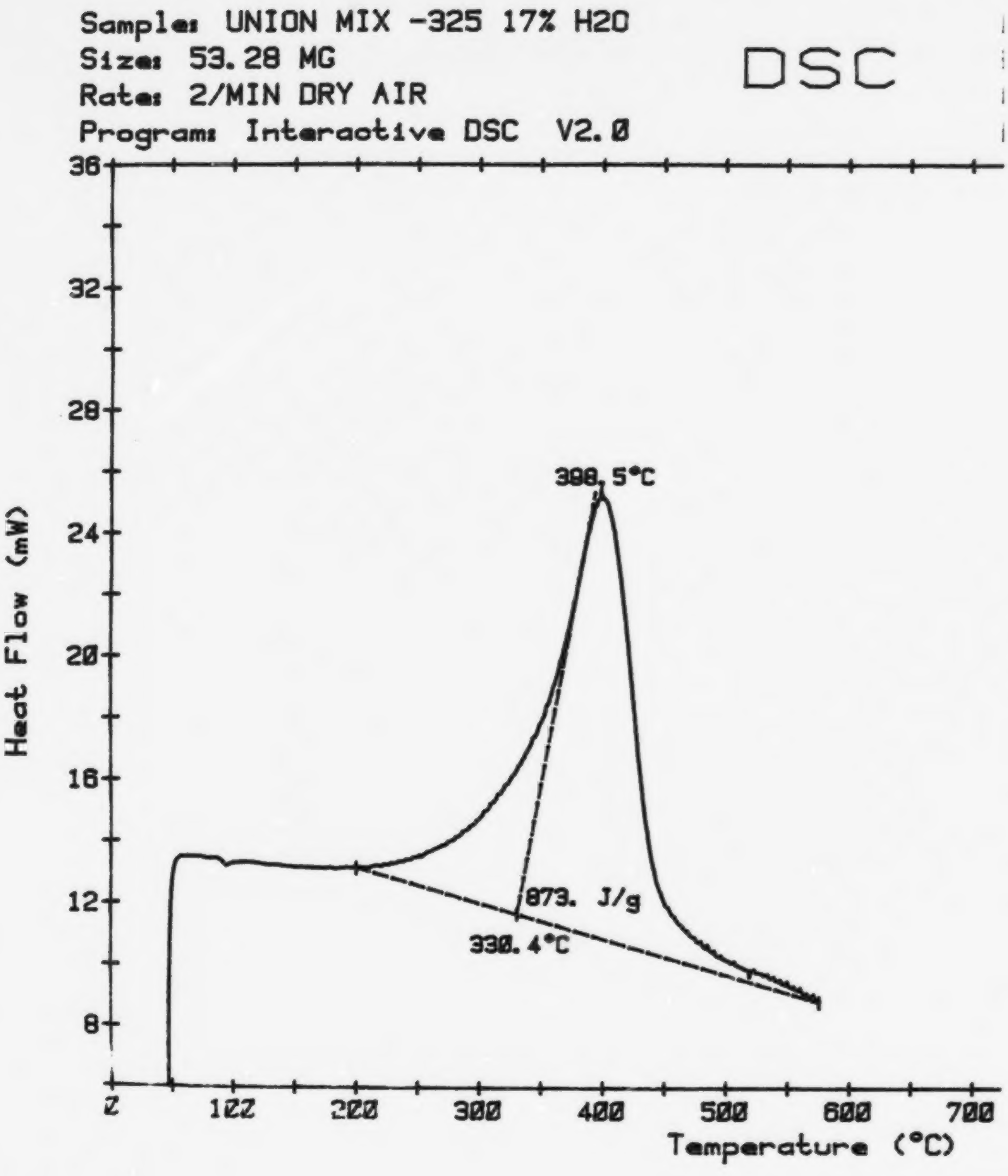

Sample: UNION MIX -325 17% H2O
Size: 53.28 MG
Rate: 2/MIN DRY AIR
Program: Interactive DSC V2.0

Figure B-24. Thermogram of Union shale mixture (-325 mesh), heated at 2°C/min in dry air. First test.

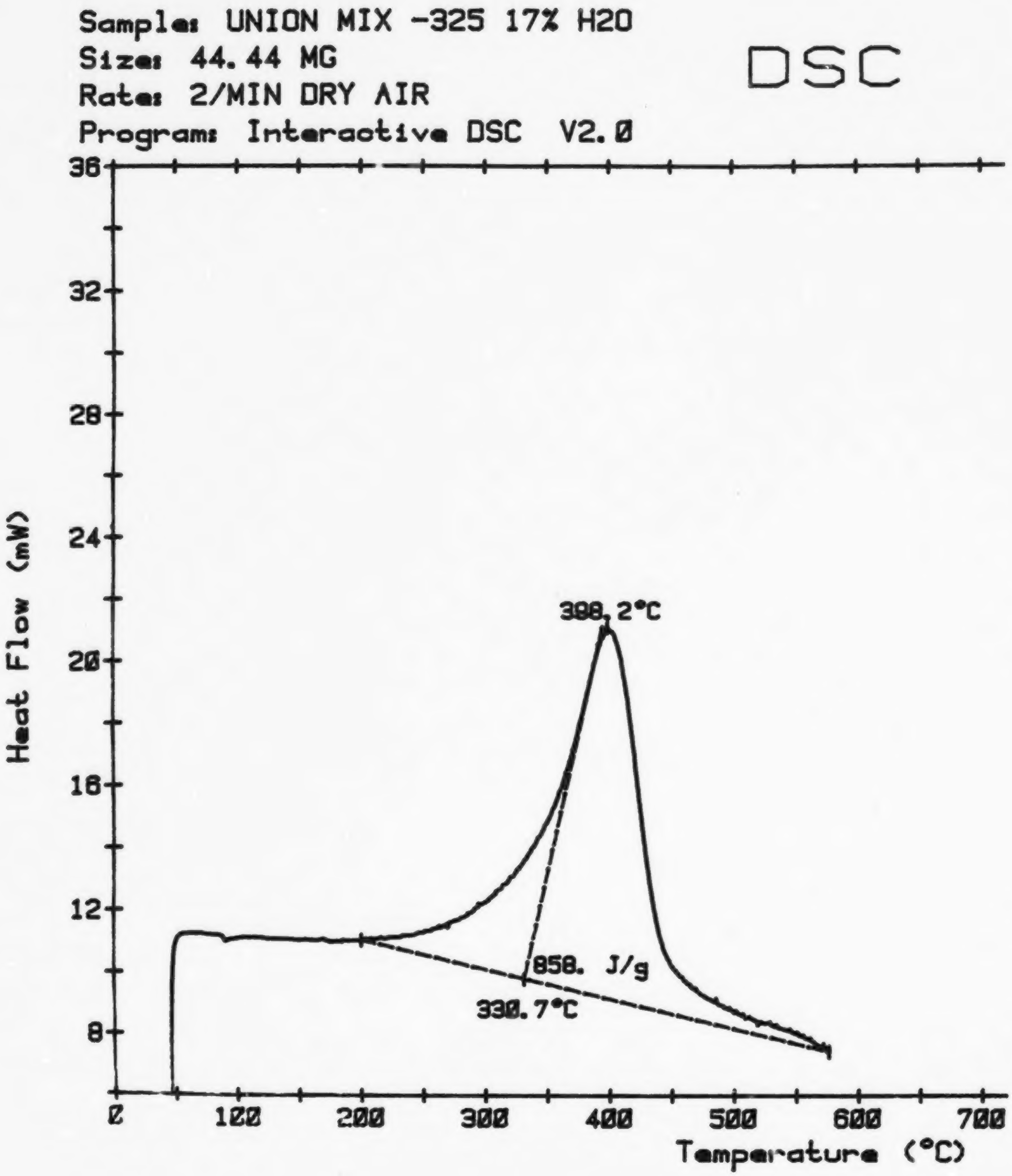

Figure B-25. Thermogram of Union shale mixture (-325 mesh), heated at 2°C/min in dry air. Second test.

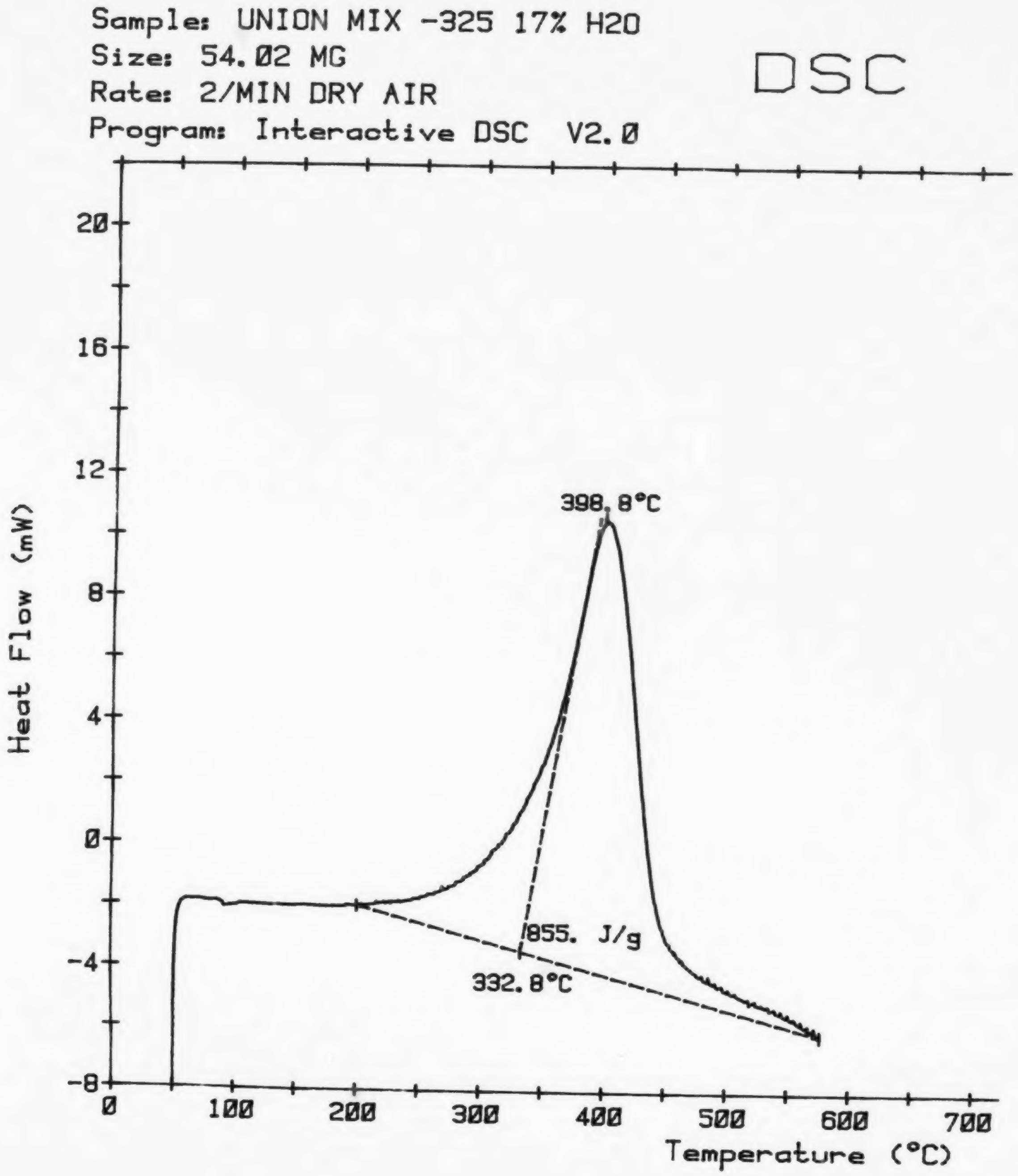

Figure B-26. Thermogram of Union shale mixture (-325 mesh), heated at 2°C/min in dry air. Third test.

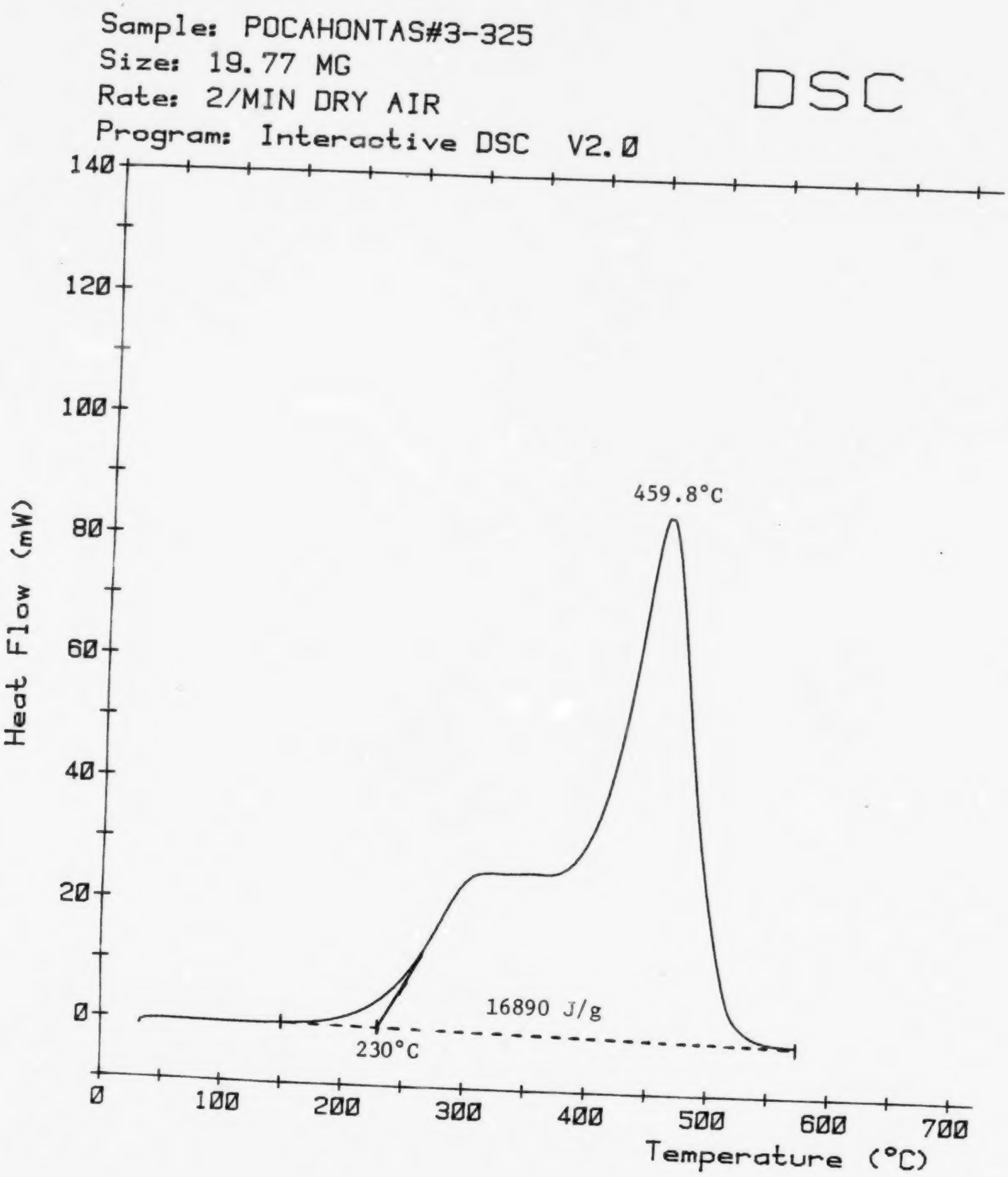

Figure B-27. Thermogram of Pocahontas #3 bituminous coal (-325 mesh), heated at 2°C/min in dry air. First test.

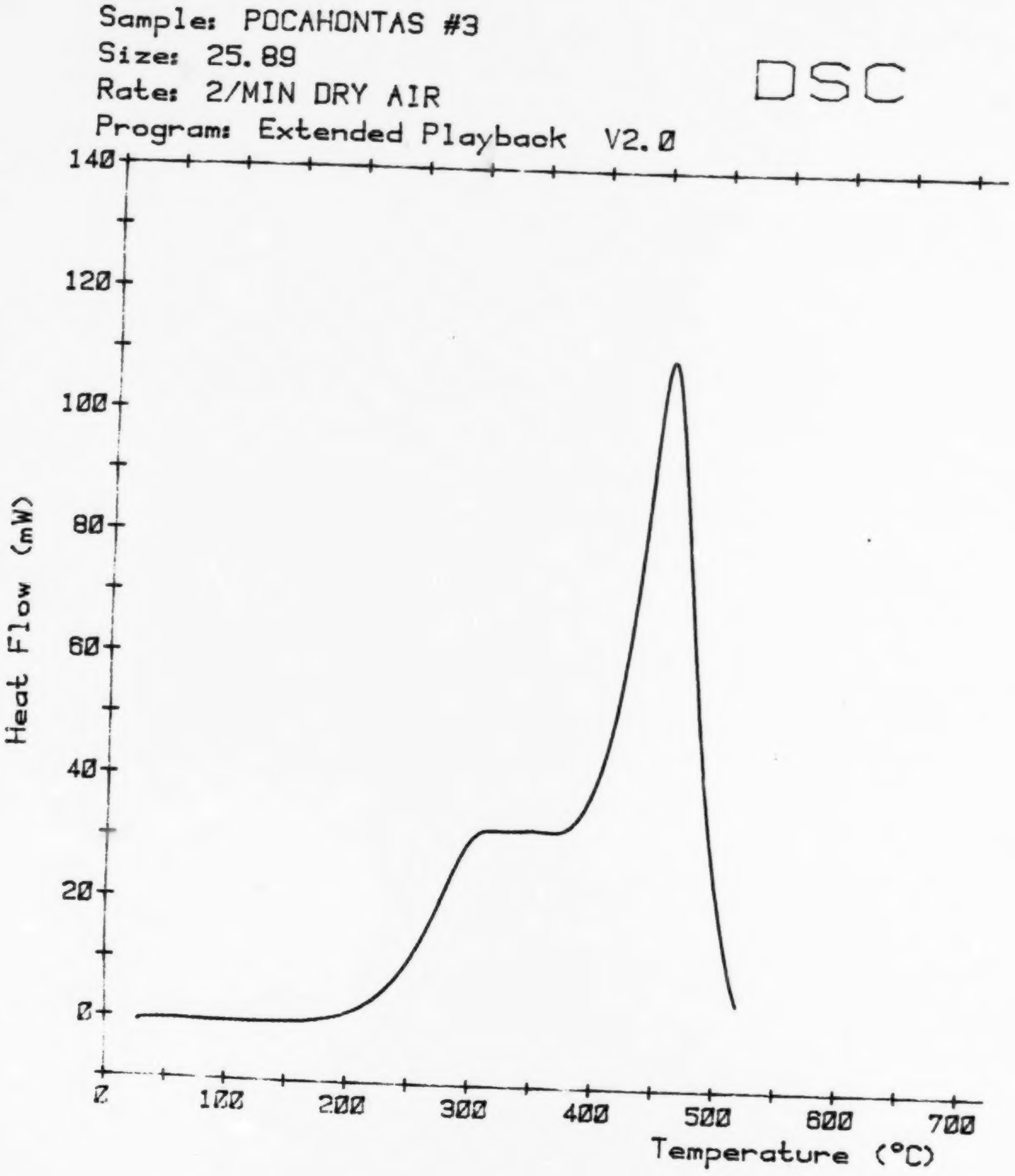

Figure B-28. Thermogram of Pocahontas #3 bituminous coal (-325 mesh), heated at 2°C/min in dry air. Second test.

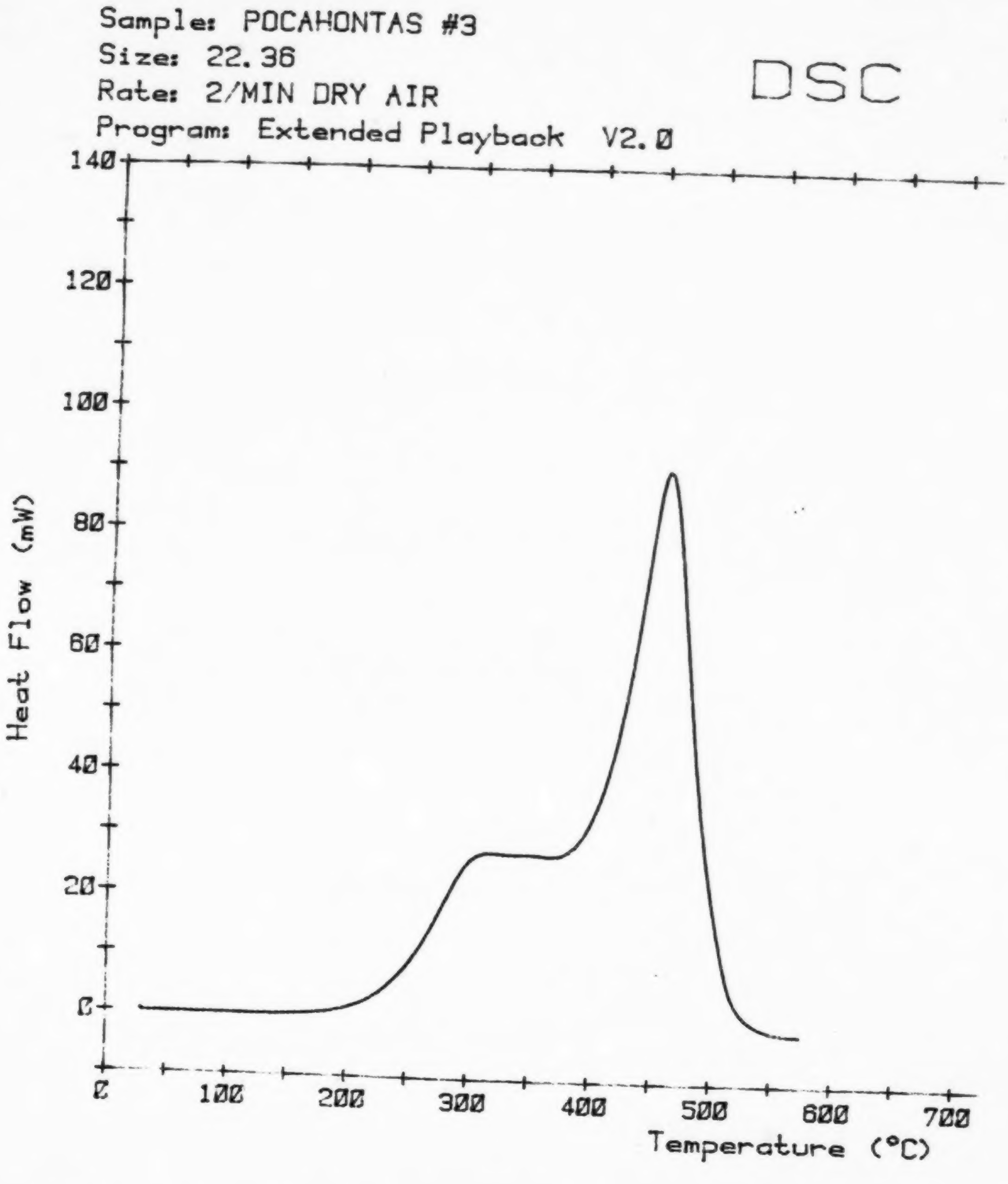

Figure B-29. Thermogram of Pocahontas #3 bituminous coal (-325 mesh), heated at 2°C/min in dry air. Third test.

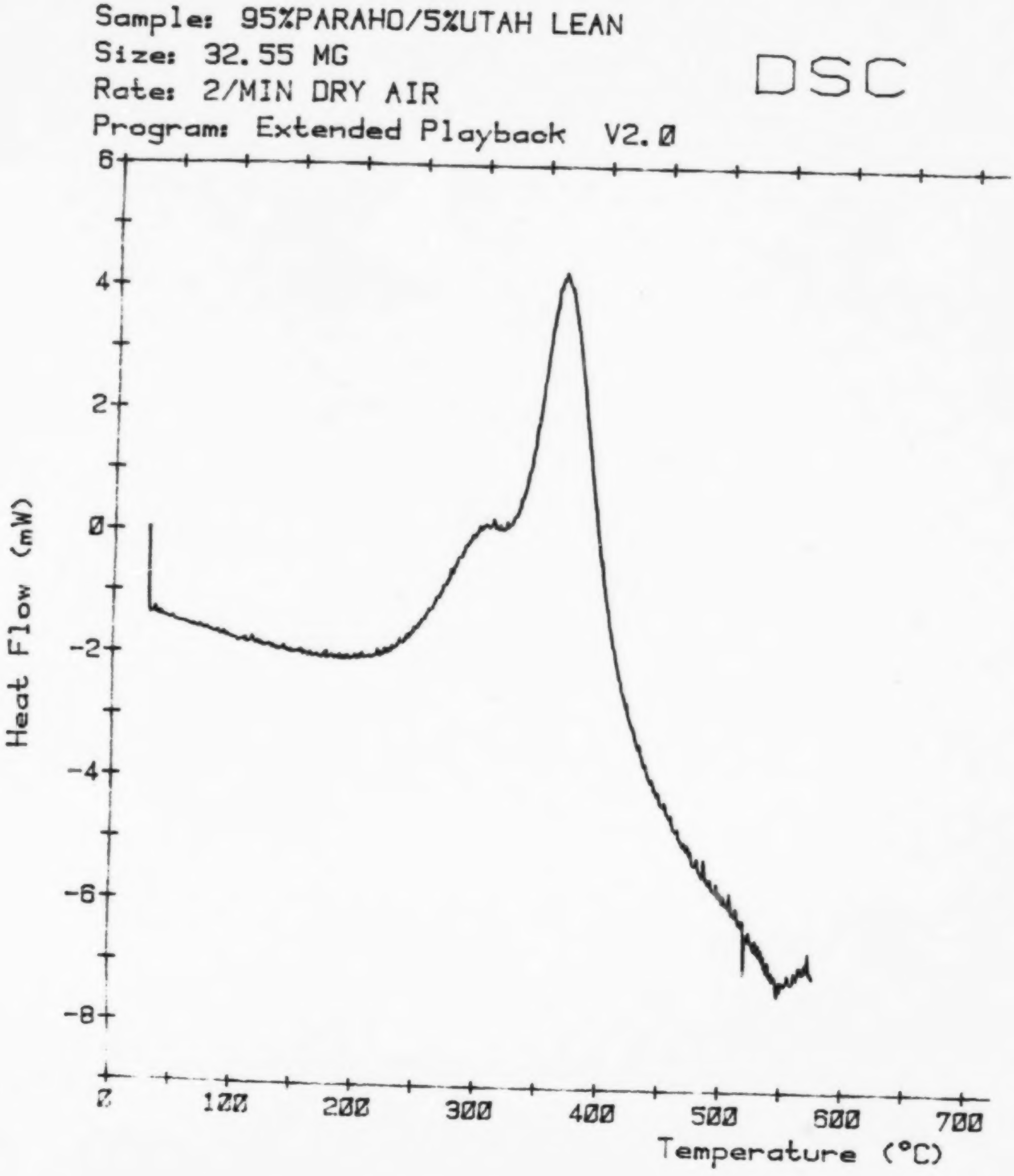

Figure B-30. Thermogram of 95% Paraho retorted shale/5% Utah raw shale (28 GPT) mixture (-325 mesh), heated at 2°C/minute in dry air.

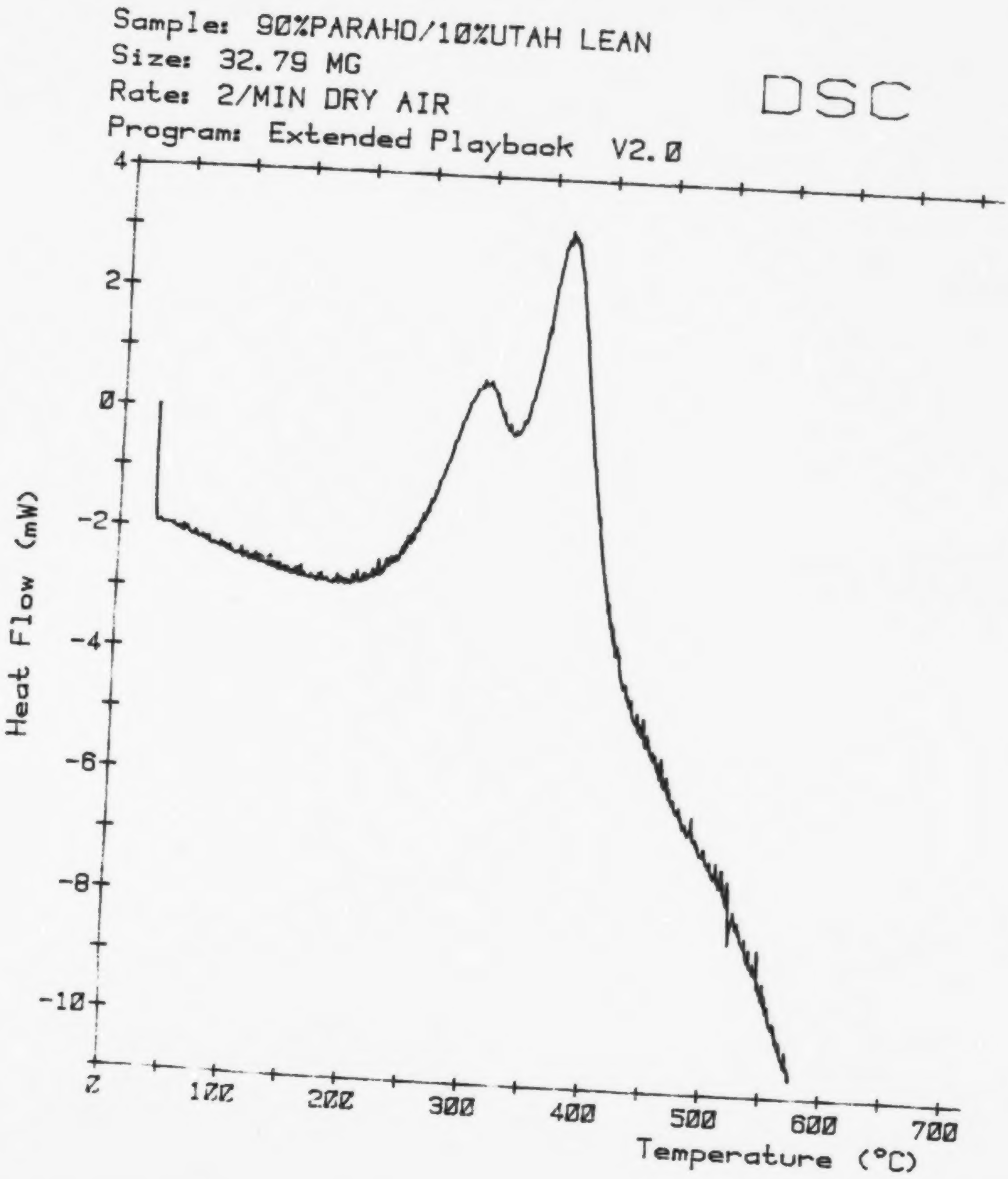

Figure B-31. Thermogram of 90% Paraho retorted shale/10% Utah raw shale (28 GPT) mixture (-325 mesh), heated at 2°C/min in dry air.

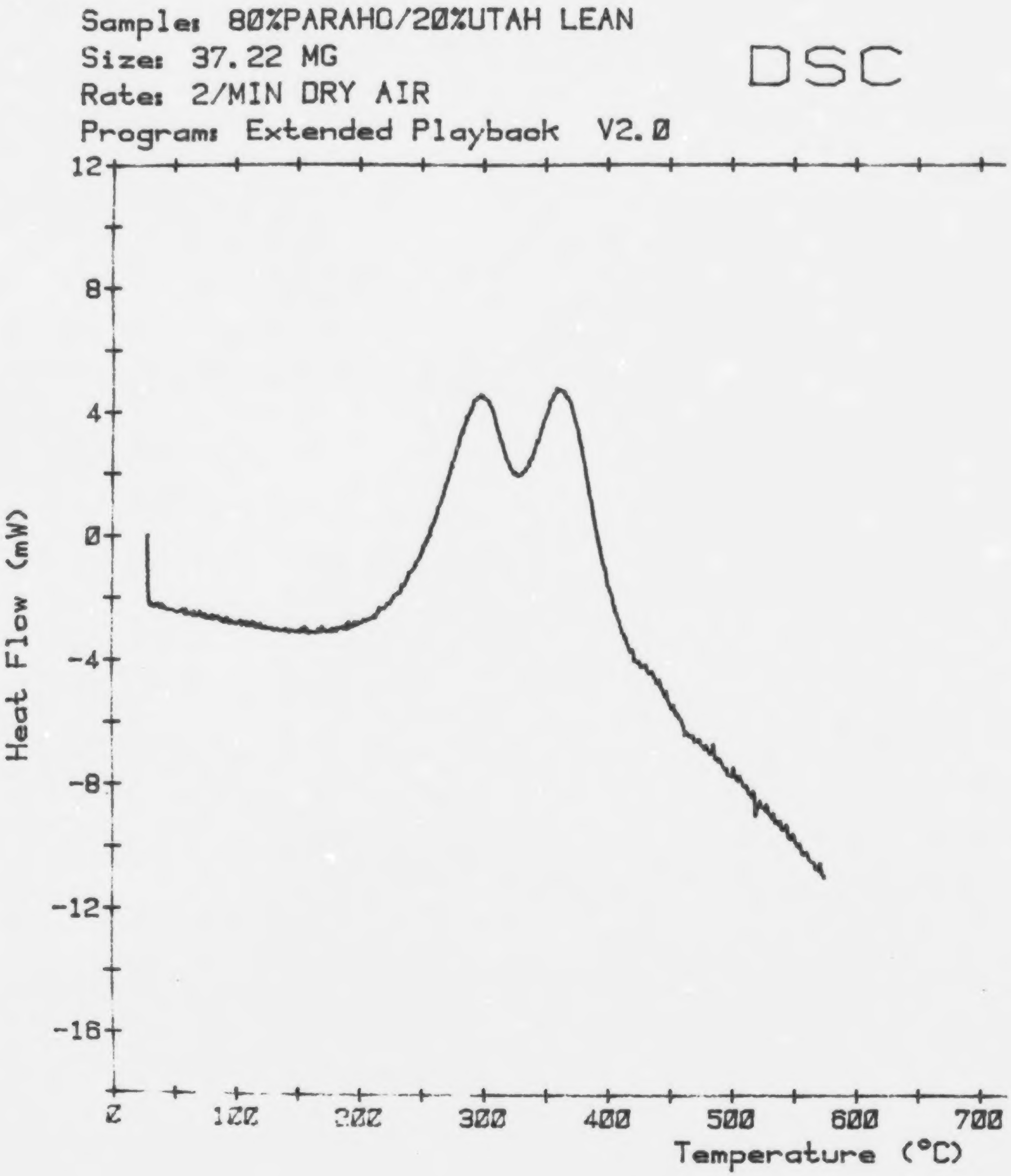

Figure B-32. Thermogram of 80% Paraho retorted shale/20% Utah raw shale (28 GPT) mixture (-325 mesh), heated at 2°C/min in dry air.

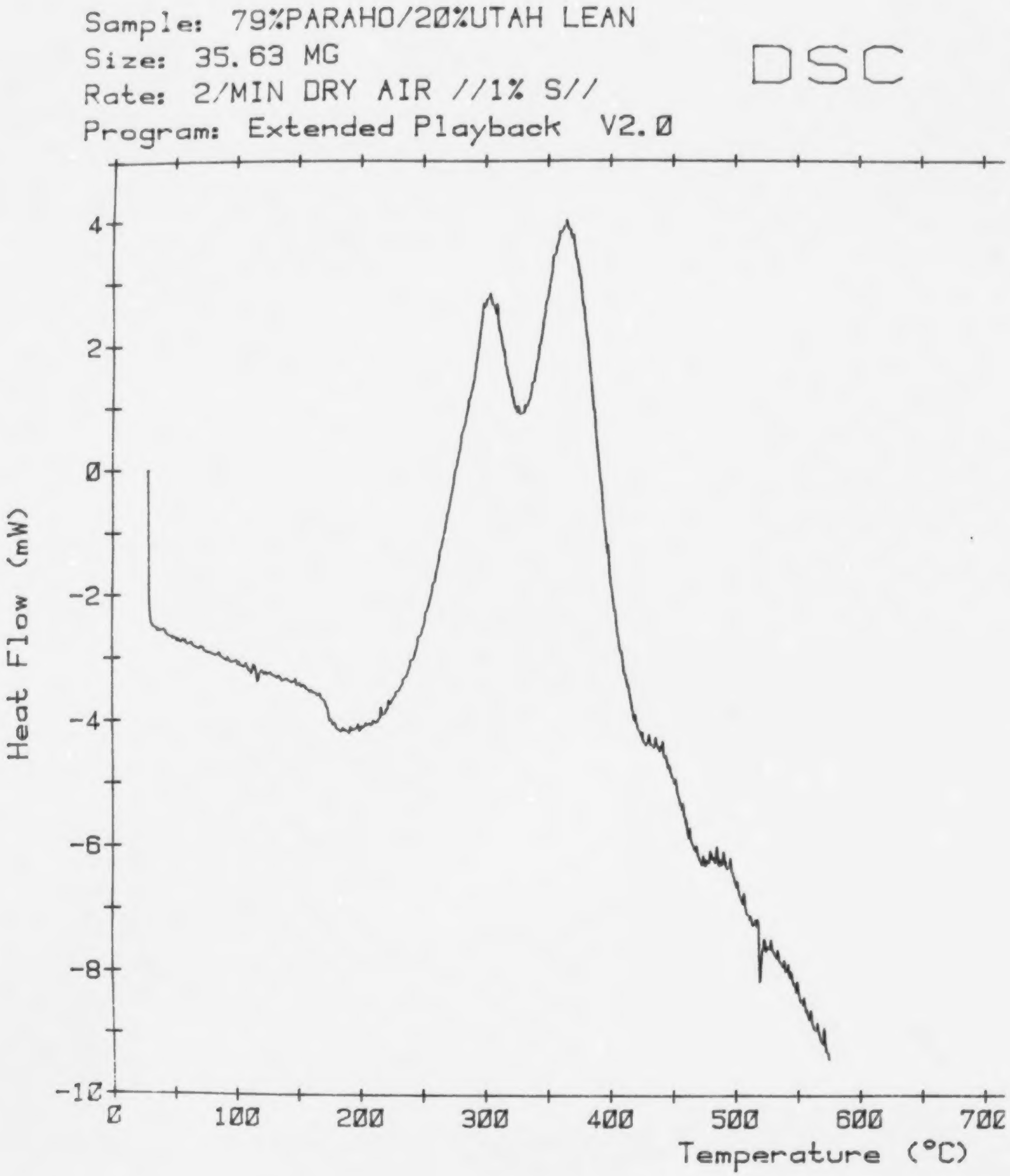

Figure B-33. Thermogram of 79% Paraho retorted shale/20% Utah raw shale (28 GPT)/1% sulfur mixture (-325 mesh), heated at 2°C/min in dry air.

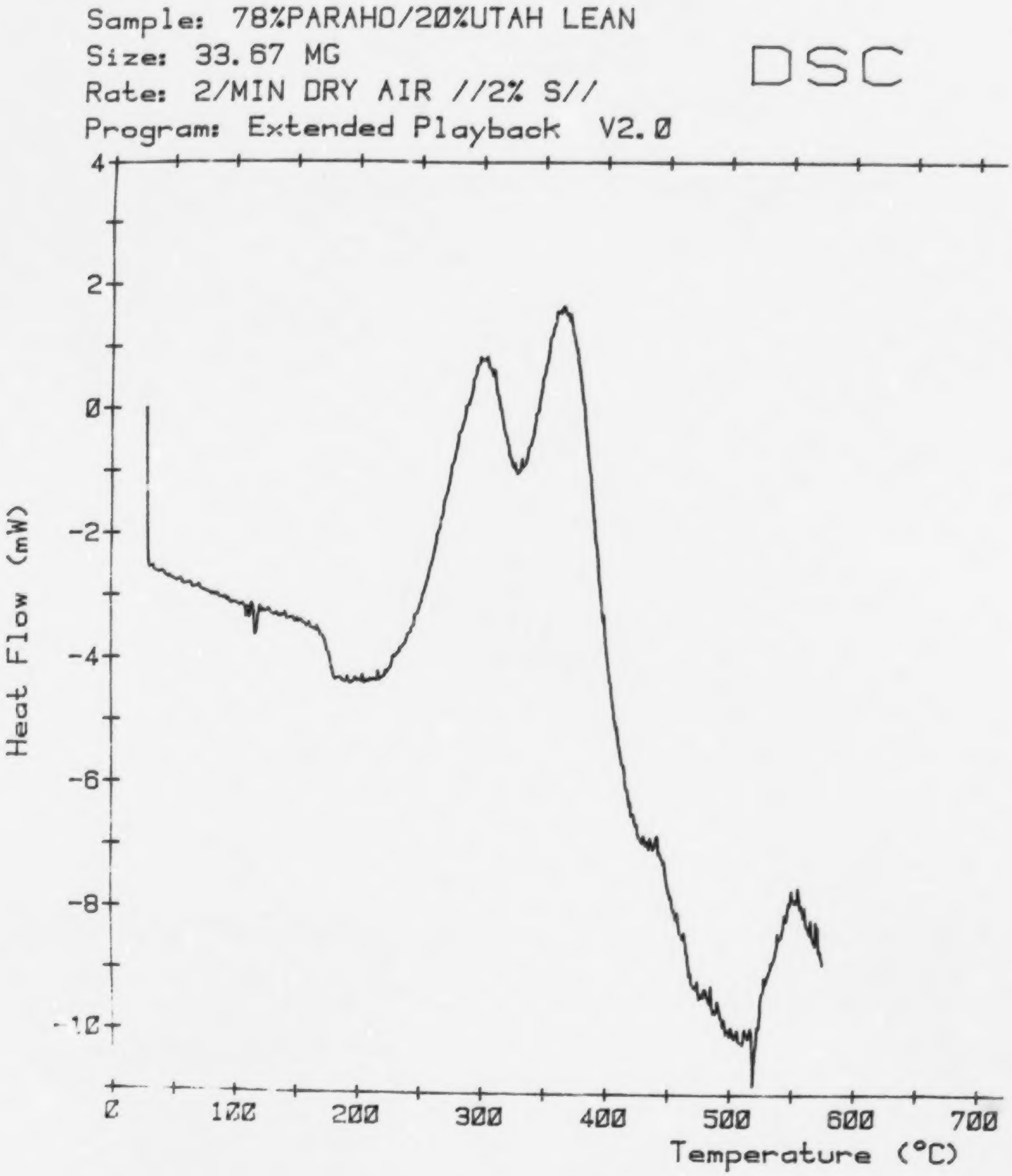

Figure B-34. Thermogram of 78% Paraho retorted shale/20% Utah raw shale (28 GPT)/12% sulfur mixture (-325 mesh), heated at 2°C/min in dry air.

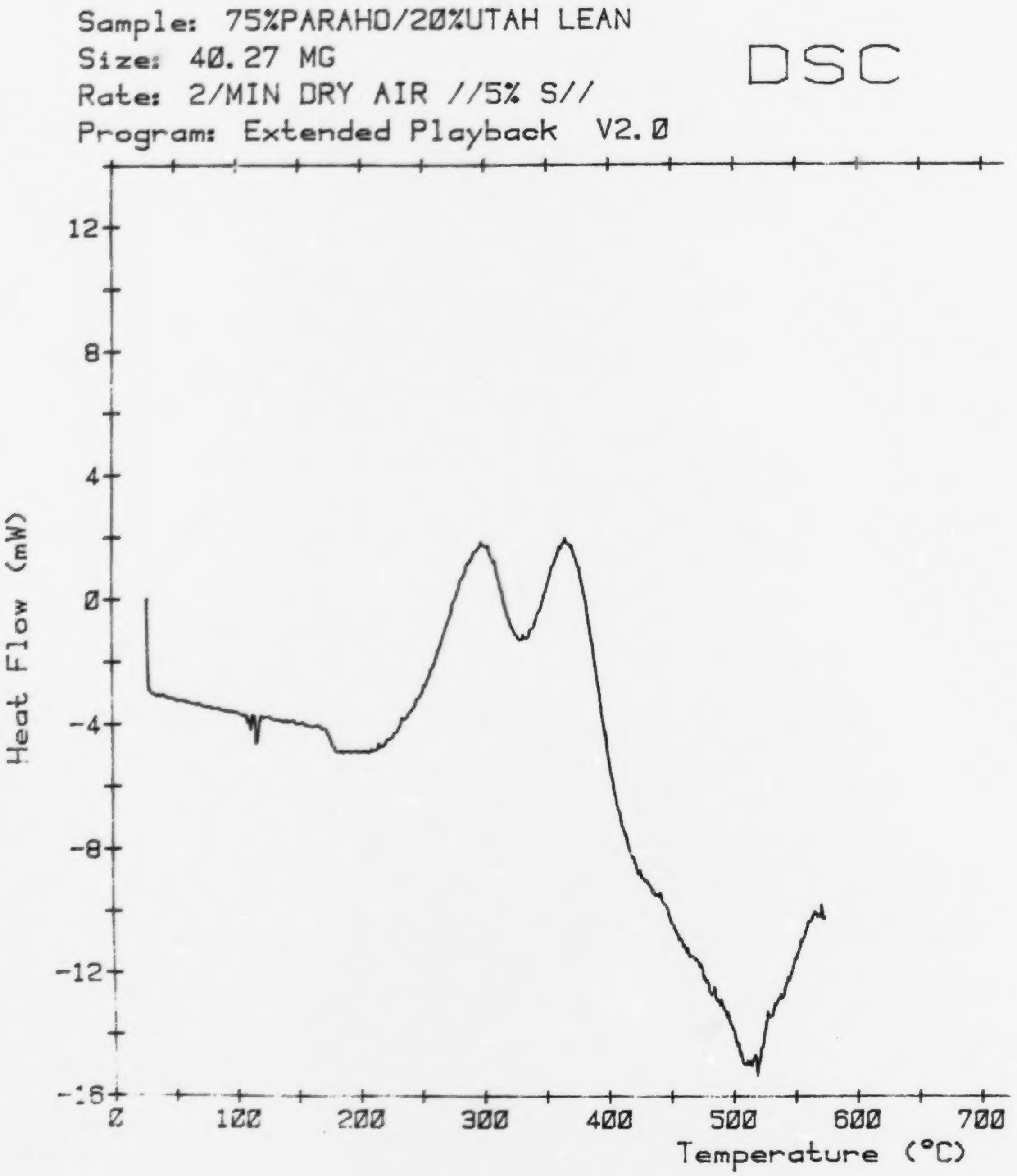

Figure B-35. Thermogram of 75% Paraho retorted shale/20% Utah raw shale (28 GPT)/15% sulfur mixture (-325 mesh), heated at 2°C/min in dry air.

TABLE B-1. COMPOSITION OF EXIT GAS FROM NONADIABATIC TEST CELL AT 125°C. MEAN VALUES FROM TRIPLICATE TESTS (VOLUME % DRY BASIS). FIRST SAMPLE SET.

Sample Type	O_2	CO_2	CO	CH_4
Wyoming Sub-bituminous Coal (-48 + 100)	17.45	2.83	0.26	0.000
Wyoming Sub-bituminous Coal (-325)	11.56	1.96	0.86	0.000
West Kentucky #9 Bituminous Coal (-48 +100)	16.15	0.55	0.95	0.000
West Kentucky #9 Bituminous Coal (-325)	18.03	0.35	0.06	0.000
C-a Raw Shale (-48 +100)	20.55	0.10	0.00	0.000
C-a Raw Shale (-325)	19.88	0.10	0.00	0.000
Paraho Retorted Shale (-48 +100)	20.32	0.05	0.00	0.000
Paraho Retorted Shale (-325)	20.90	0.07	0.00	0.000
Tosco II Retorted Shale (-48 +100)	19.90	0.11	0.00	0.000
Tosco II Retorted Shale (-325)	20.43	0.19	0.00	0.000
Lurgi Retorted Shale (-200 +325)	20.68	0.03	0.00	0.000
Lurgi Retorted Shale (-325)	20.62	0.02	0.00	0.000

Source: Denver Research Institute.

TABLE B-2. COMPOSITION OF EXIT GAS FROM NONADIABATIC TEST CELL AT 125°C MEAN VALUES FROM TRIPLICATE TESTS (VOLUME % DRY BASIS). SECOND SAMPLE SET, -325 mesh.

Sample Type	O_2	CO_2	CO	CH_4
Pocahontas #3 Bituminous Coal	17.6	0.6	0.05	0.02
Hytort Retorted Shale	20.1	0.27	<.01	<.01
Utah Raw Shale (28GPT)	19.5	0.28	0.05	<.01
Utah Raw Shale (66GPT)	13.6	1.16	0.15	<.01
Union Shale Mixture Dry	20.6	0.59	<.01	<.01

TABLE B-3. COMPOSITION OF EXIT GAS FROM NONADIABATIC TEST CELL AT 150°C. MEAN VALUES FROM TRIPLICATE TESTS (VOLUME % DRY BASIS). FIRST SAMPLE SET.

Sample Type	O_2	CO_2	CO	CH_4
Wyoming Sub-bituminous Coal (-48 + 100)	3.40	5.63	0.61	0.000
Wyoming Sub-bituminous Coal (-325)	3.58	6.44	0.83	0.000
West Kentucky #9 Bituminous Coal (-48 +100)	8.66	1.68	0.32	0.000
West Kentucky #9 Bituminous Coal (-325)	8.41	1.51	0.59	0.000
C-a Raw Shale (-48 +100)	18.40	0.33	0.03	0.000
C-a Raw Shale (-325)	18.50	0.27	0.08	0.000
Paraho Retorted Shale (-48 +100)	20.16	0.07	0.00	0.000
Paraho Retorted Shale (-325)	20.53	0.08	0.00	0.000
Tosco II Retorted Shale (-48 +100)	19.56	0.33	0.00	0.000
Tosco II Retorted Shale (-325)	19.72	0.27	0.00	0.000
Lurgi Retorted Shale (-200 +325)	20.86	0.03	0.00	0.000
Lurgi Retorted Shale (-325)	21.04	0.02	0.00	0.000

Source: Denver Research Institute.

TABLE B-4. COMPOSITION OF EXIT GAS FROM NONADIABATIC TEST CELL AT 150°C MEAN VALUES FROM TRIPLICATE TESTS (VOLUME % DRY BASIS). SECOND SAMPLE SET, -325 mesh.

Sample Type	O_2	CO_2	CO	CH_4
Pocahontas #3 Bituminous Coal	9.8	1.6	0.45	0.01
Hytort Retorted Shale	17.9	0.70	0.07	<.01
Utah Raw Shale (28GPT)	12.5	1.38	0.32	<.01
Utah Raw Shale (66GPT)	1.3	4.7	0.61	<.01
Union Shale Mixture (Dry)	18.0	1.20	0.07	<.01

TABLE B-5. COMPOSITION OF EXIT GAS FROM NONADIABATIC TEST CELL AT 175°C. MEAN VALUES FROM TRIPLICATE TESTS (VOLUME %, DRY BASIS). FIRST SAMPLE SET.

Sample Type	O_2	CO_2	CO	CH_4
Wyoming Sub-bituminous Coal (-48 + 100)	0.12	9.37	1.59	0.021
Wyoming Sub-bituminous Coal (-325)	0.03	11.92	1.91	0.036
West Kentucky #9 Bituminous Coal (-48 +100)	0.65	3.38	1.08	0.017
West Kentucky #9 Bituminous Coal (-325)	0.13	4.56	1.56	0.039
C-a Raw Shale (-48 +100)	14.45	1.76	0.32	0.003
C-a Raw Shale (-325)	14.91	1.50	0.25	0.001
Paraho Retorted Shale (-48 +100)	19.96	0.28	0.00	0.000
Paraho Retorted Shale (-325)	20.22	0.50	0.02	0.000
Tosco II Retorted Shale (-48 +100)	18.21	1.90	0.15	0.000
Tosco II Retorted Shale (-325)	18.98	1.06	0.10	0.000
Lurgi Retorted Shale (-200 +325)	20.85	0.04	0.00	0.000
Lurgi Retorted Shale (-325)	21.00	0.02	0.00	0.000

Source: Denver Research Institute.

TABLE B-6. COMPOSITION OF EXIT GAS FROM NONADIABATIC TEST CELL AT 175°C MEAN VALUES FROM TRIPLICATE TESTS (VOLUME % DRY BASIS). SECOND SAMPLE SET, -325 mesh.

Sample Type	O_2	CO_2	CO	CH_4
Pocahontas #3 Bituminous Coal	0.0	3.8	0.08	0.03
Hytort Retorted Shale	15.7	1.38	0.16	<.01
Utah Raw Shale (28GPT)	2.8	4.3	1.1	<.01
Utah Raw Shale (66GPT)	0.2	6.6	1.1	.02
Union Shale Mixture (Dry)	14.6	1.1	0.23	<.01

TABLE B-7. COMPOSITION OF EXIT GAS FROM NONADIABATIC TEST CELL AT 200°C. MEAN VALUES FROM TRIPLICATE TESTS (VOLUME %, DRY BASIS). FIRST SAMPLE SET.

Sample Type	O_2	CO_2	CO	CH_4
Wyoming Sub-bituminous Coal (-48 + 100)	0.02	12.64	2.64	0.035
Wyoming Sub-bituminous Coal (-325)	0.01	14.83	2.71	0.081
West Kentucky #9 Bituminous Coal (-48 +100)	0.01	4.35	1.37	0.027
West Kentucky #9 Bituminous Coal (-325)	0.01	4.09	1.38	0.035
C-a Raw Shale (-48 +100)	7.84	2.95	0.99	0.032
C-a Raw Shale (-325)	8.42	2.13	0.83	0.014
Paraho Retorted Shale (-48 +100)	19.40	0.31	0.01	0.000
Paraho Retorted Shale (-325)	19.56	0.45	0.07	0.000
Tosco II Retorted Shale (-48 +100)	16.48	1.46	0.22	0.000
Tosco II Retorted Shale (-325)	16.31	1.58	0.54	0.000
Lurgi Retorted Shale (-200 +325)	20.63	0.04	0.00	0.000
Lurgi Retorted Shale (-325)	20.42	0.03	0.00	0.000

Source: Denver Research Institute.

TABLE B-8. COMPOSITION OF EXIT GAS FROM NONADIABATIC TEST CELL AT 250°C. MEAN VALUES FROM TRIPLICATE TESTS (VOLUME %, DRY BASIS). FIRST SAMPLE SET.

Sample Type	O_2	CO_2	CO	CH_4
Wyoming Sub-bituminous Coal (-48 + 100)	0.01	16.56	3.43	0.045
Wyoming Sub-bituminous Coal (-325)	0.02	13.75	3.04	0.068
West Kentucky #9 Bituminous Coal (-48 +100)	0.01	7.87	2.36	0.031
West Kentucky #9 Bituminous Coal (-325)	0.01	8.52	2.55	0.028
C-a Raw Shale (-48 +100)	0.05	7.98	2.23	0.065
C-a Raw Shale (-325)	0.02	8.64	2.34	0.052
Paraho Retorted Shale (-48 +100)	18.82	1.08	0.14	0.000
Paraho Retorted Shale (-325)	16.95	1.99	0.21	0.000
Tosco II Retorted Shale (-48 +100)	9.51	6.99	0.86	0.000
Tosco II Retorted Shale (-325)	7.62	7.57	1.02	0.000
Lurgi Retorted Shale (-200 +325)	20.53	0.09	0.00	0.000
Lurgi Retorted Shale (-325)	20.66	0.14	0.00	0.000

Source: Denver Research Institute.

TABLE B-9. COMPOSITION OF EXIT GAS FROM NONADIABATIC TEST CELL AT 300°C. MEAN VALUES FROM TRIPLICATE TESTS (VOLUME %, DRY BASIS). FIRST SAMPLE SET.

Sample Type	O_2	CO_2	CO	CH_4
Wyoming Sub-bituminous Coal (-48 + 100)	0.01	20.13	3.55	0.196
Wyoming Sub-bituminous Coal (-325)	0.01	19.40	3.82	0.131
West Kentucky #9 Bituminous Coal (-48 +100)	0.01	12.22	2.95	0.108
West Kentucky #9 Bituminous Coal (-325)	0.01	14.59	3.32	0.059
C-a Raw Shale (-48 +100)	0.01	12.42	3.01	0.726
C-a Raw Shale (-325)	0.01	15.24	2.95	0.513
Paraho Retorted Shale (-48 +100)	15.03	4.99	0.64	0.000
Paraho Retorted Shale (-325)	8.32	7.61	1.08	0.000
Tosco II Retorted Shale (-48 +100)	1.79	16.45	1.60	0.000
Tosco II Retorted Shale (-325)	0.22	17.68	1.72	0.000
Lurgi Retorted Shale (-200 +325)	20.48	0.16	0.00	0.000
Lurgi Retorted Shale (-325)	20.41	0.29	0.00	0.000

Source: Denver Research Institute.

TABLE B-10. MEAN OXYGEN CONCENTRATIONS IN EFFLUENT GAS AT VARIOUS TEMPERATURES (VOLUME %, DRY BASIS) NONADIABATIC TEST OF FIRST SAMPLE SET.

Sample Type	Temperature (°C) 125	150	175	200	250	300
Wyoming Sub-bituminous Coal (-48 +100)	17.45	3.40	0.12	0.02	0.01	0.01
Wyoming Sub-bituminous Coal (-325)	11.56	3.58	0.03	0.01	0.02	0.01
West Kentucky #9 Bituminous Coal (-48 +100)	16.15	8.66	0.65	0.01	0.01	0.01
West Kentucky #9 Bituminous Coal (-325)	18.03	8.41	0.13	0.01	0.01	0.01
C-a Raw Shale (-48 +100)	0.55	18.40	14.45	7.84	0.05	0.01
C-a Raw Shale (-325)	19.88	18.50	14.91	8.42	0.02	0.01
Paraho Retorted Shale (-48 +100)	20.32	20.16	19.96	19.40	18.82	15.03
Paraho Retorted Shale (-325)	20.90	20.53	20.22	19.56	16.95	8.32
Tosco II Retorted Shale (-48 +100)	19.90	19.56	18.21	16.48	9.51	1.79
Tosco II Retorted Shale (-325)	20.43	19.72	18.98	16.31	7.62	0.22
Lurgi Retorted Shale (-200 +325)	20.68	20.86	20.85	20.63	20.53	20.48
Lurgi Retorted Shale (-325)	20.62	21.04	21.00	20.42	20.66	20.41

Source: Denver Research Institute.

TABLE B-11. MEAN OXYGEN CONCENTRATIONS IN EFFLUENT GAS FROM NONADIABATIC TEST OF SECOND SAMPLE SET (VOLUME %, DRY BASIS, -325 mesh)

Sample type	Temperature (°C)		
	125	150	175
Pocahontas #3 Bituminous Coal	17.6	9.8	0.0
Hytort Retorted Shale	20.1	17.9	15.7
Utah Raw Shale (28 GPT)	19.5	12.5	2.8
Utah Raw Shale (66 GPT)	13.6	1.3	0.2
Union Shale Mixture (Dry)	20.6	18.0	14.6

TABLE B-12. MEAN CARBON MONOXIDE CONCENTRATIONS IN EFFLUENT GAS AT VARIOUS TEMPERATURES (VOLUME %, DRY BASIS). NONADIABATIC TEST OF FIRST SAMPLE SET

Sample Type	Temperature (°C)					
	125	150	175	200	250	300
Wyoming Sub-bituminous Coal (-48 +100)	0.26	0.61	1.59	2.64	3.43	3.55
Wyoming Sub-bituminous Coal (-325)	0.86	0.83	1.91	2.71	3.04	3.82
West Kentucky #9 Bituminous Coal (-48 +100)	0.95	0.32	1.08	1.37	2.36	2.95
West Kentucky #9 Bituminous Coal (-325)	0.60	0.59	1.56	1.38	2.55	3.32
C-a Raw Shale (-48 +100)	0.00	0.03	0.32	0.99	2.23	3.01
C-a Raw Shale (-325)	0.00	0.08	0.25	0.83	2.34	2.95
Paraho Retorted Shale (-48 +100)	0.00	0.00	0.00	0.01	0.14	0.64
Paraho Retorted Shale (-325)	0.00	0.00	0.02	0.07	0.21	1.08
Tosco II Retorted Shale (-48 +100)	0.00	0.00	0.15	0.22	0.86	1.60
Tosco II Retorted Shale (-325)	0.00	0.00	0.10	0.54	1.02	1.72
Lurgi Retorted Shale (-200 +325)	0.00	0.00	0.00	0.00	0.00	0.00
Lurgi Retorted Shale (-325)	0.00	0.00	0.00	0.00	0.00	0.00

Source: Denver Research Institute.

TABLE B-13. MEAN CARBON MONOXIDE CONCENTRATIONS IN EFFLUENT GAS FROM NONADIABATIC TEST OF SECOND SAMPLE SET (VOLUME %, DRY BASIS -325 mesh)

Sample type	Temperature (°C)		
	125	150	175
Pocahontas #3 Bituminous Coal	0.05	0.45	0.08
Hytort Retorted Shale	<0.1	0.07	0.16
Utah Raw Shale (28 GPT)	0.05	0.32	0.16
Utah Raw Shale (66 GPT)	0.15	0.61	1.1
Union Shale Mixture (Dry)	<.01	0.07	0.23

TABLE B-14. MEAN CARBON DIOXIDE CONCENTRATIONS IN EFFLUENT GAS AT VARIOUS TEMPERATURES (VOLUME %, DRY BASIS). NONADIABATIC TEST OF FIRST SAMPLE SET.

Sample Type	Temperature (°C)					
	125	150	175	200	250	300
Wyoming Sub-bituminous Coal (-48 +100)	2.83	5.63	9.73	12.64	16.56	20.13
Wyoming Sub-bituminous Coal (-325)	1.96	6.44	11.92	14.83	13.75	19.40
West Kentucky #9 Bituminous Coal (-48 +100)	0.55	1.68	3.38	4.35	7.87	12.22
West Kentucky #9 Bituminous Coal (-325)	0.35	1.51	4.56	4.09	8.52	14.59
C-a Raw Shale (-48 +100)	0.10	0.33	1.76	2.95	7.98	12.42
C-a Raw Shale (-325)	0.10	0.27	1.50	2.13	8.64	15.24
Paraho Retorted Shale (-48 +100)	0.05	0.07	0.28	0.31	1.08	4.99
Paraho Retorted Shale (-325)	0.07	0.08	0.50	0.45	1.99	7.61
Tosco II Retorted Shale (-48 +100)	0.11	0.33	1.90	1.46	6.99	16.45
Tosco II Retorted Shale (-325)	0.19	0.27	1.06	1.58	7.57	17.68
Lurgi Retorted Shale (-200 +325)	0.03	0.03	0.04	0.04	0.09	0.16
Lurgi Retorted Shale (-325)	0.02	0.02	0.02	0.03	0.14	0.29

Source: Denver Research Institute.

TABLE B-15. MEAN CARBON DIOXIDE CONCENTRATIONS IN EFFLUENT GAS FROM NONADIABATIC TEST OF SECOND SAMPLE SET (VOLUME %, DRY BASIS, -325 mesh)

Sample type	Temperature (°C) 125	150	175
Pocahontas #3 Bituminous Coal	0.60	1.6	3.8
Hytort Retorted Shale	0.27	0.70	1.4
Utah Raw Shale (28 GPT)	0.28	1.4	4.3
Utah Raw Shale (66 GPT)	1.16	4.7	6.6
Union Shale Mixture (Dry)	0.59	1.2	1.1

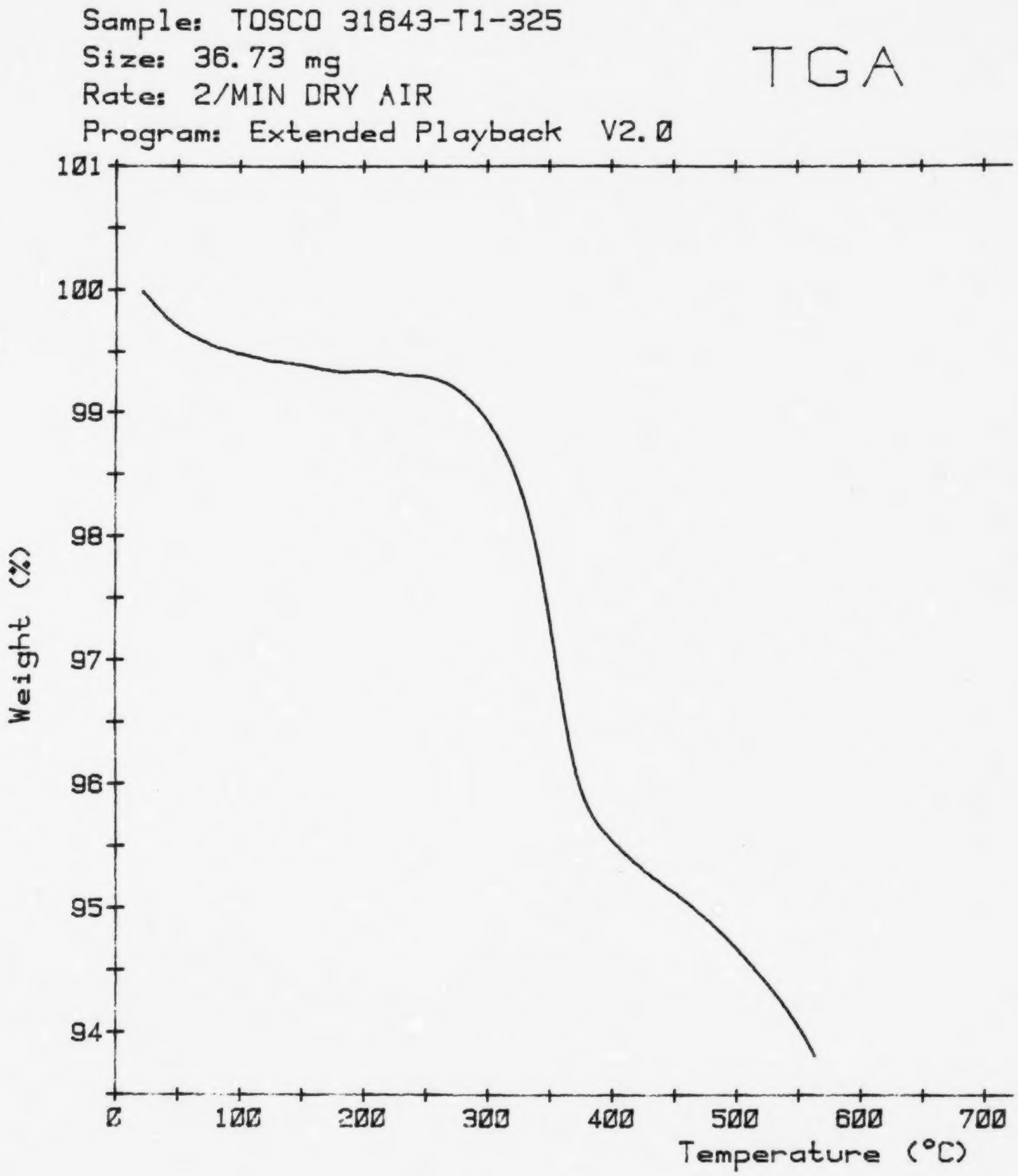

Figure C-1. Thermogravimetric test data, Tosco II retorted shale, (-325 mesh, 2°C/min heating ramp). Test 1.

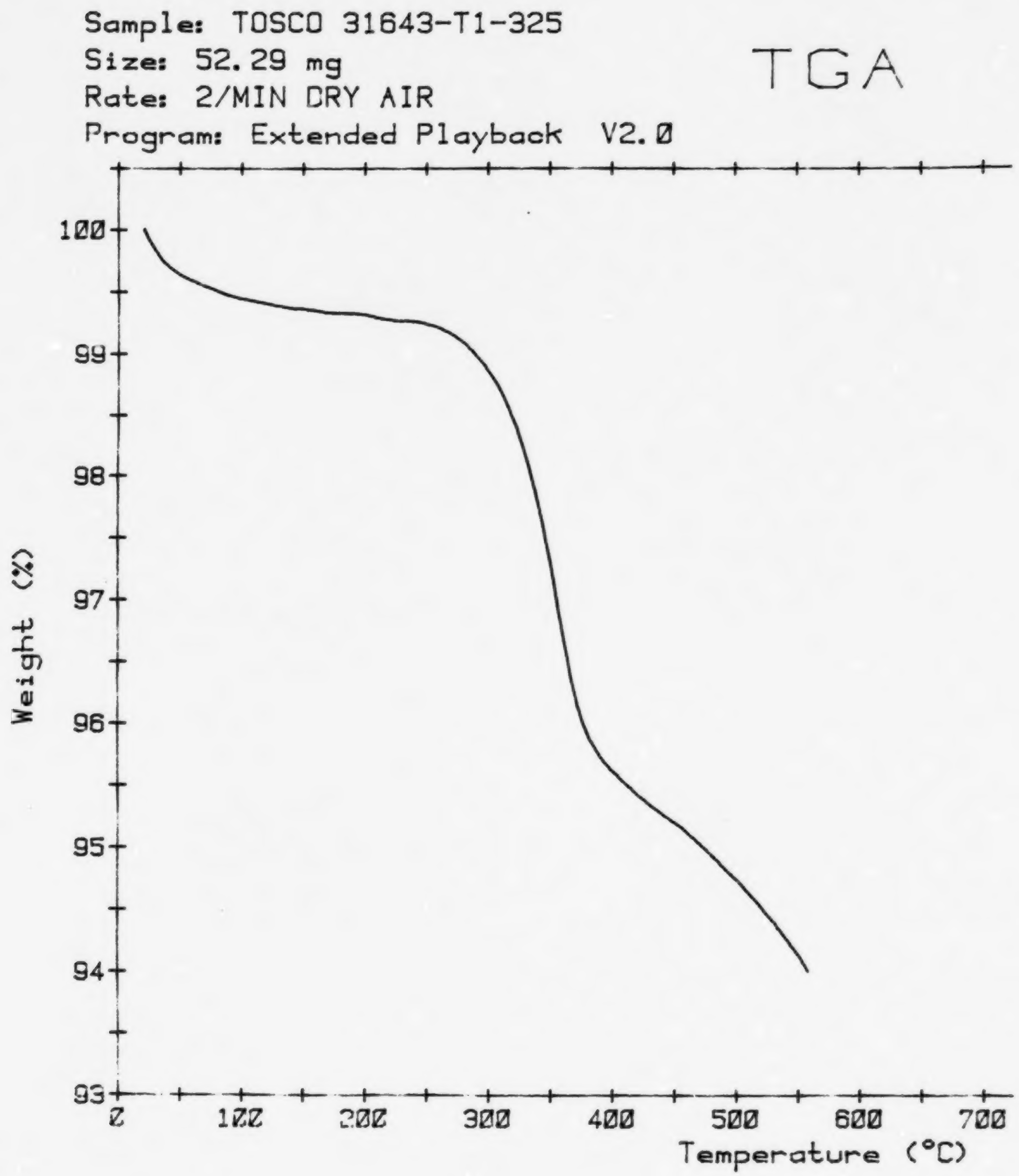

Figure C-2. Thermogravimetric test data, Tosco II retorted shale (-325 mesh, 2°C/min heating ramp). Test 2.

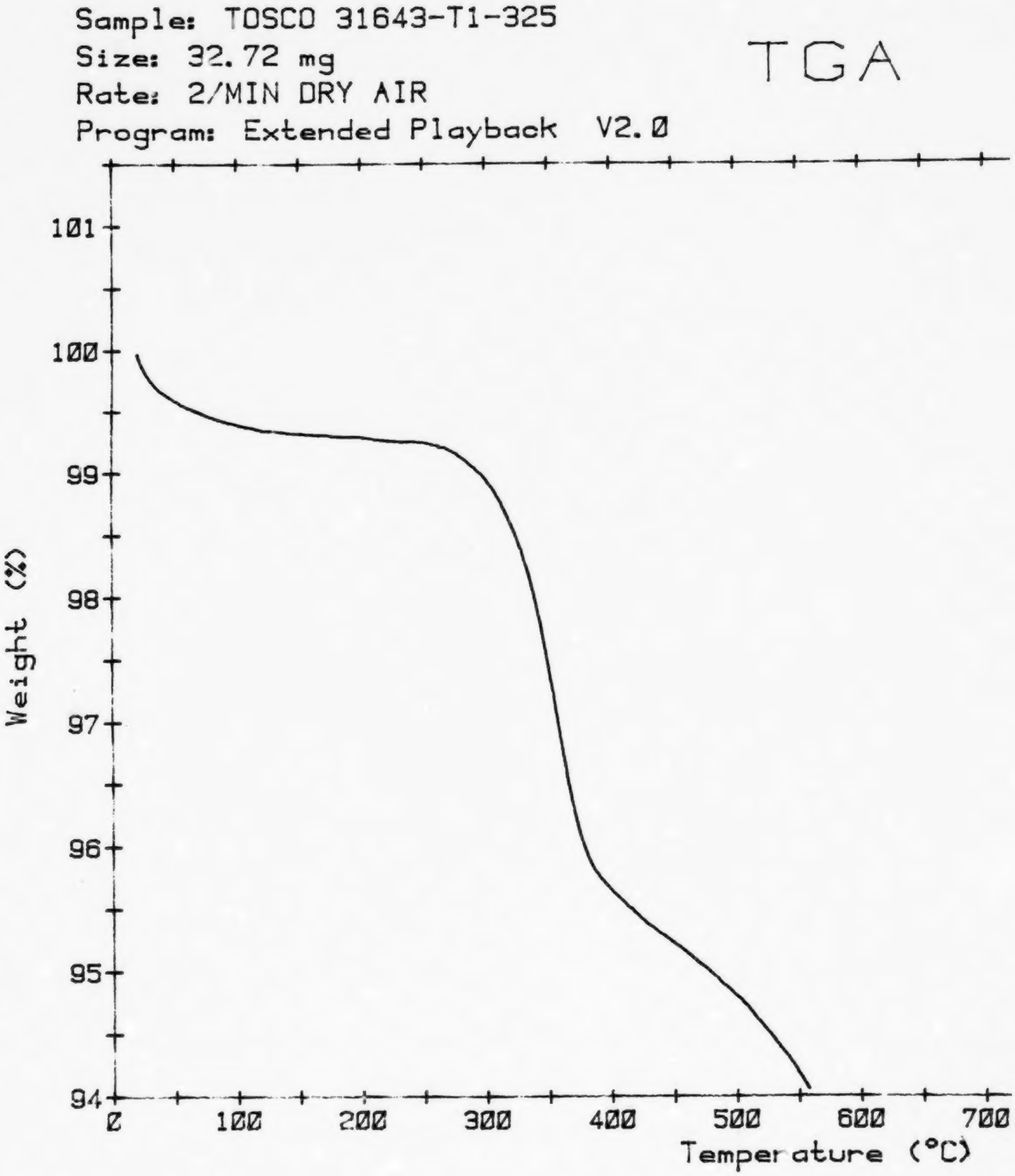

Figure C-3. Thermogravimetric test data, Tosco II retorted shale (-325 mesh, 2°C/min heating ramp). Test 3.

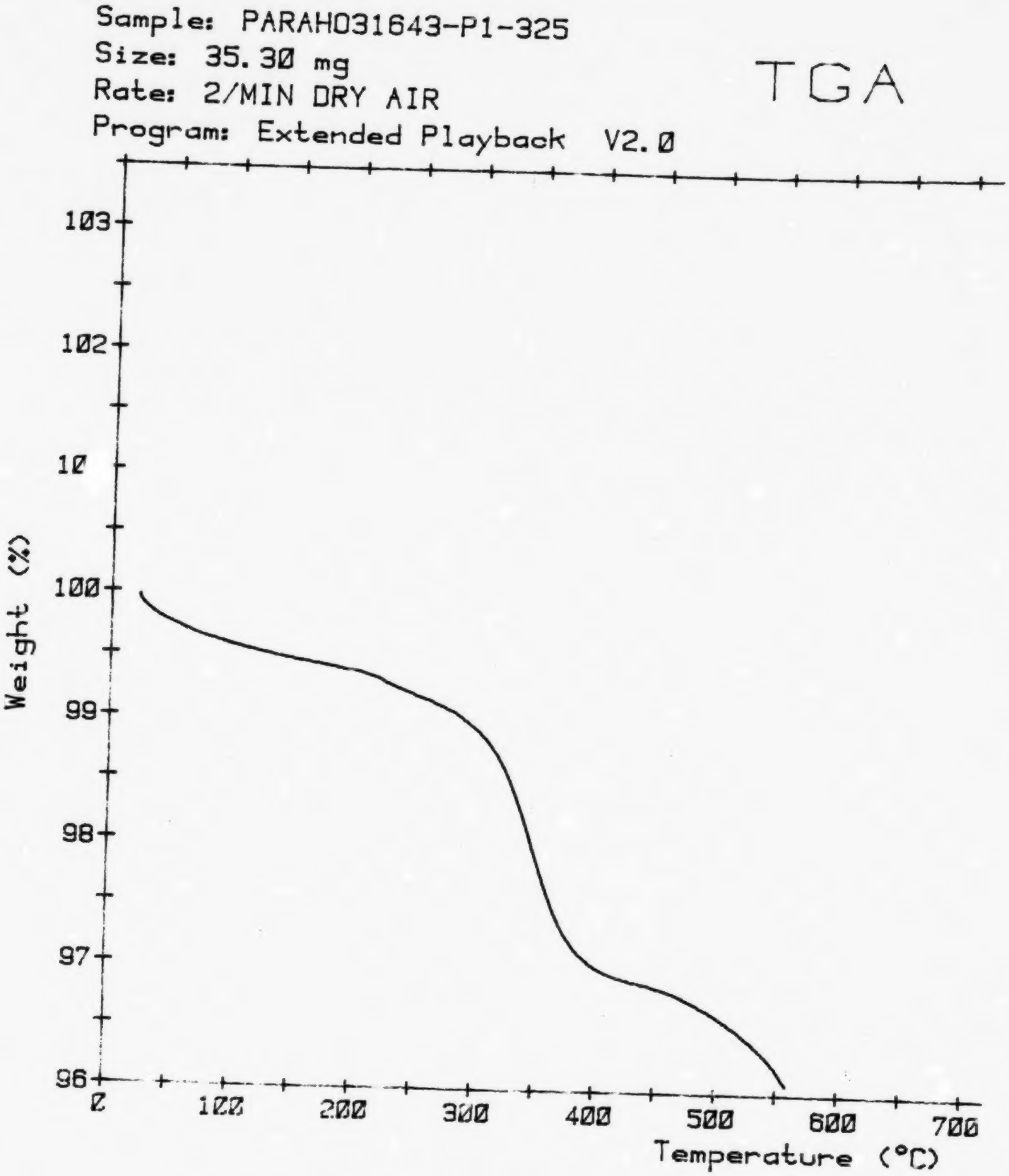

Sample: PARAH031643-P1-325
Size: 35.30 mg
Rate: 2/MIN DRY AIR
Program: Extended Playback V2.0

Figure C-4. Thermogravimetric test data, Paraho retorted shale (-325 mesh, 2°C/min heating ramp). Test 1.

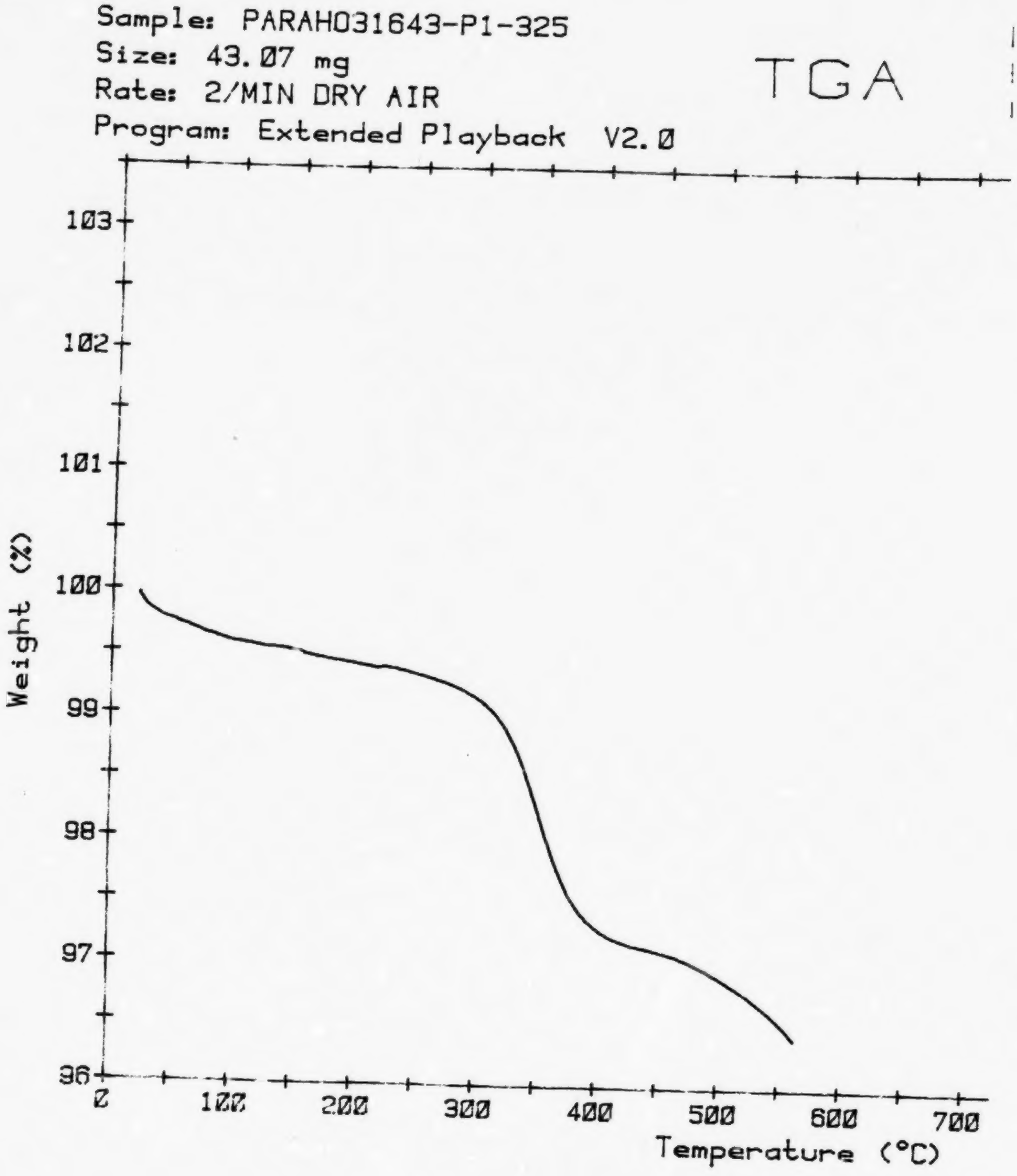

Figure C-5. Thermogravimetric test data, Paraho retorted shale (-325 mesh, 2°C/min heating ramp). Test 2.

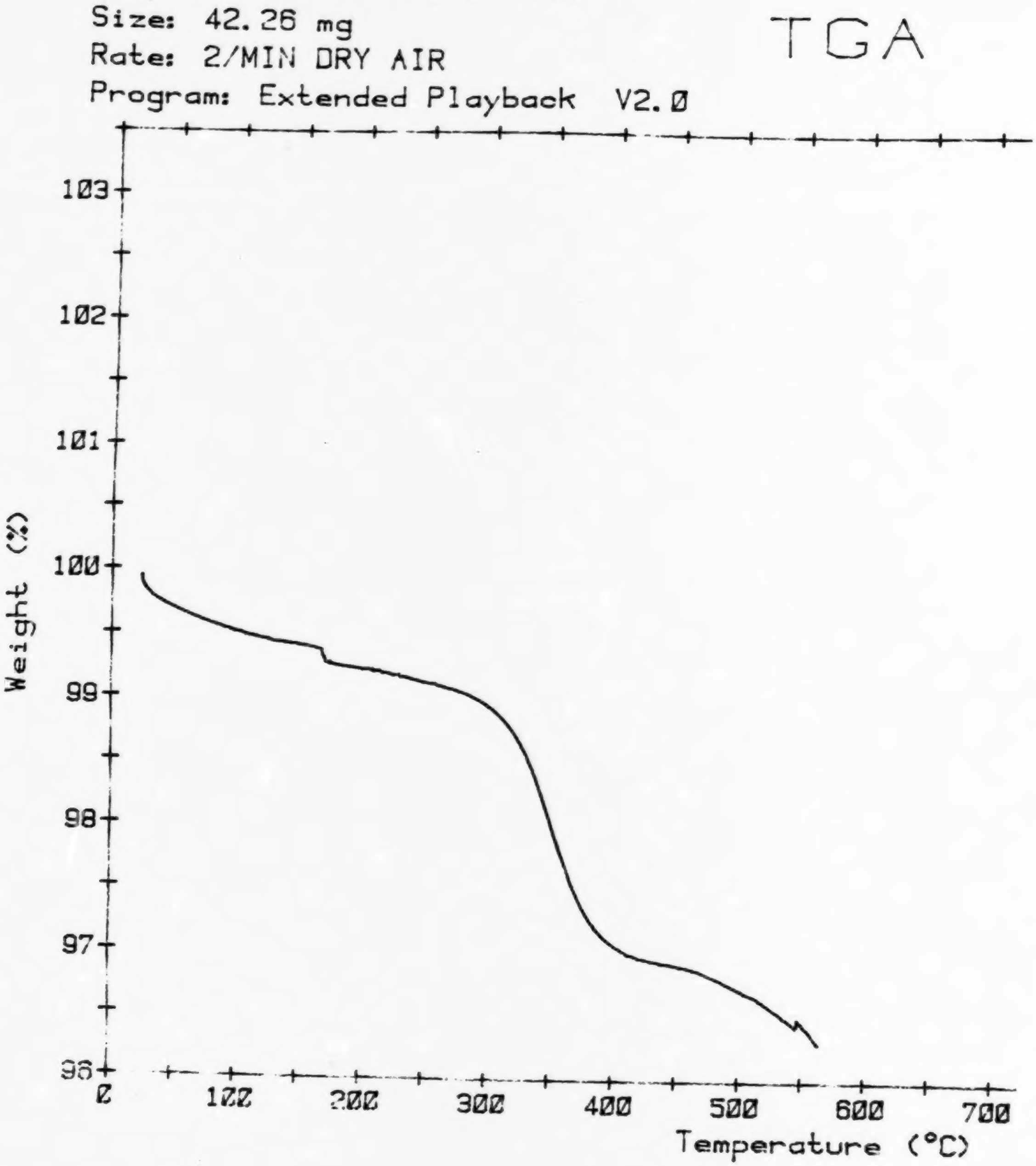

Figure C-6. Thermogravimetric test data, Paraho retorted shale (-325 mesh, 2°C/min heating ramp). Test 3.

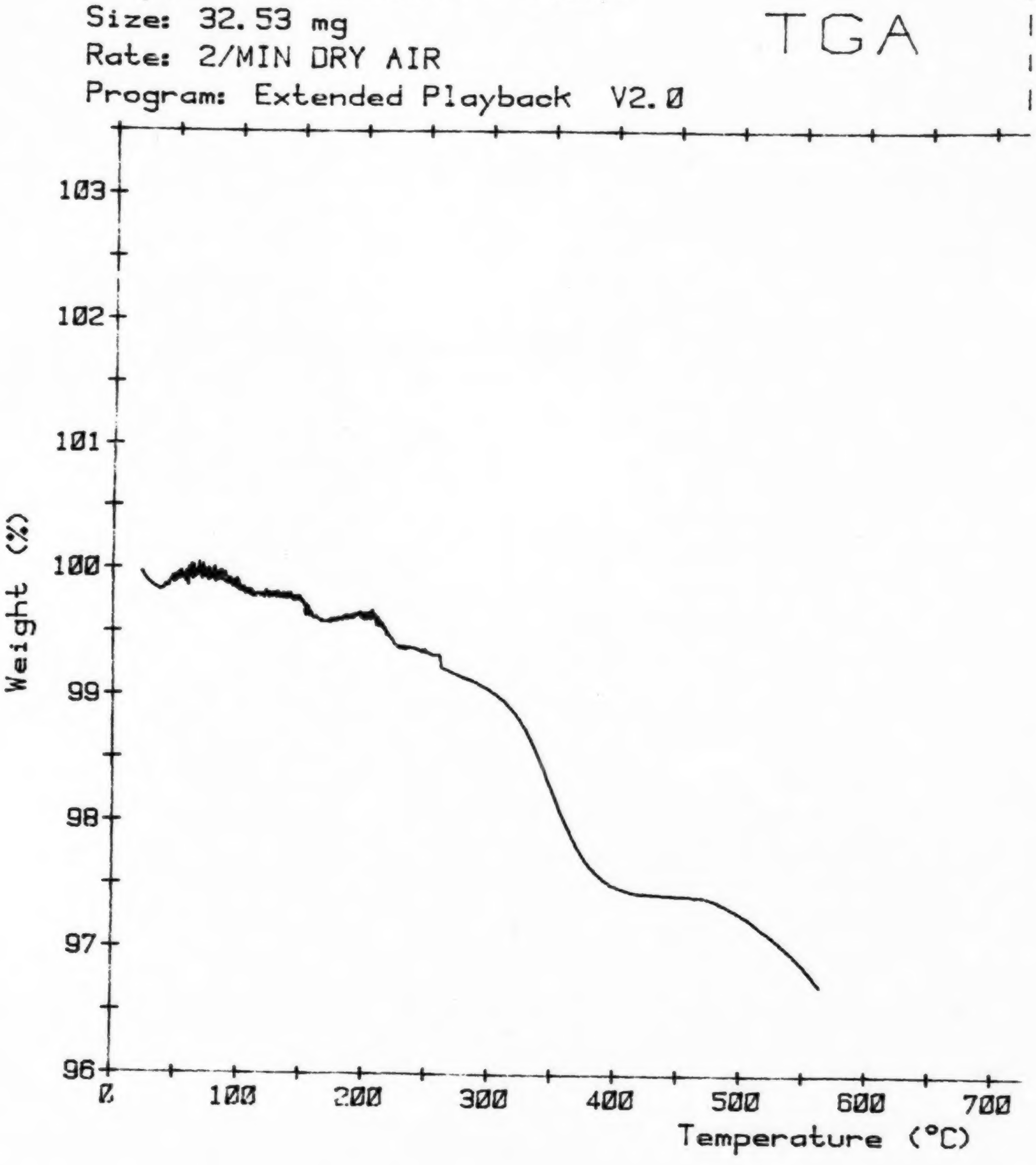

Figure C-7. Thermogravimetric test data, Paraho retorted shale (48 x 100 mesh, 2°C/min heating ramp). Test 1.

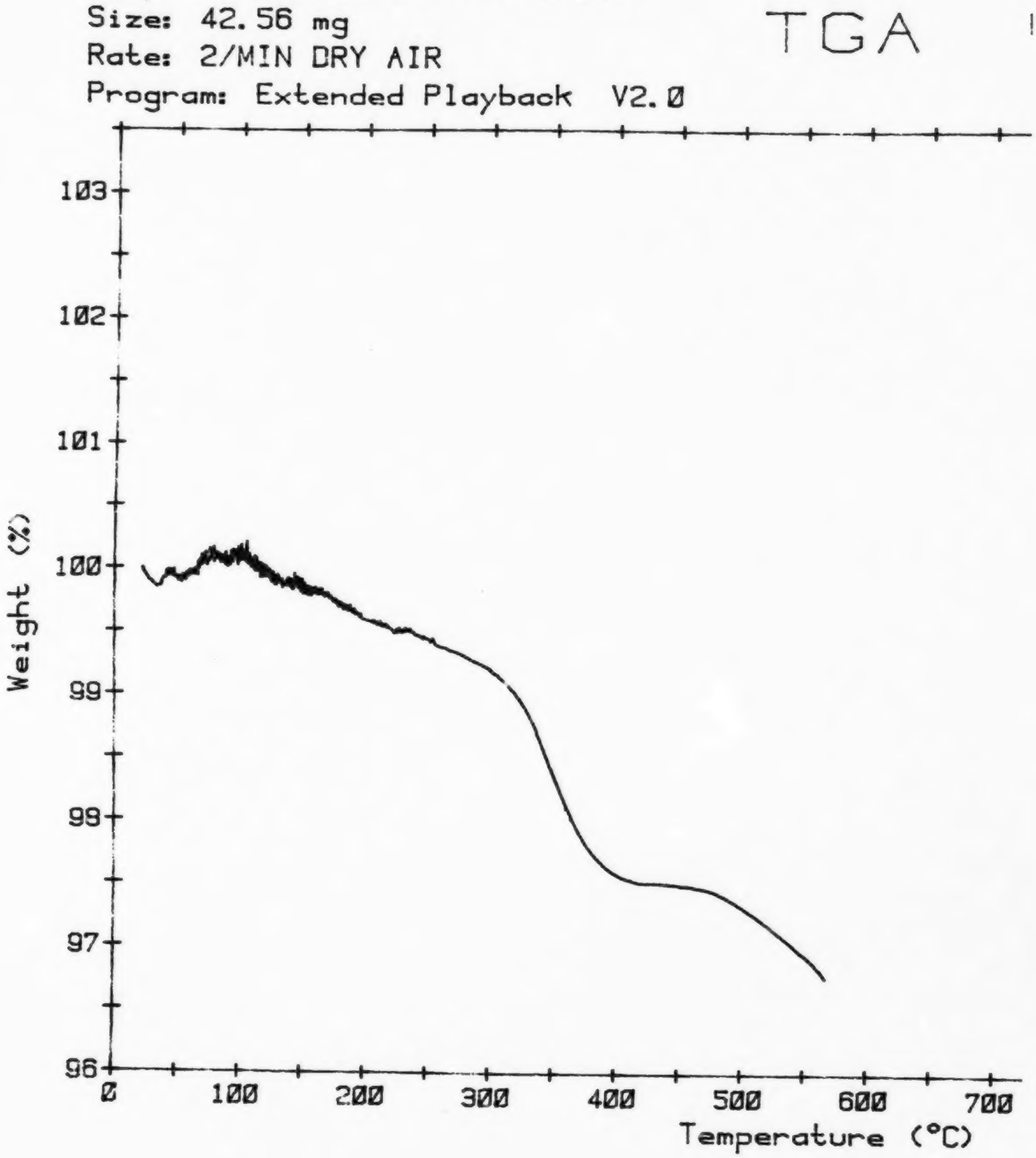

Figure C-8. Thermogravimetric test data, Paraho retorted shale (-48 +100 mesh, 2°C/min heating ramp). Test 2.

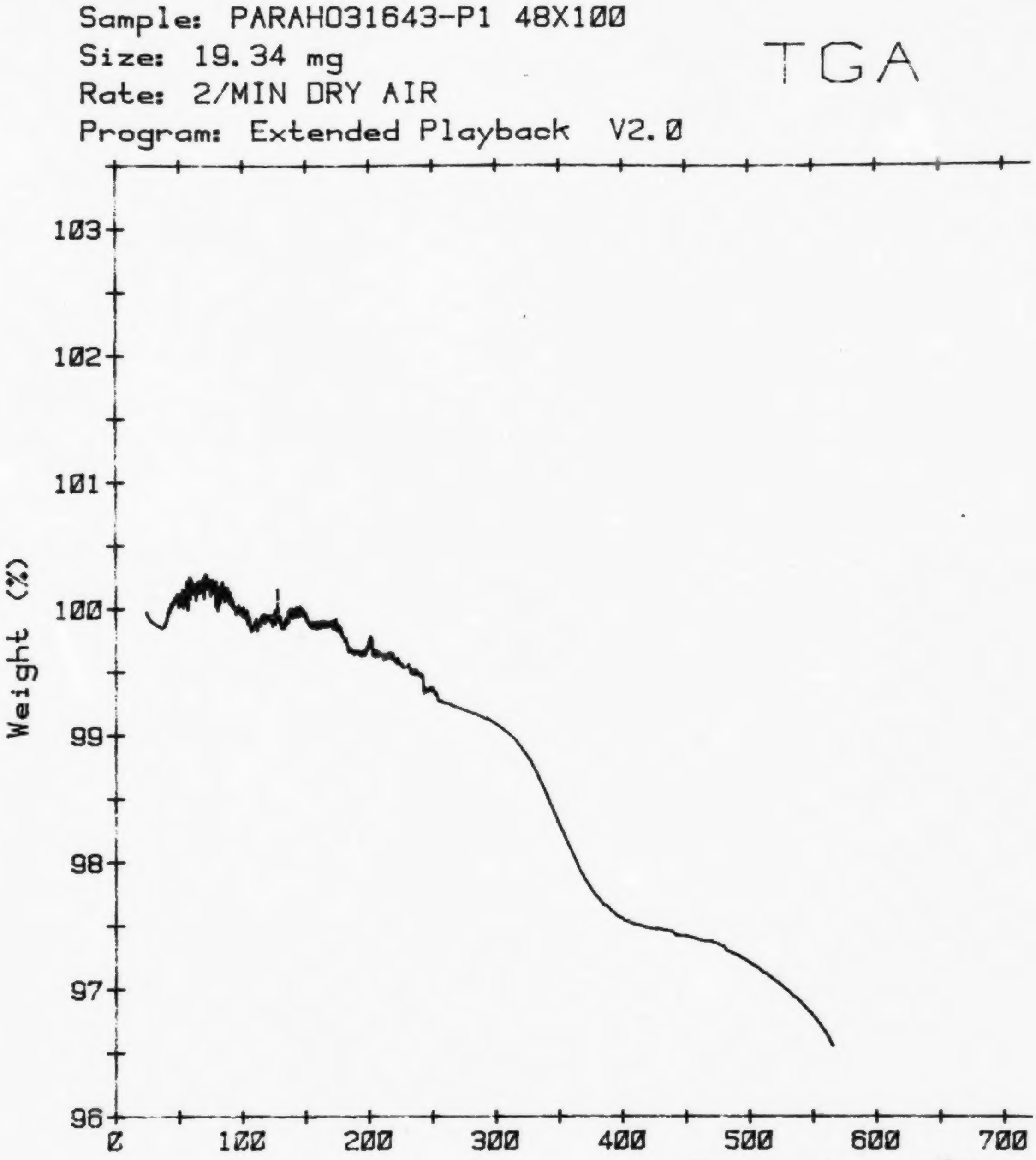

Figure C-9. Thermogravimetric test data, Paraho retorted shale (-48 +100 mesh, 2°C/min heating ramp). Test 3.

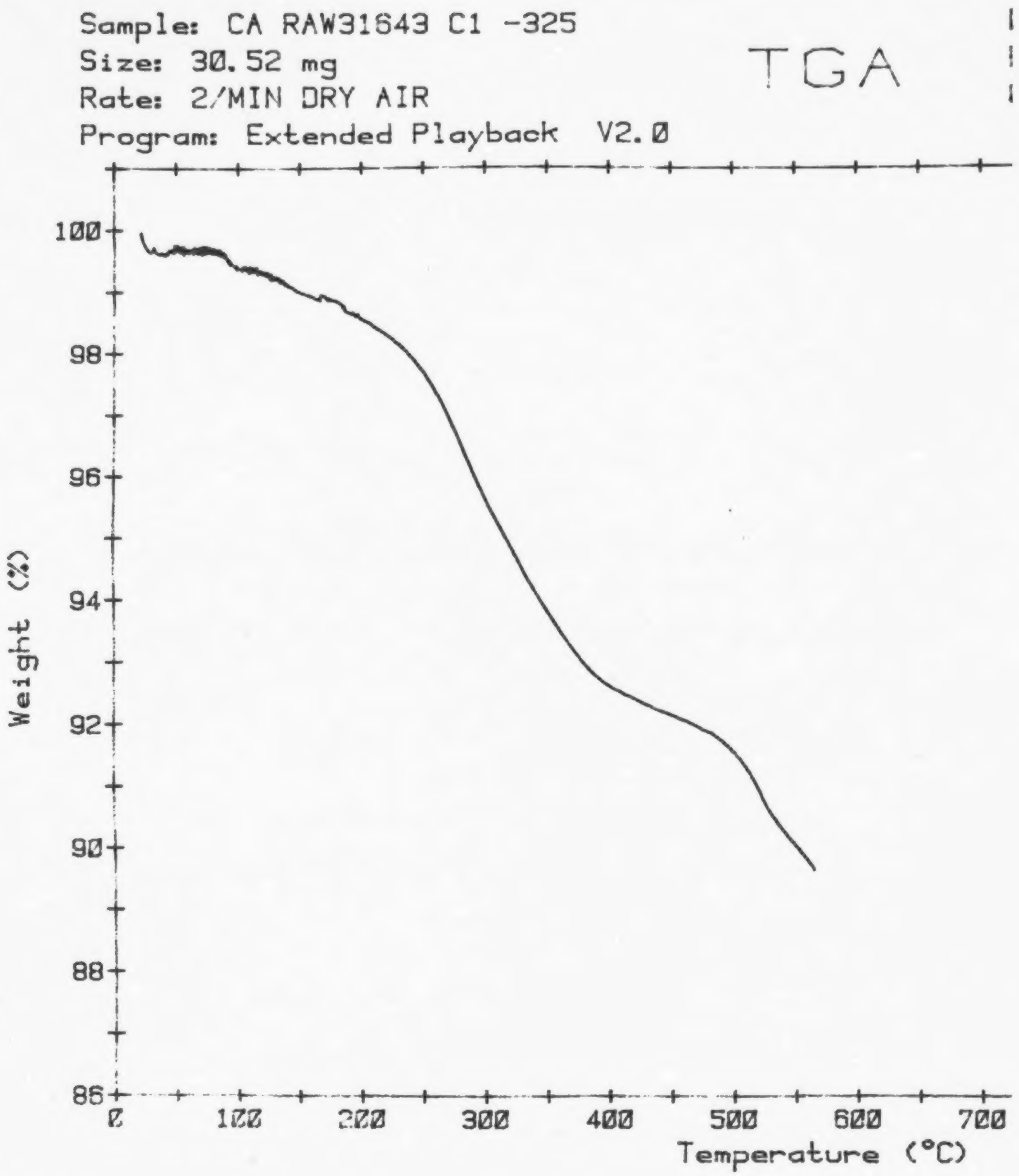

Figure C-10. Thermogravimetric test data, C-a raw shale (-325 mesh, 2°C/min heating ramp). Test 1.

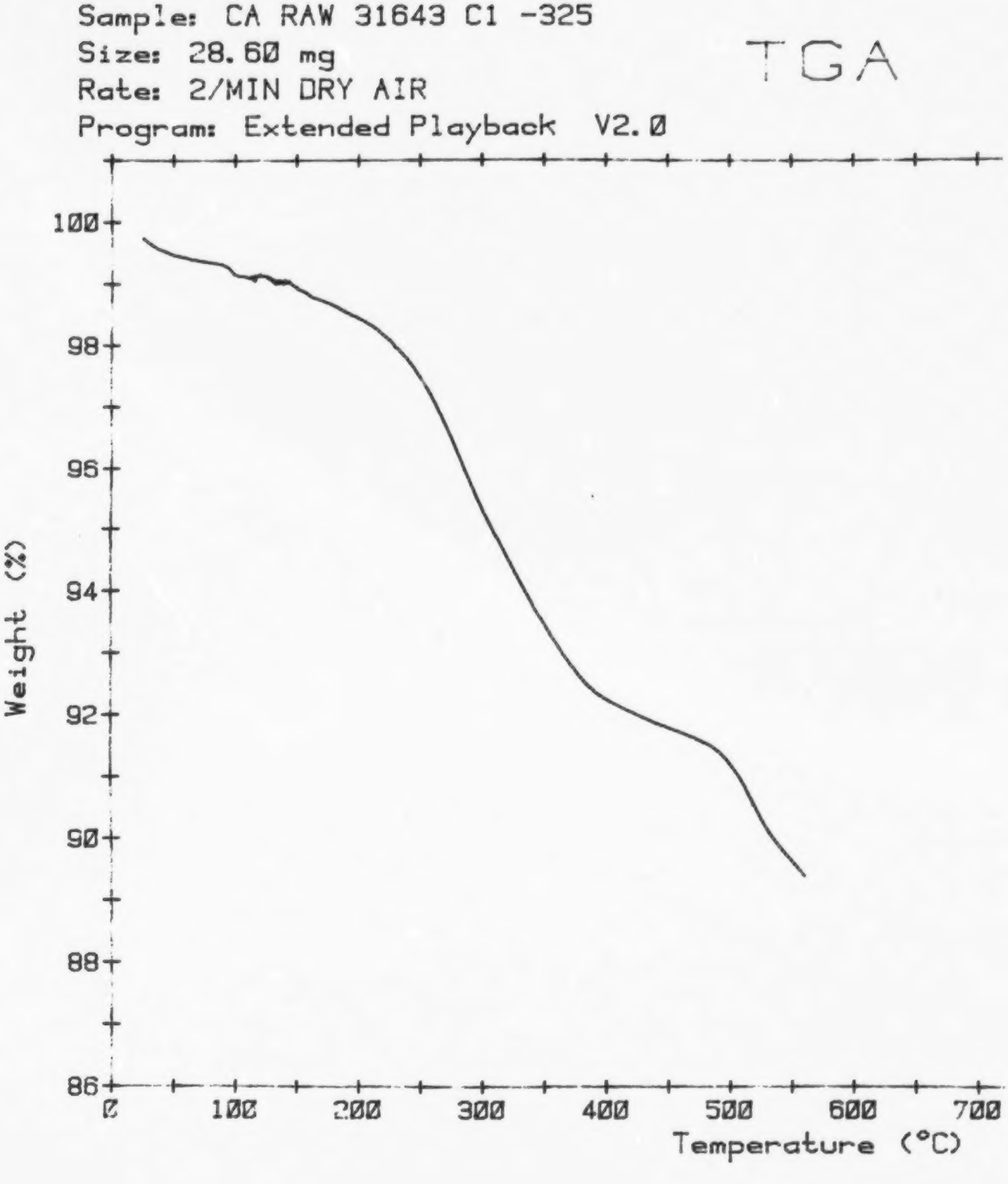

Figure C-11. Thermogravimetric test data, C-a raw shale (-325 mesh, 2°C/min heating ramp). Test 2.

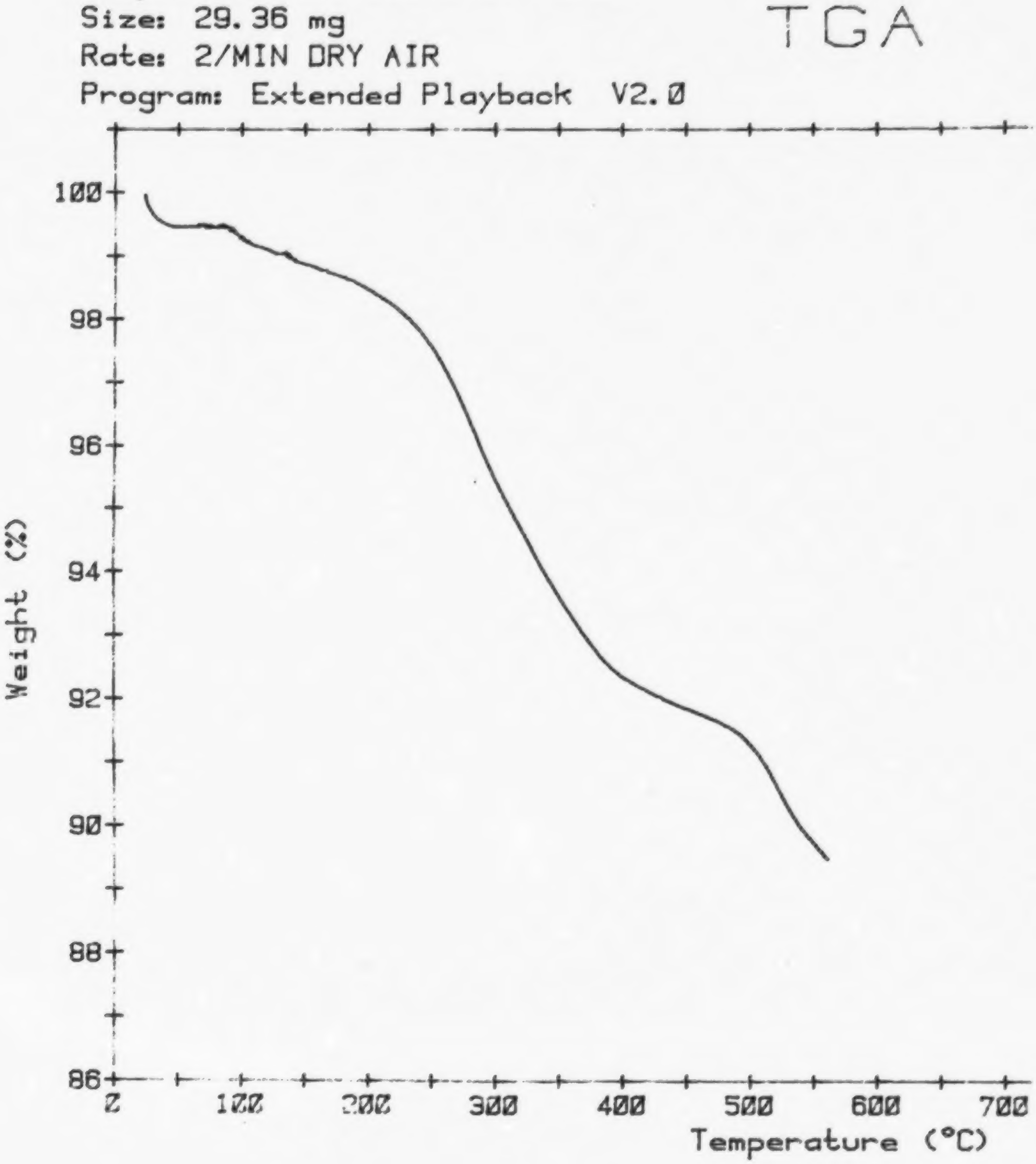

Figure C-12. Thermogravimetric test data, C-a raw shale (-325 mesh, 2°C/min heating ramp). Test 3.

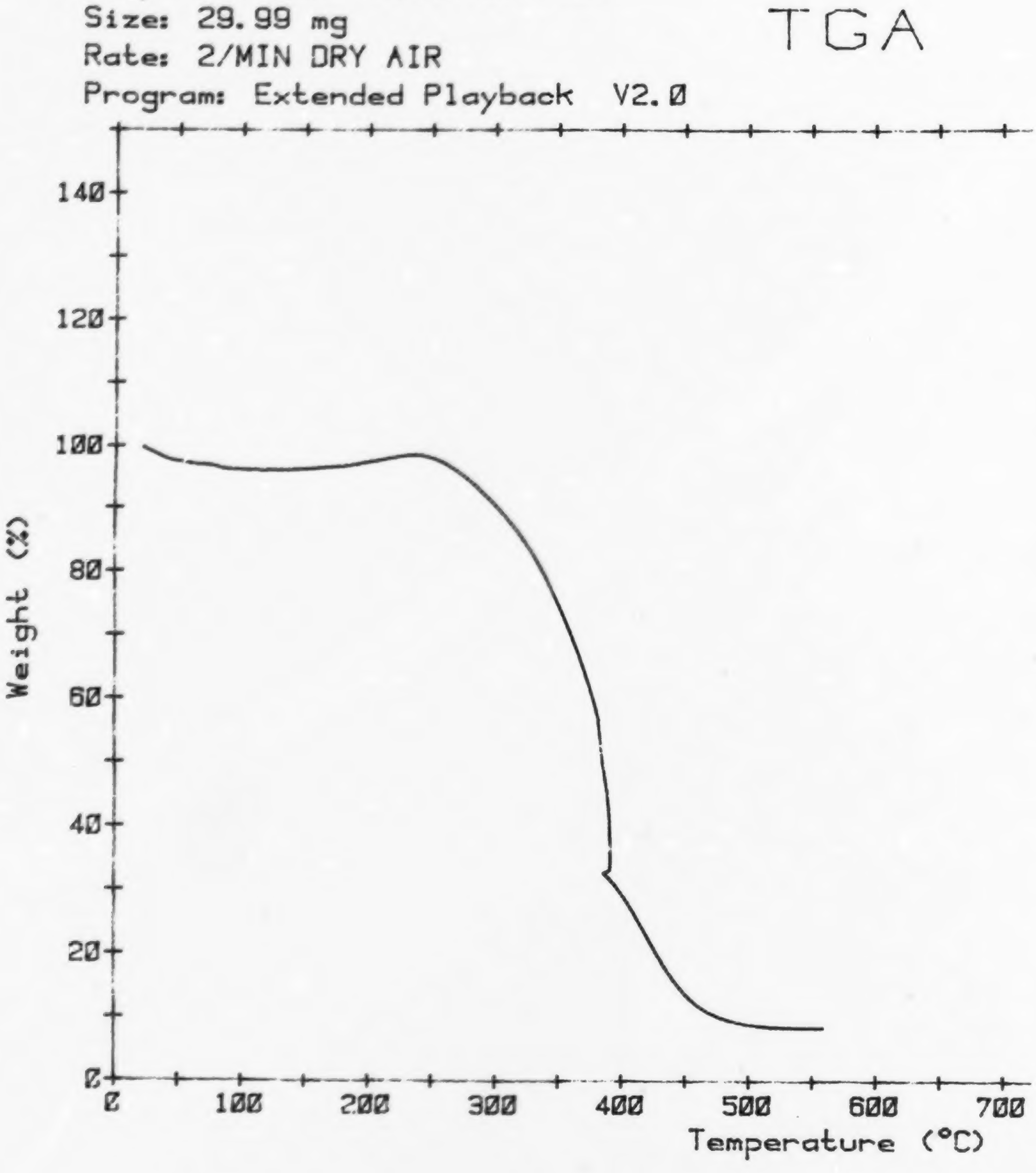

Figure C-13. Thermogravimetric test data, Western Kentucky #9 bituminous coal (-325 mesh 2°C/min heating ramp). Test 1.

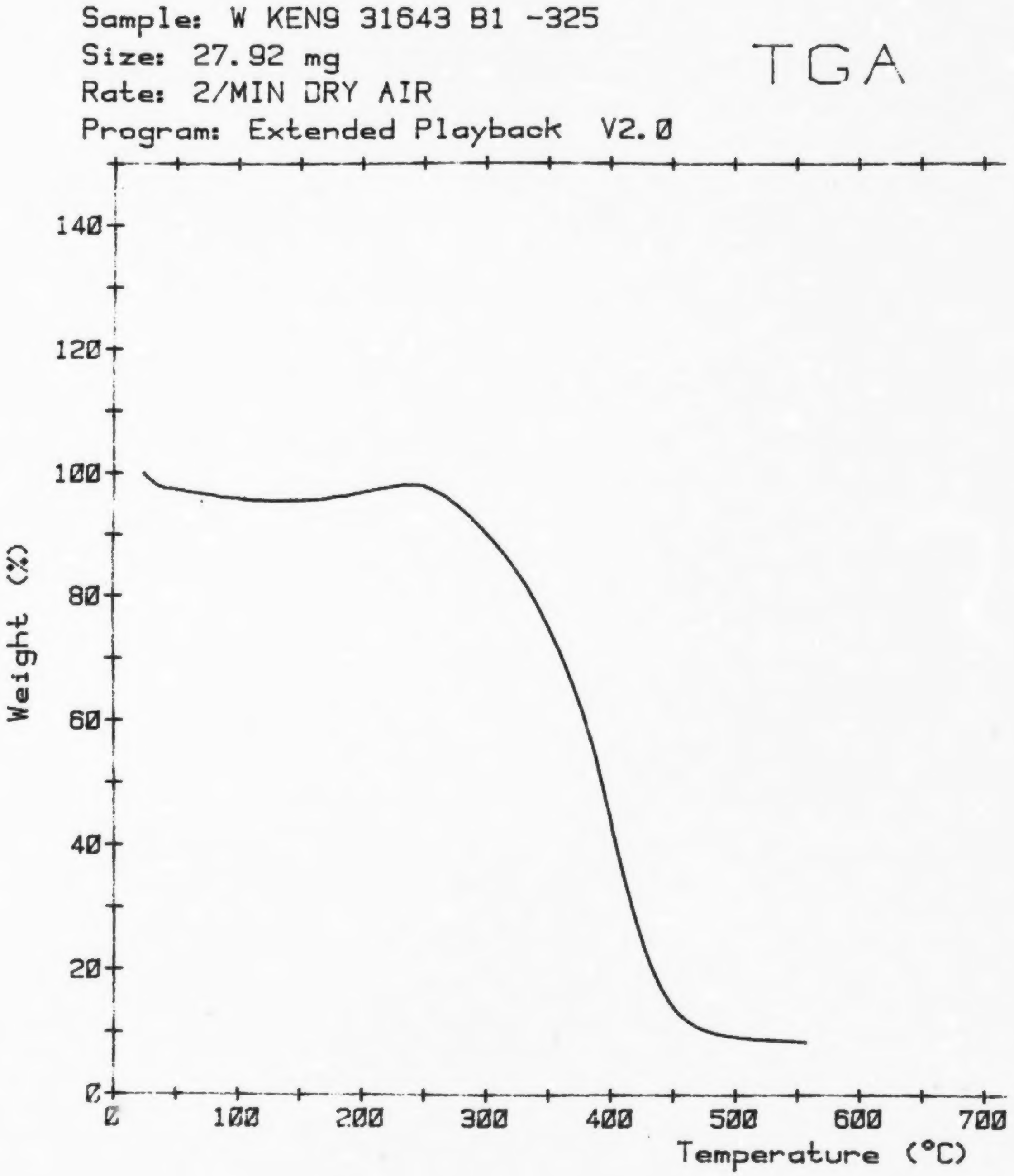

Figure C-14. Thermogravimetric test data, Western Kentucky #9 bituminous coal (-325 mesh 2°C/min heating ramp). Test 2.

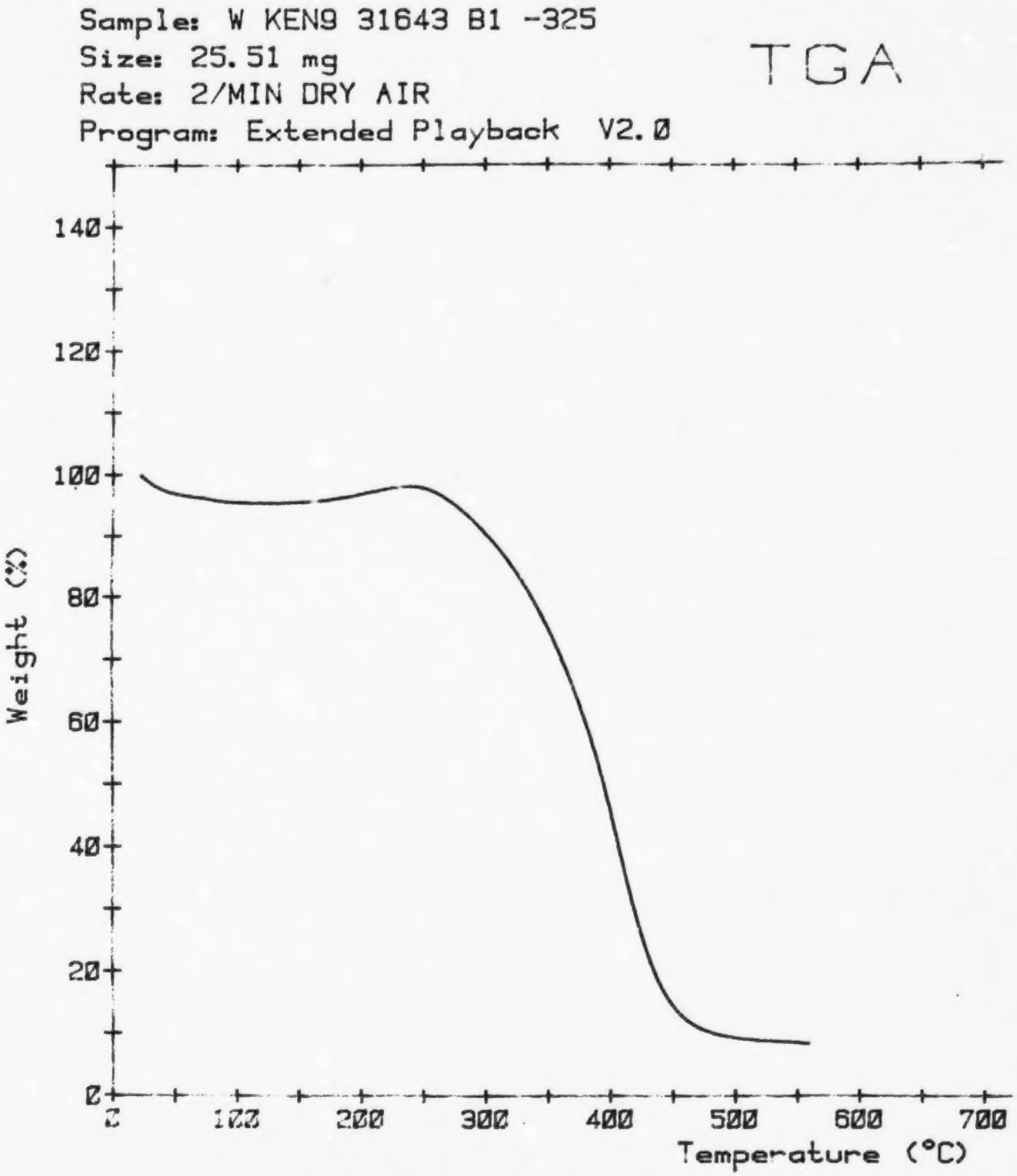

Figure C-15. Thermogravimetric test data, Western Kentucky #9 bituminous coal (-325 mesh 2°C/min heating ramp). Test 3.

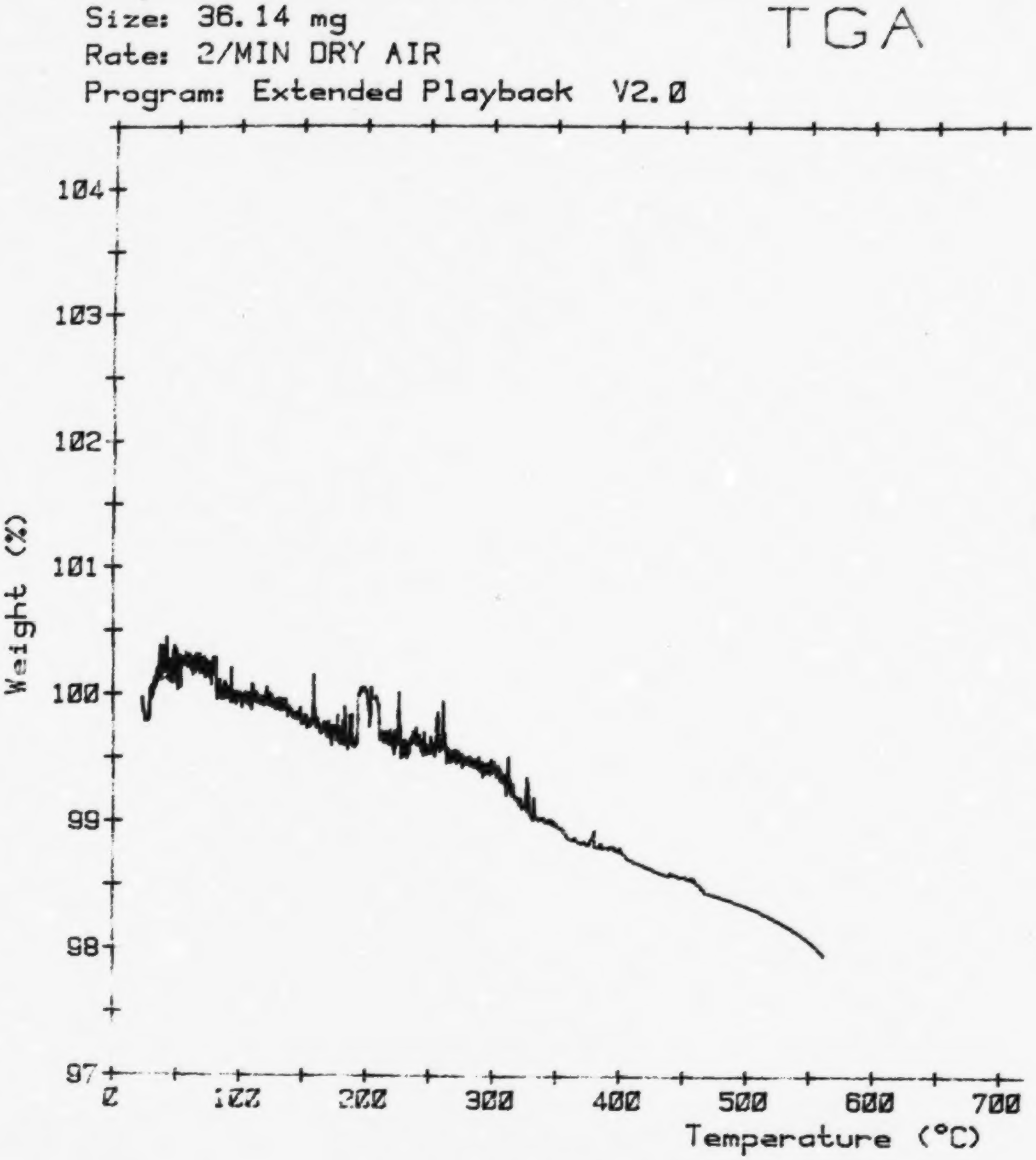

Figure C-16. Thermogravimetric test data, Lurgi retorted shale (-325 mesh 2°C/min heating ramp). Test 1.

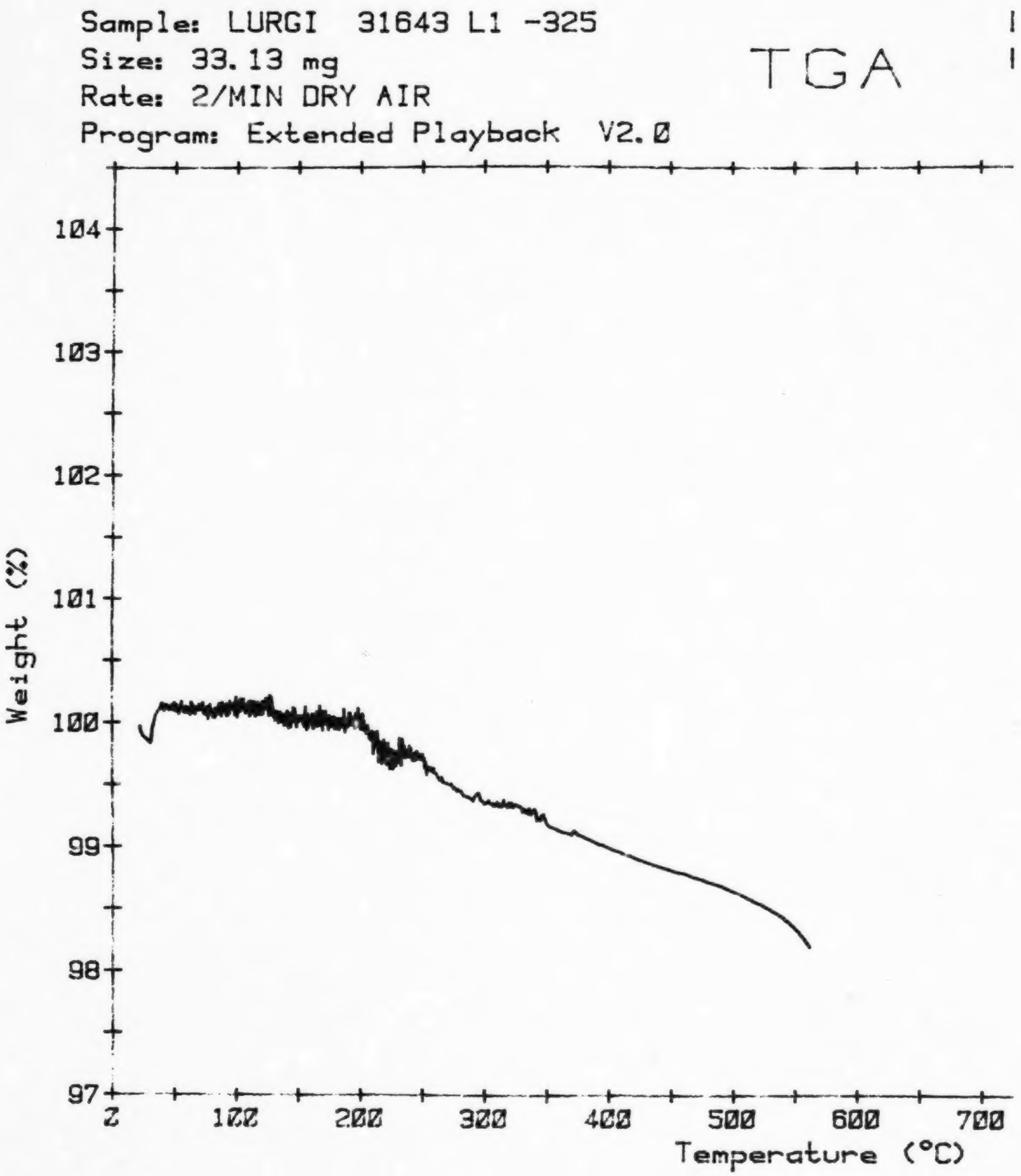

Figure C-17. Thermogravimetric test data, Lurgi retorted shale (-325 mesh 2°C/min heating ramp). Test 2.

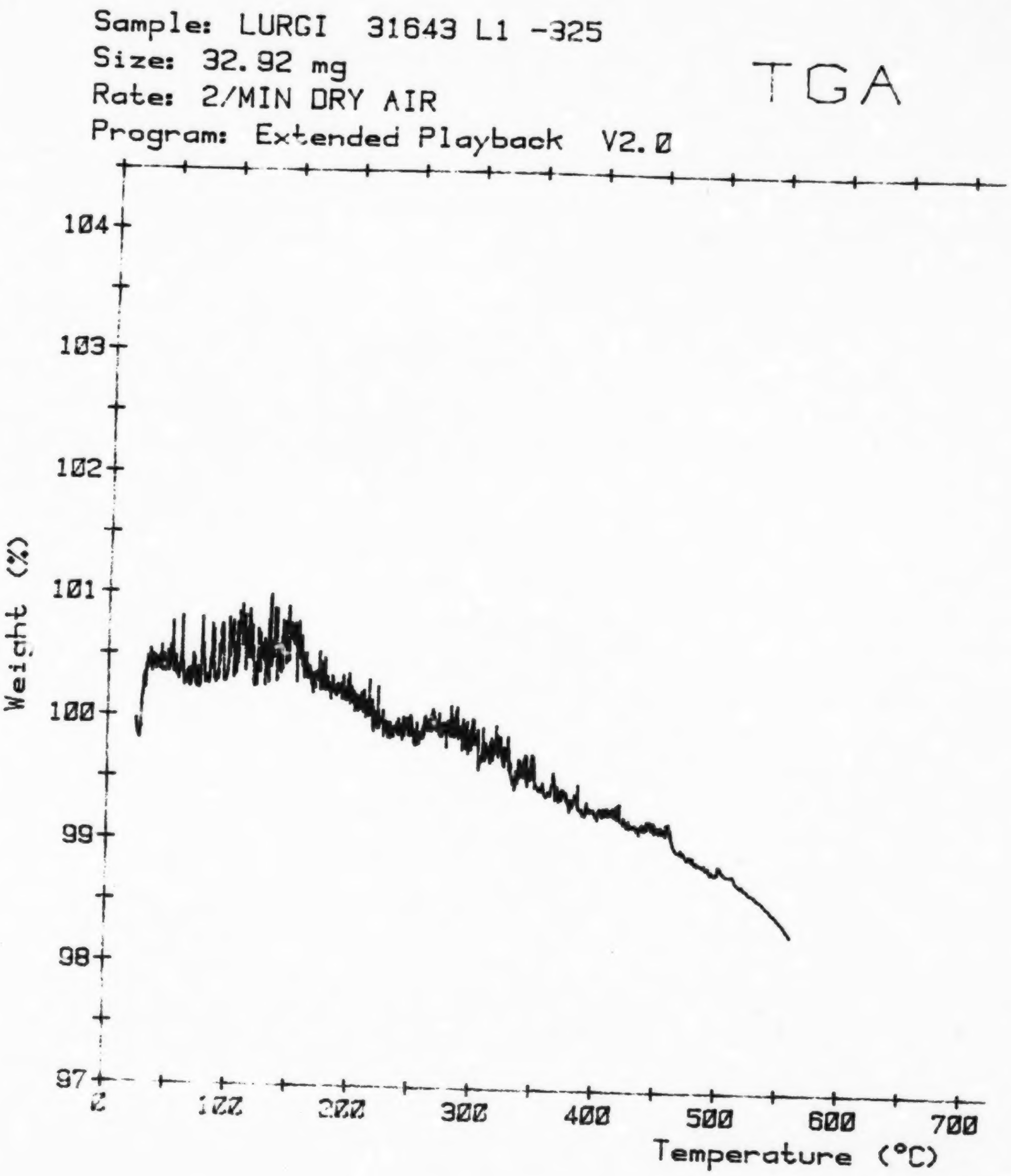

Figure C-18. Thermogravimetric test data, Lurgi retorted shale (-325 mesh 2°C/min heating ramp). Test 3.

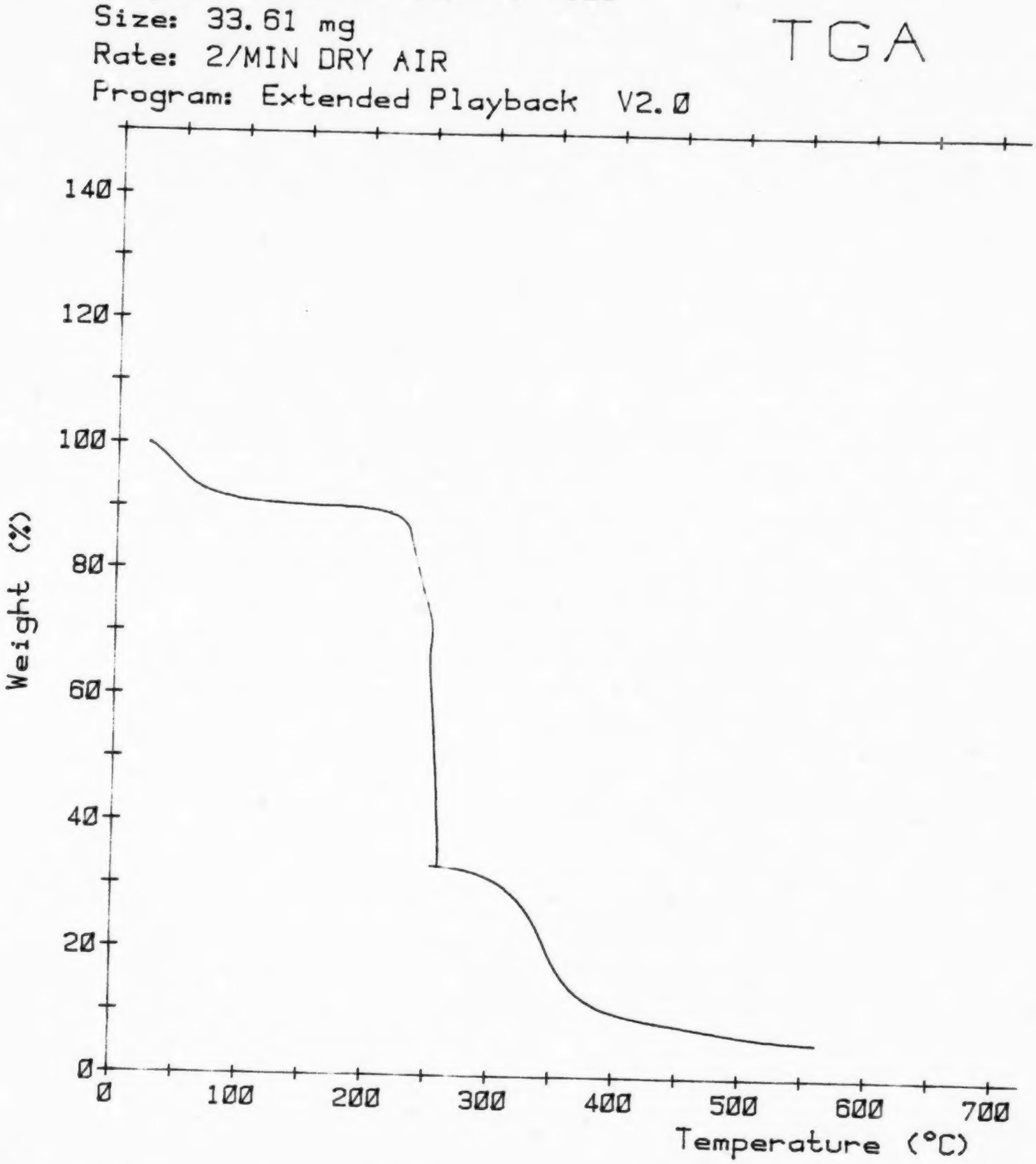

Figure C-19. Thermogravimetric test data, Wyoming subbituminous coal (-325 mesh 2°C/min heating ramp). Test 1.

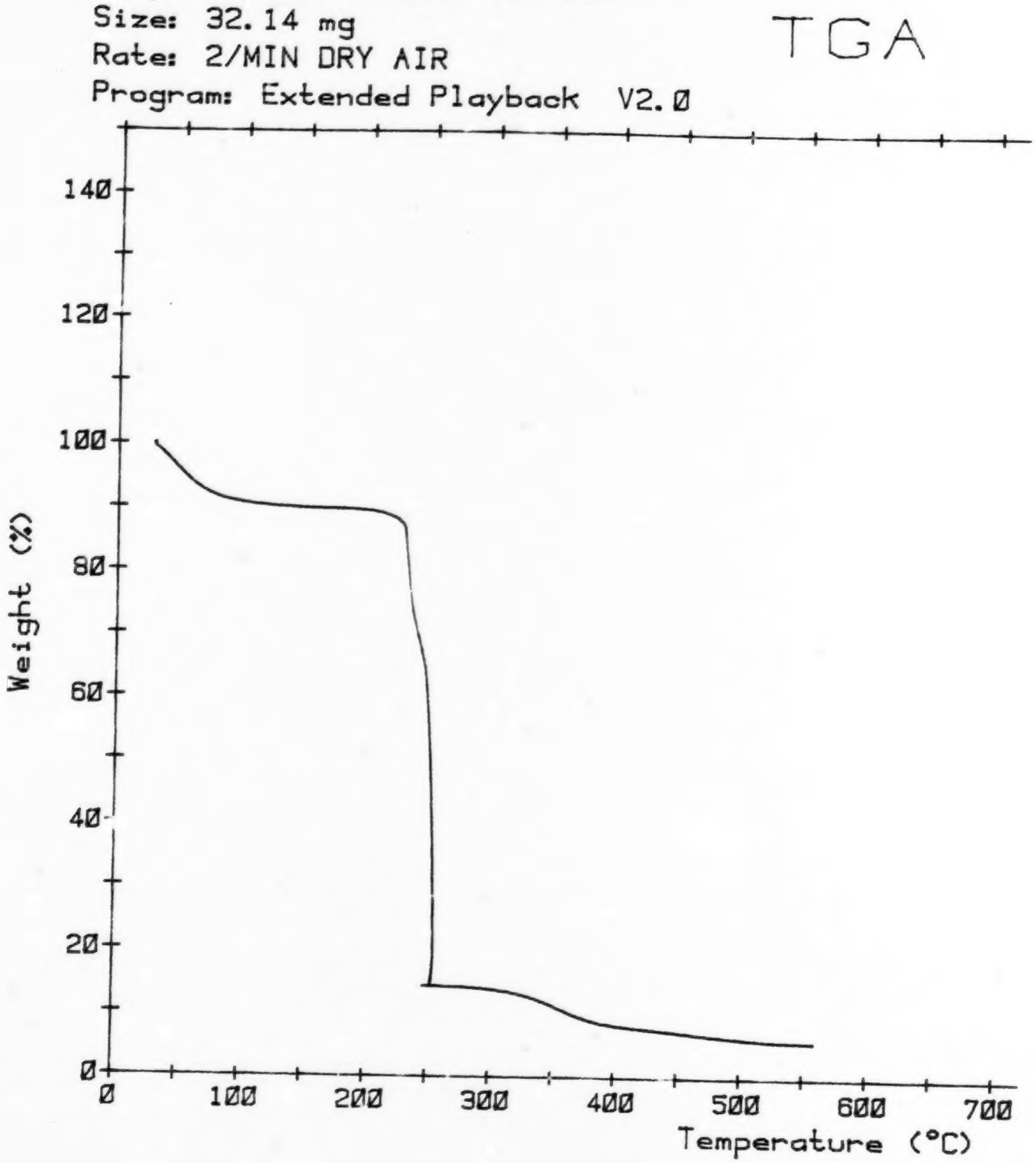

Figure C-20. Thermogravimetric test data, Wyoming subbituminous coal (-325 mesh 2°C/min heating ramp). Test 2.

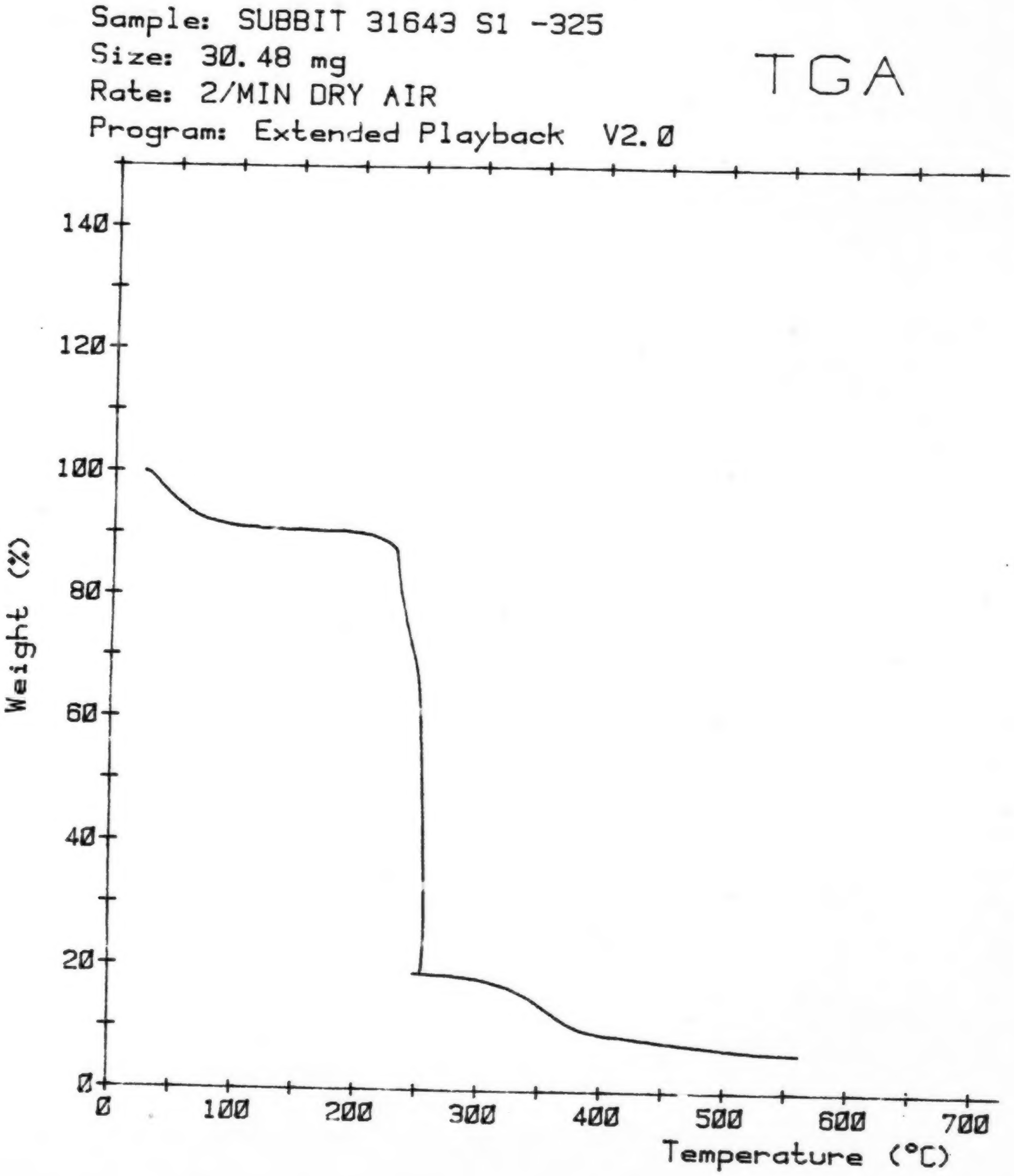

Figure C-21. Thermogravimetric test data, Wyoming subbituminous coal (-325 mesh 2°C/min heating ramp). Test 3.

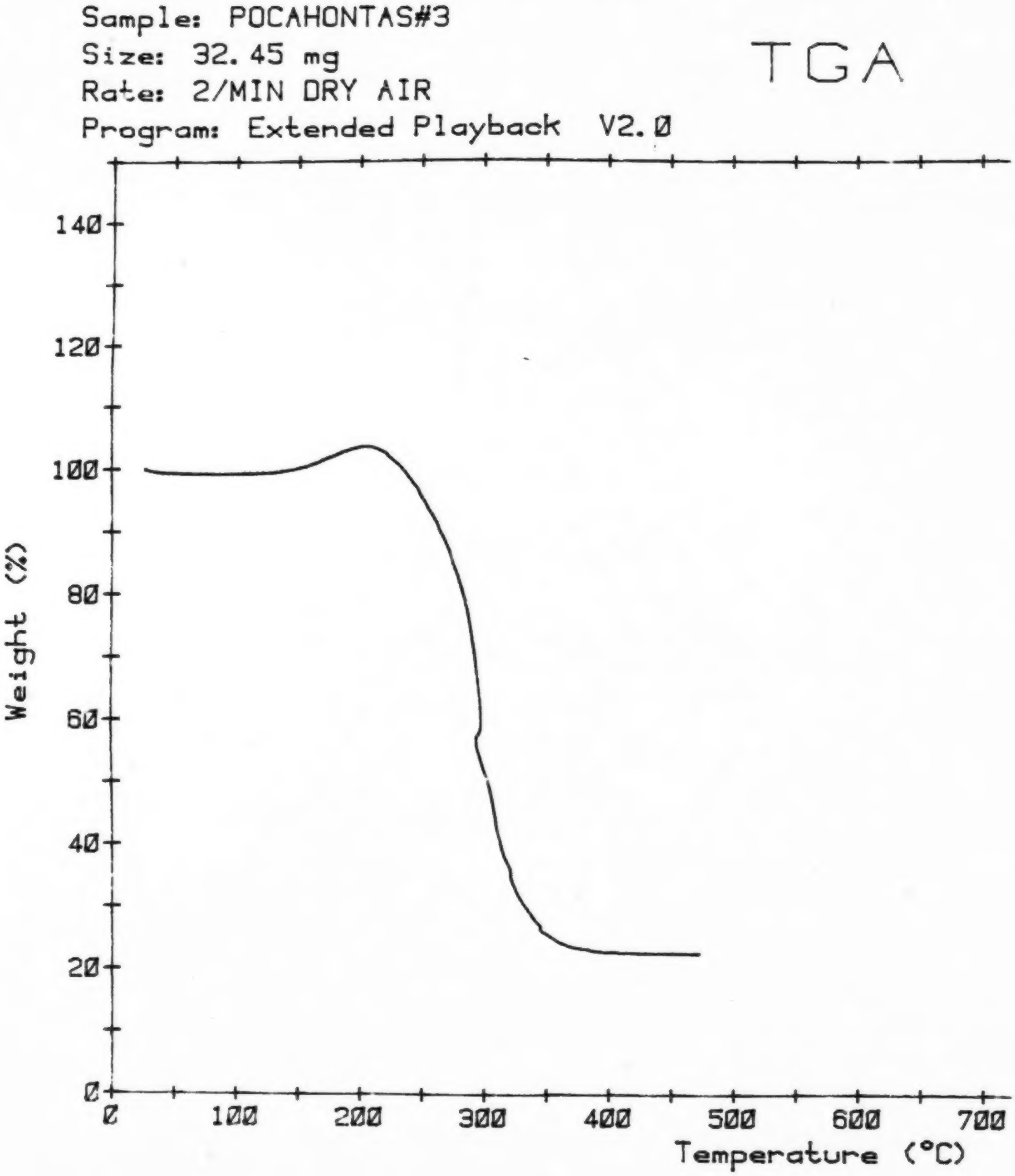

Figure C-22. Thermogravimetric test data, Pocahontas #3 bituminous coal (-325 mesh 2°C/min heating ramp). Test 1.

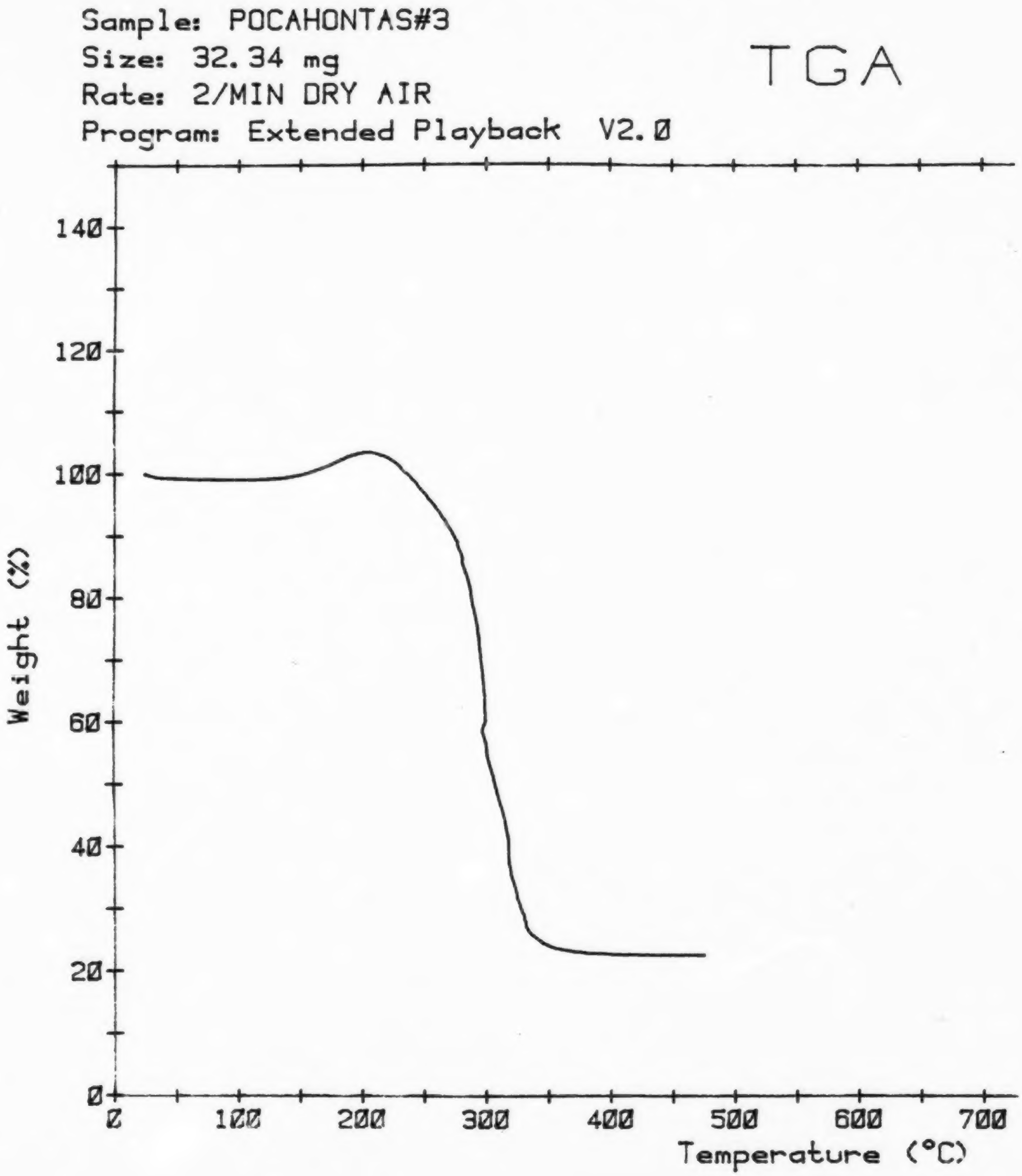

Figure C-23. Thermogravimetric test data, Pocahontas #3 bituminous coal (-325 mesh 2°C/min heating ramp). Test 2.

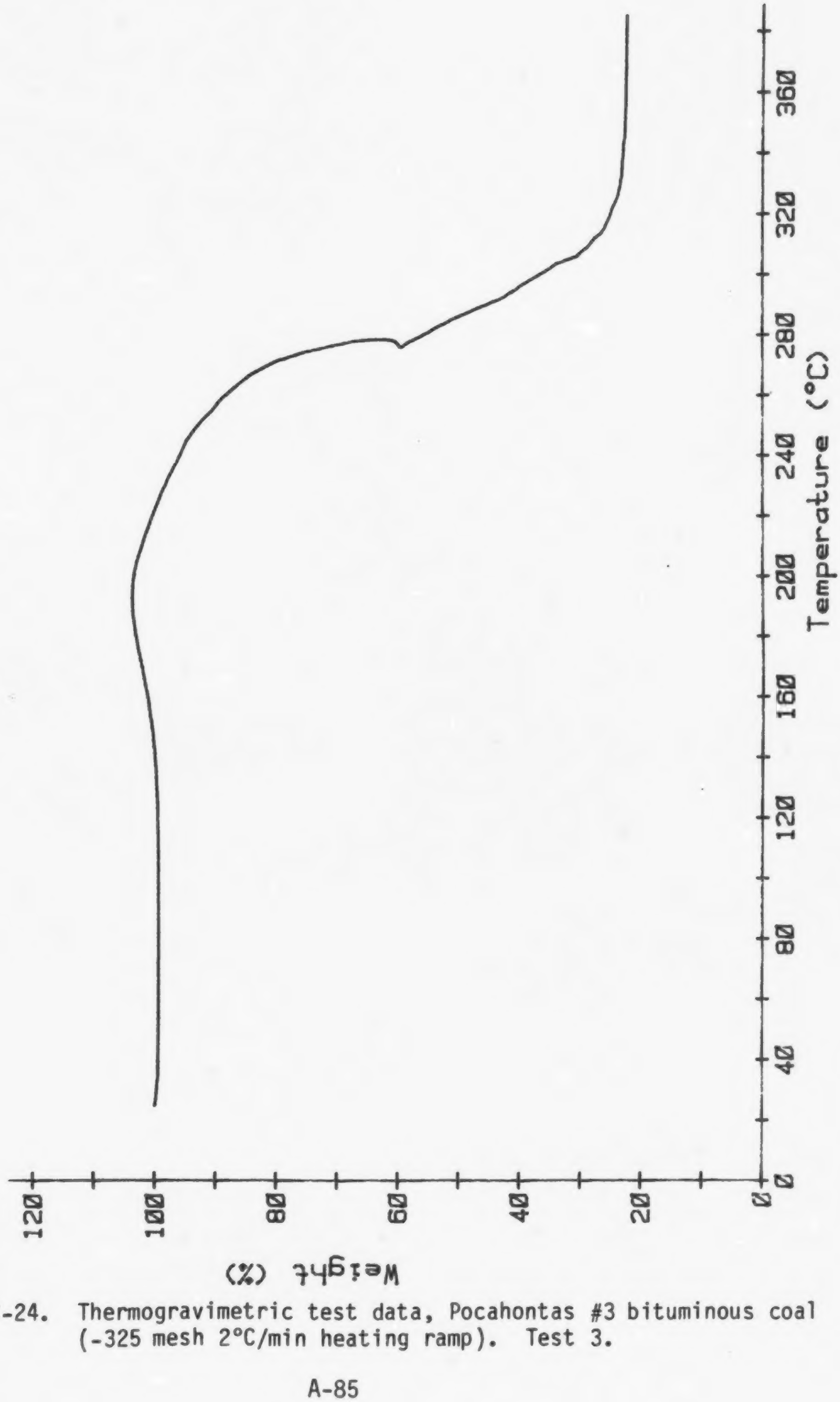

Figure C-24. Thermogravimetric test data, Pocahontas #3 bituminous coal (-325 mesh 2°C/min heating ramp). Test 3.

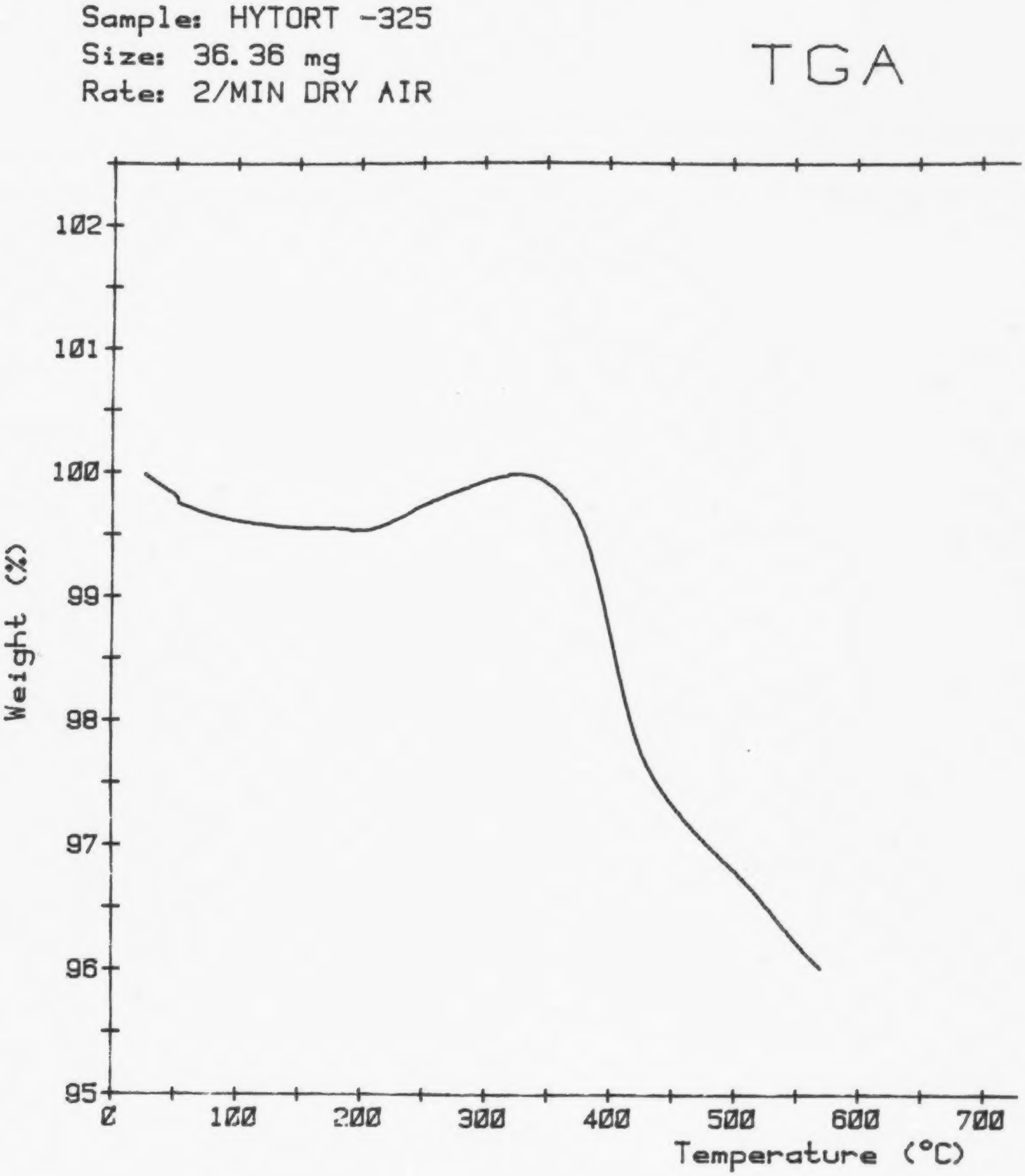

Figure C-25. Thermogravimetric test data, Hytort retorted shale (-325 mesh 2°C/min heating ramp). Test 1.

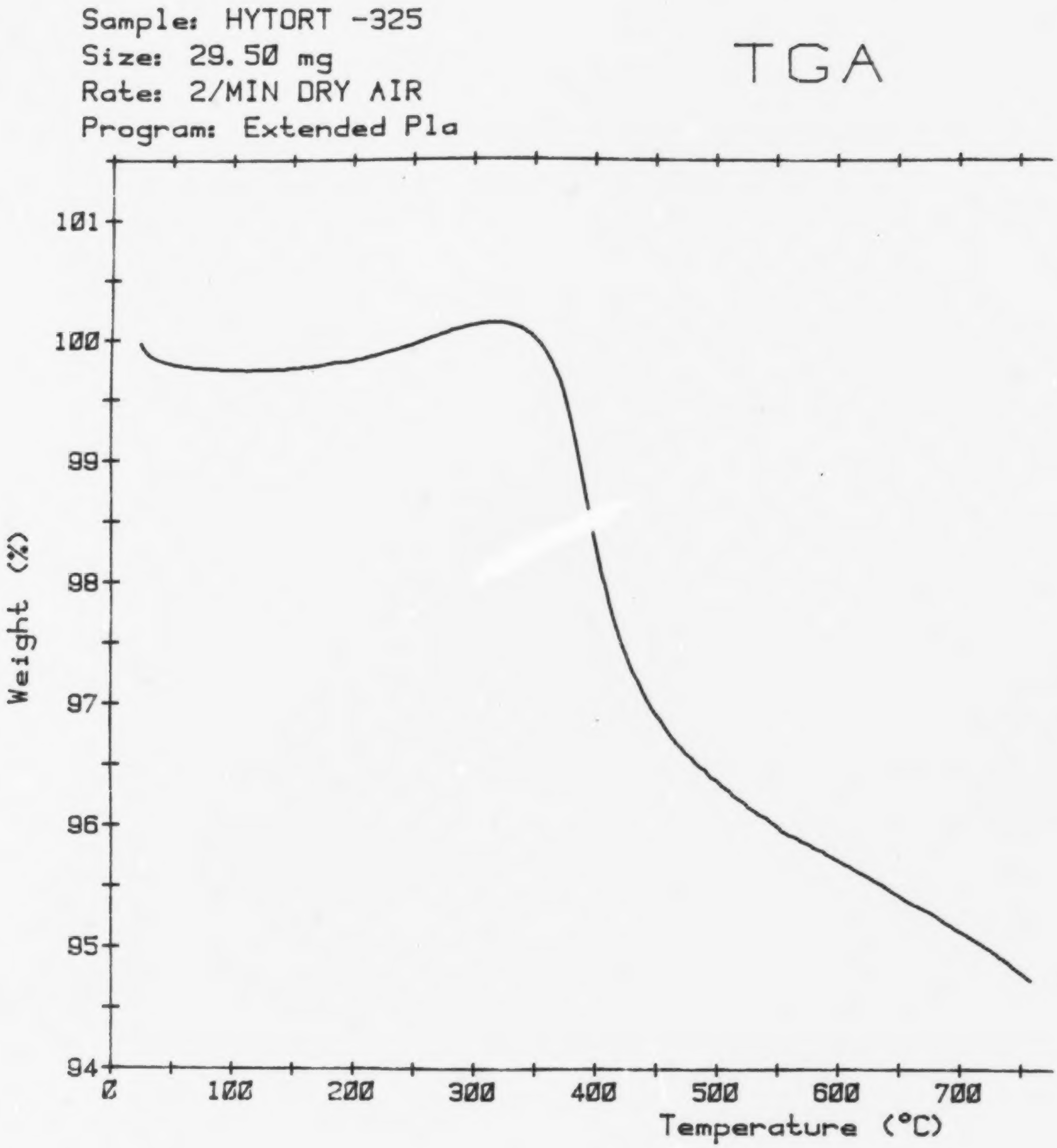

Figure C-26. Thermogravimetric test data, Hytort retorted shale (-325 mesh 2°C/min heating ramp). Test 2.

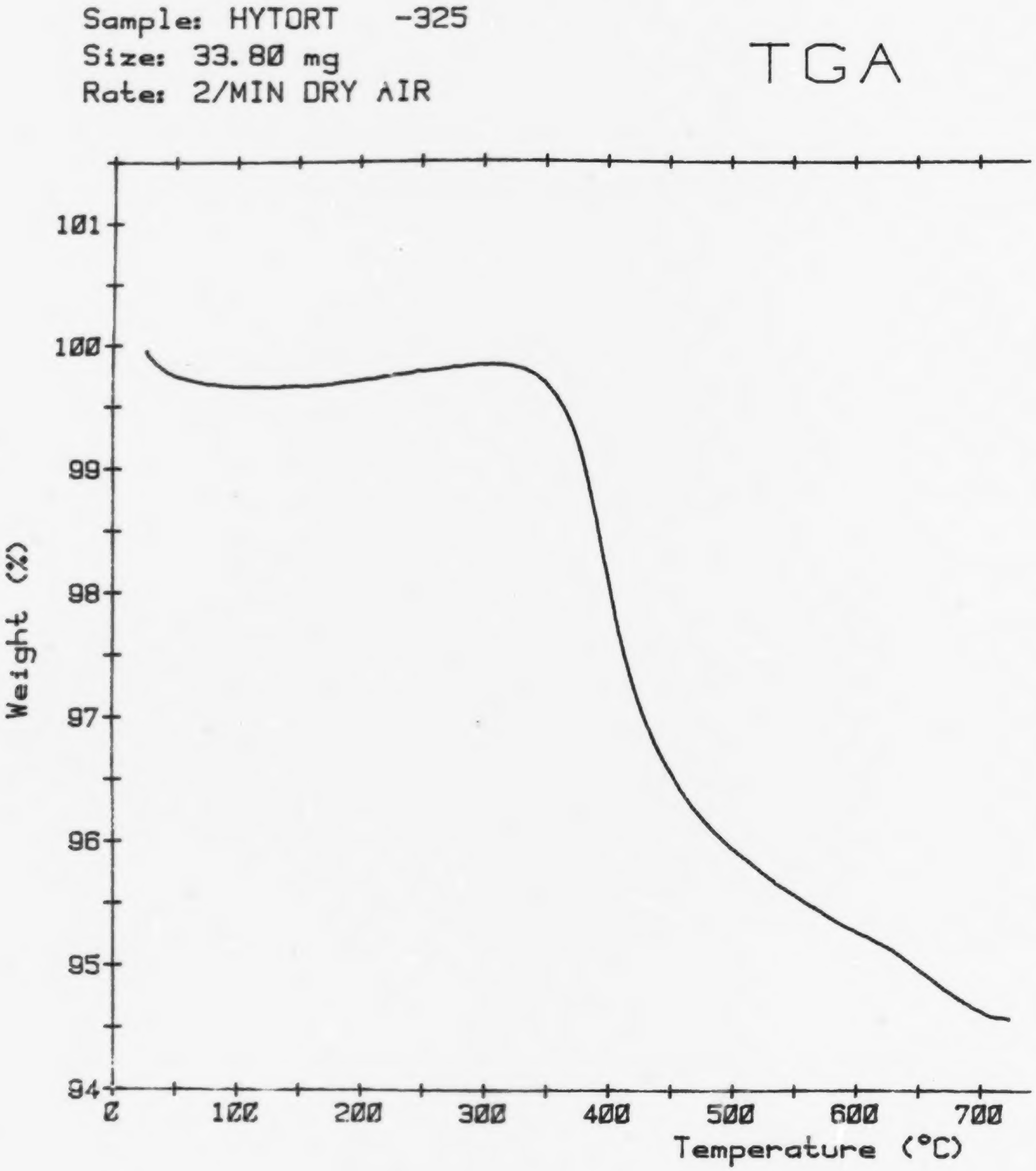

Figure C-27. Thermogravimetric test data, Hytort retorted shale (-325 mesh 2°C/min heating ramp). Test 3.

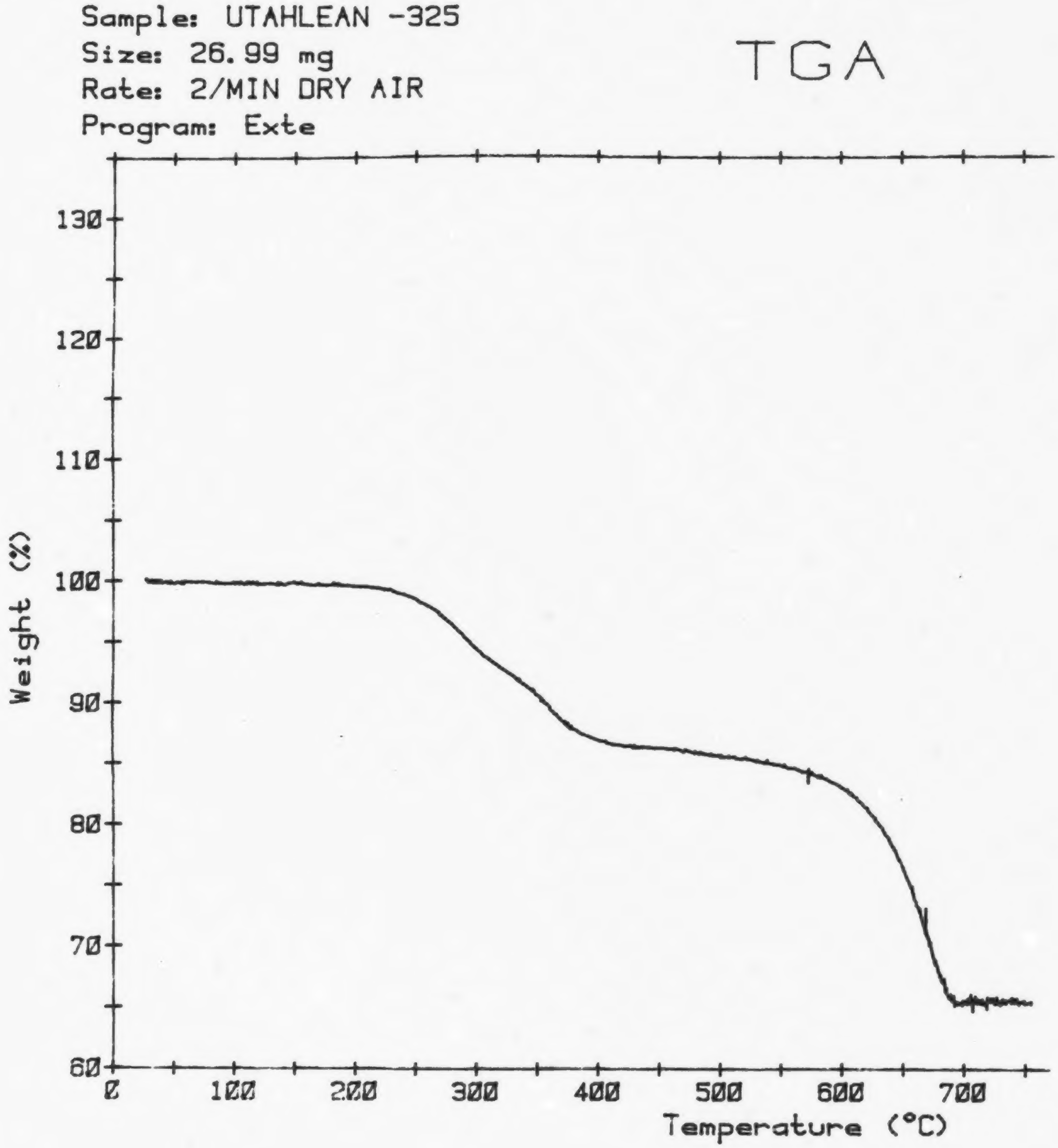

Figure C-28. Thermogravimetric test data, Utah raw shale (28 GPT) (-325 mesh 2°C/min heating ramp). Test 1.

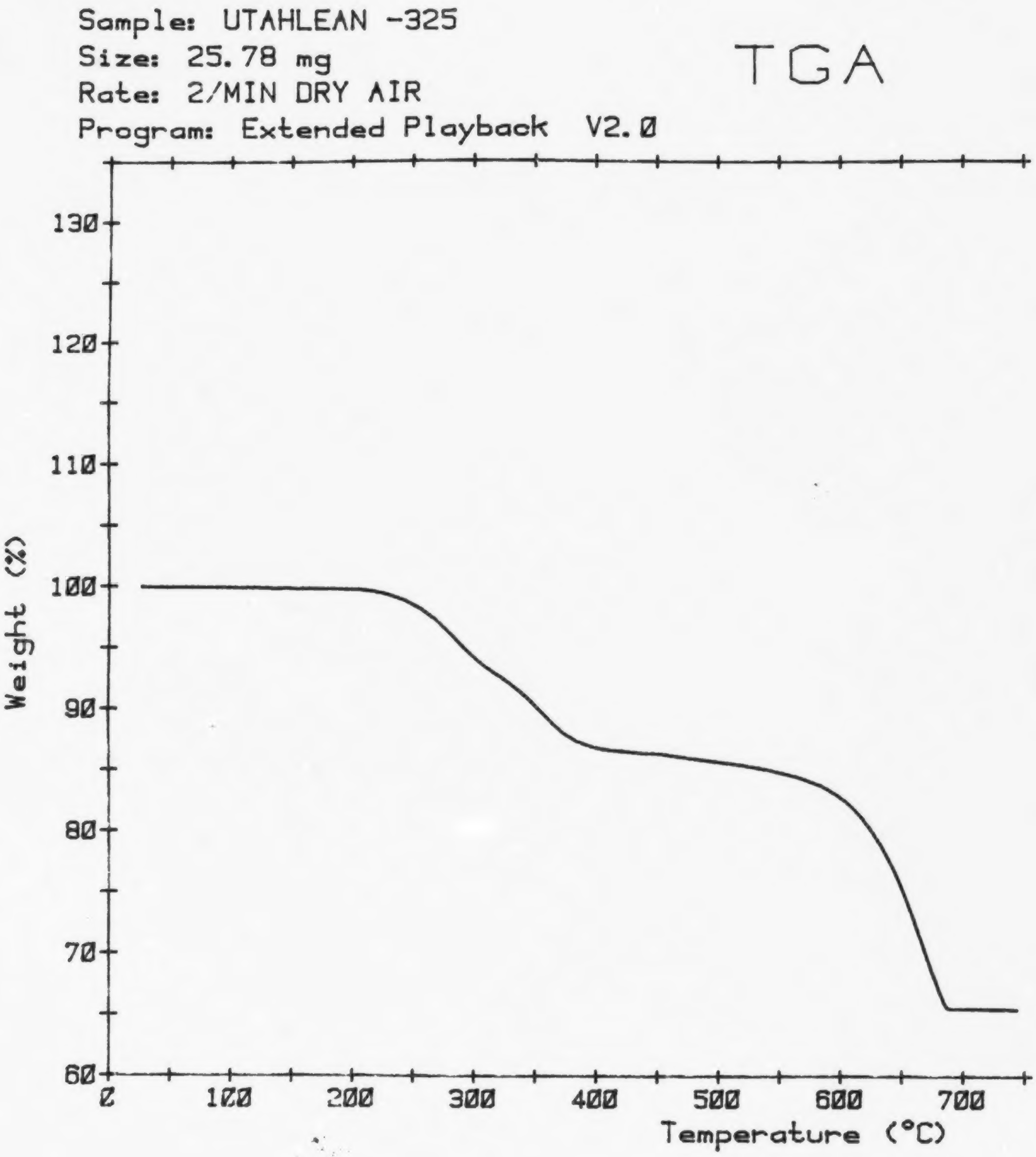

Figure C-29. Thermogravimetric test data, Utah raw shale (28 GPT) (-325 mesh 2°C/min heating ramp). Test 2.

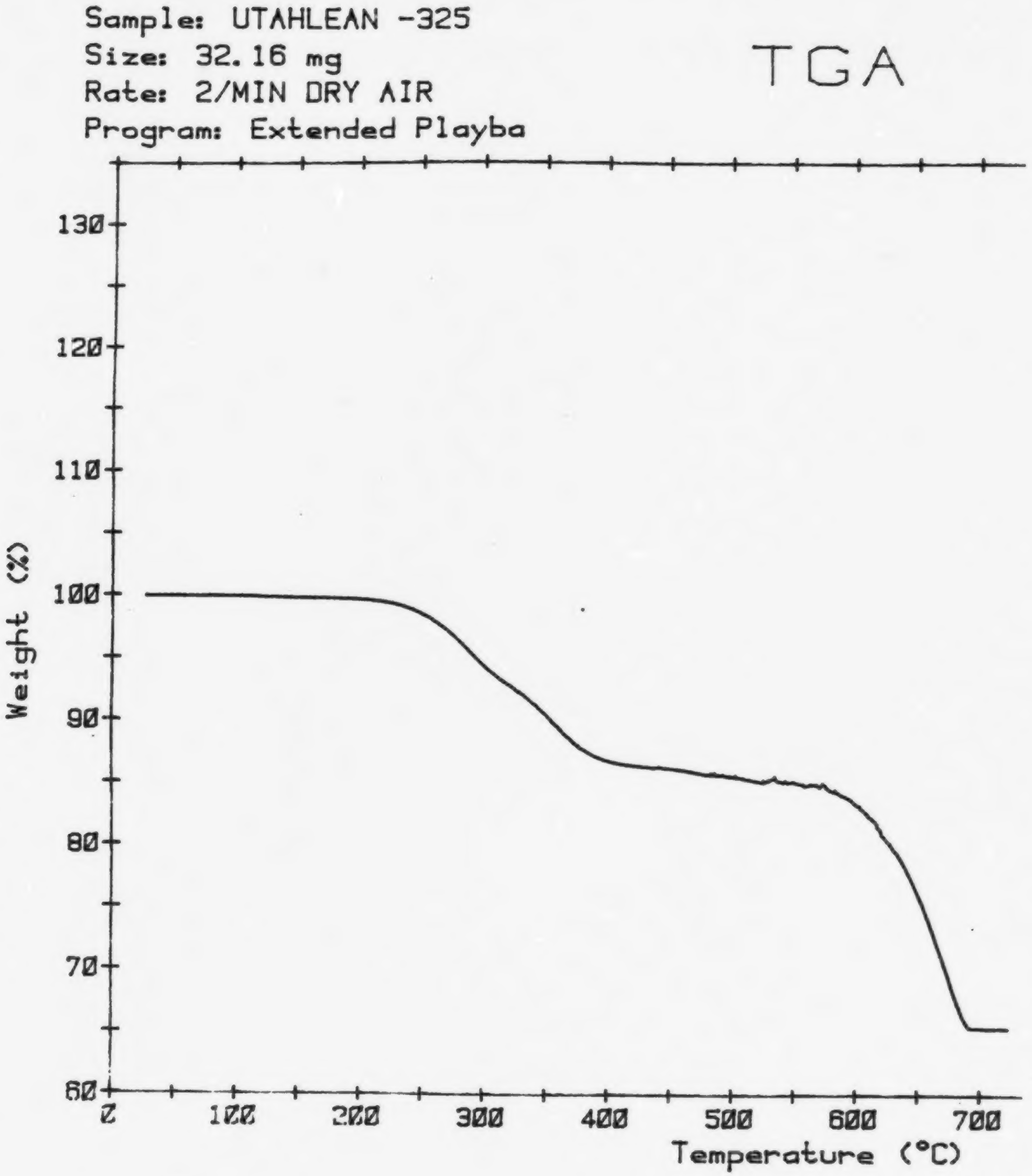

Figure C-30. Thermogravimetric test data, Utah raw shale (28 GPT) (-325 mesh 2°C/min heating ramp). Test 3.

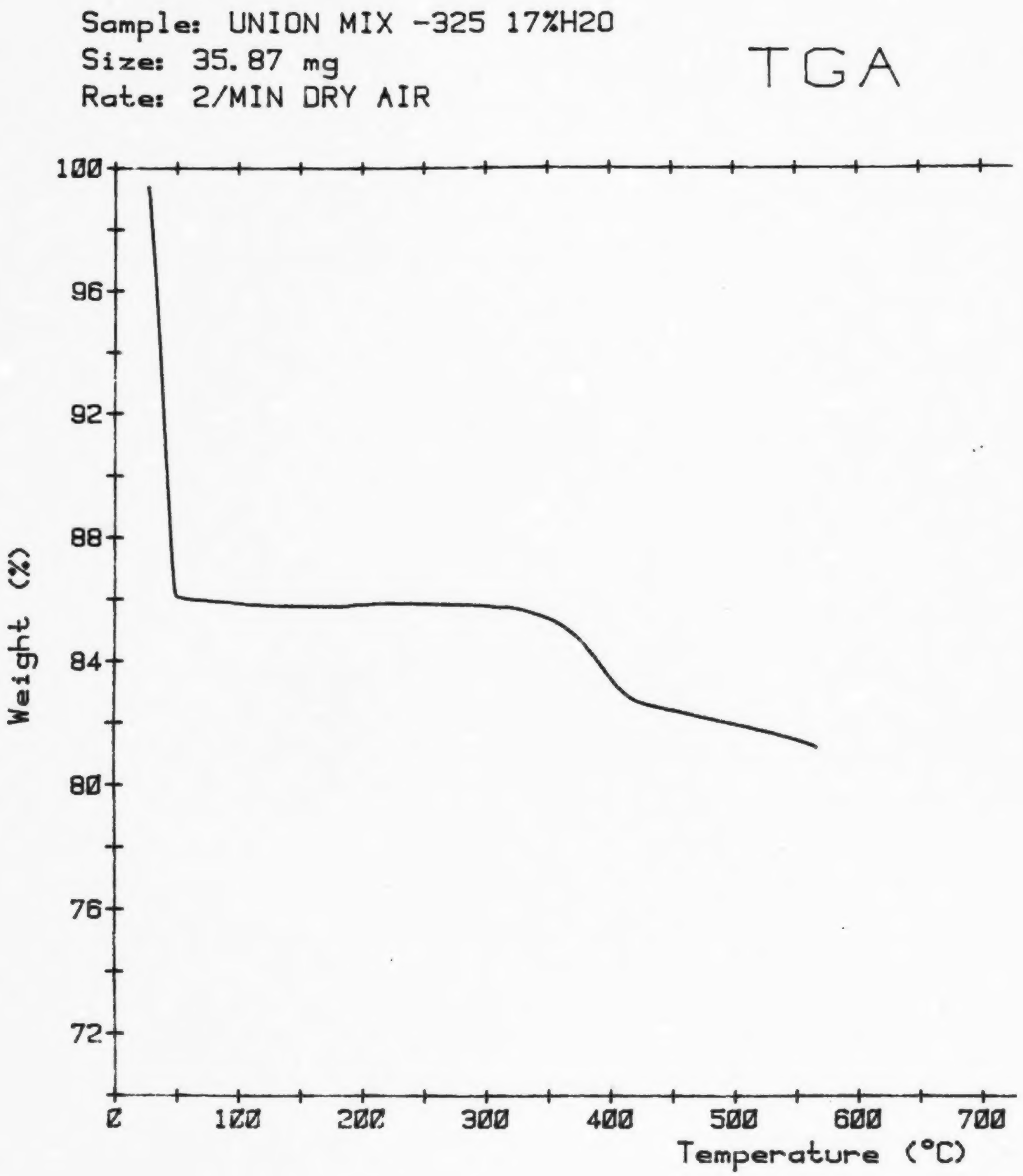

Figure C-31. Thermogravimetric test data, Union shale mixture (-325 mesh 2°C/min heating ramp). Test 1.

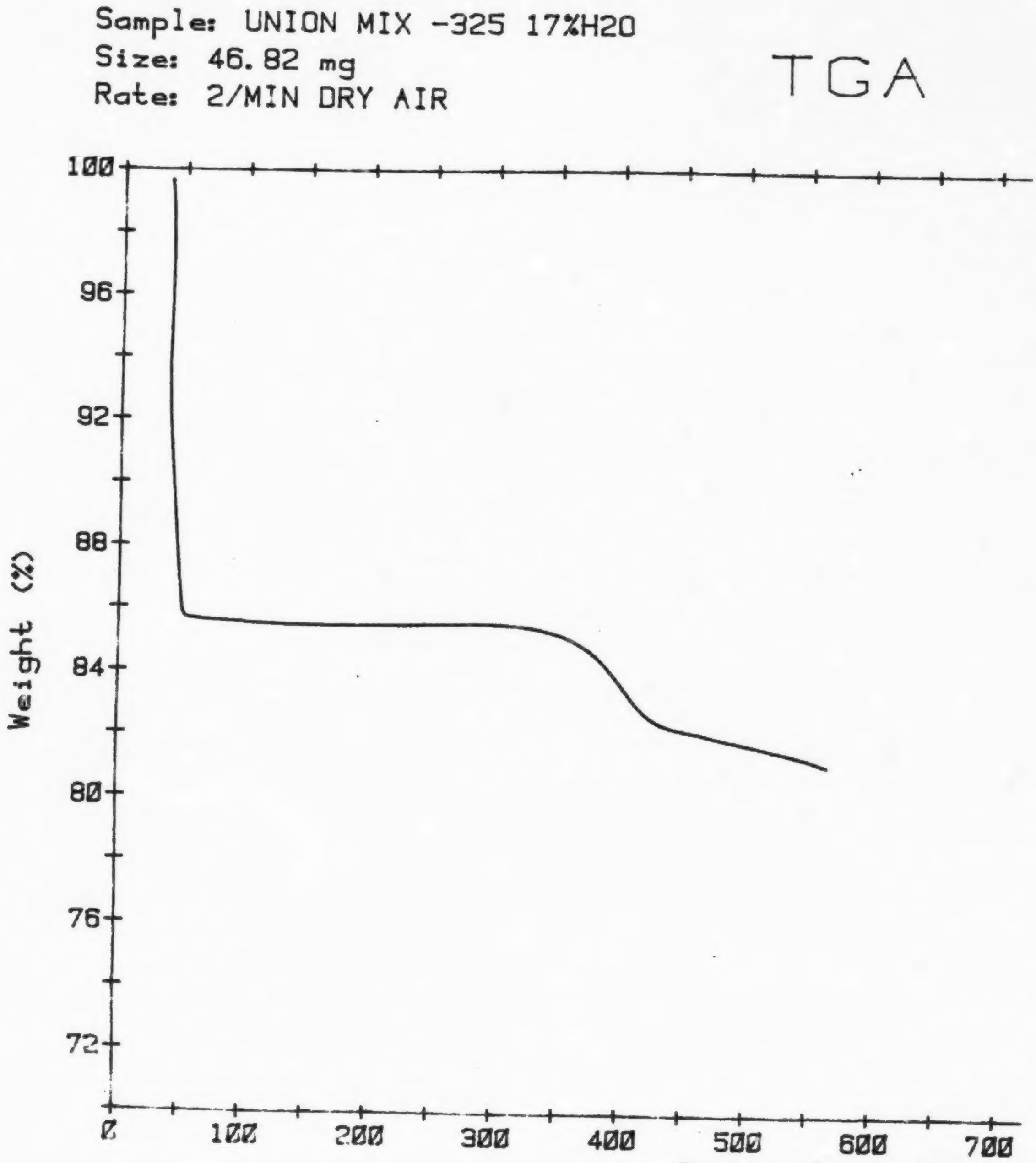

Figure C-32. Thermogravimetric test data, Union shale mixture (-325 mesh 2°C/min heating ramp). Test 2.

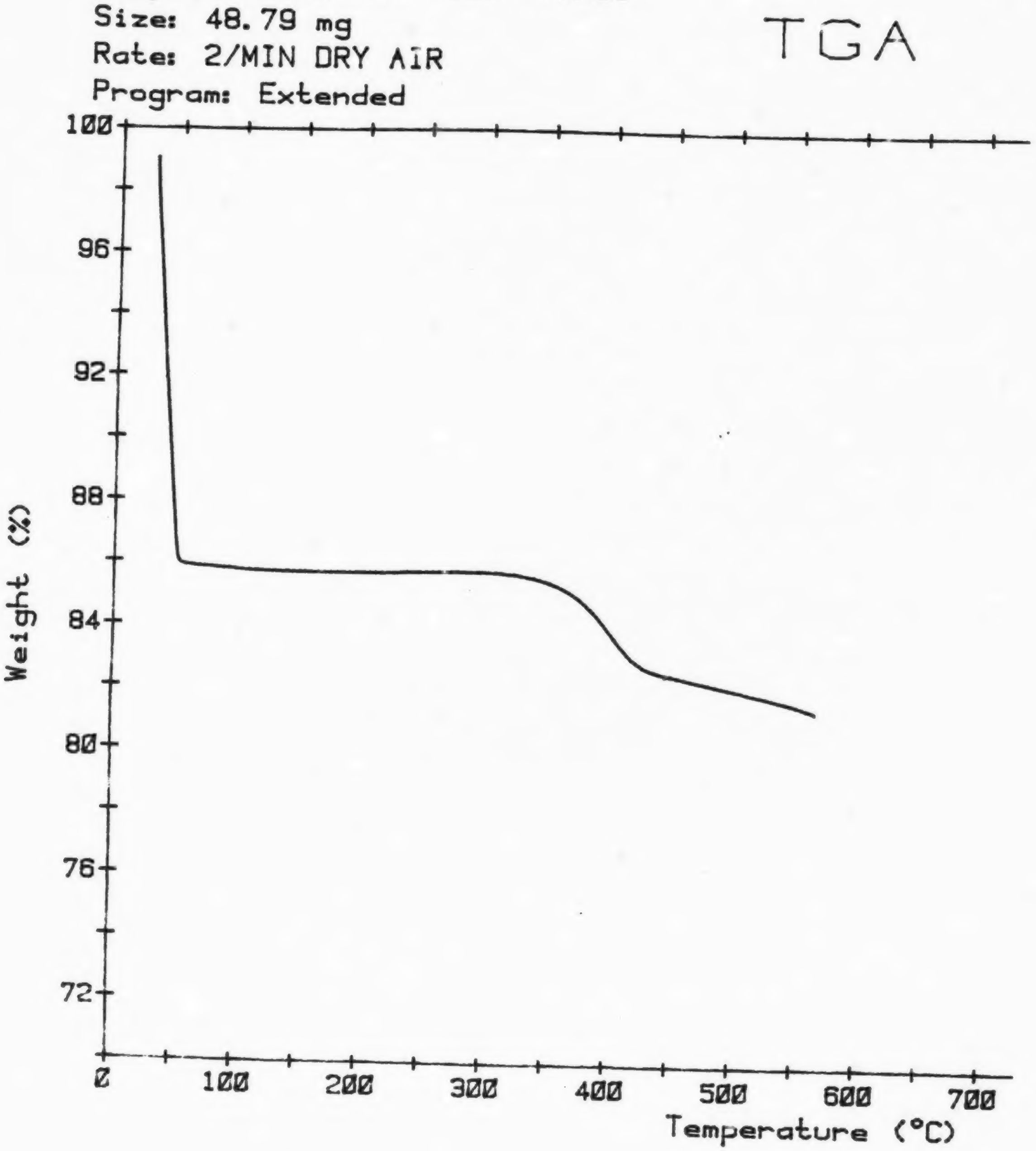

Figure C-33. Thermogravimetric test data, Union shale mixture (-325 mesh 2°C/min heating ramp). Test 3.

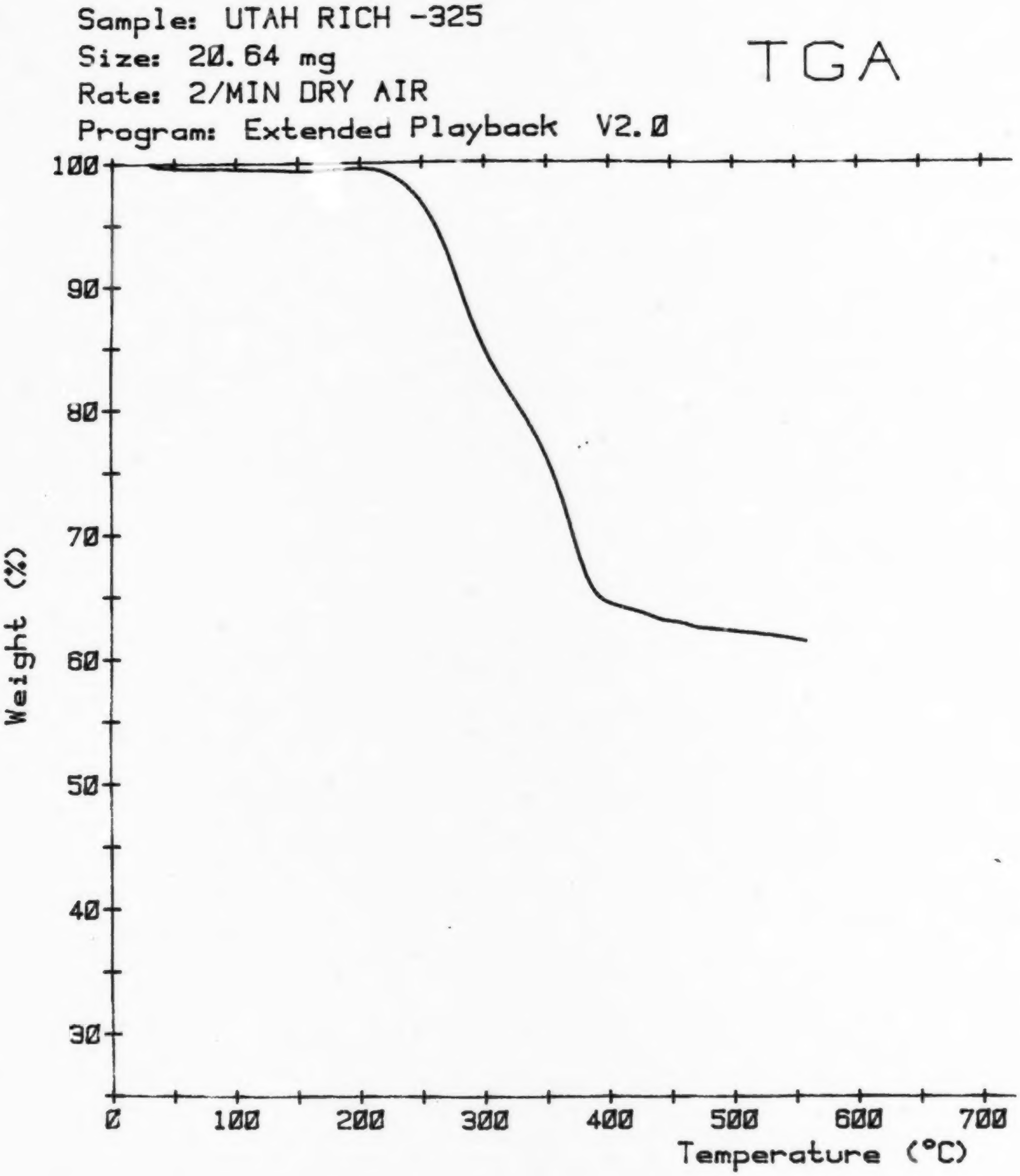

Figure C-34. Thermogravimetric test data, Utah raw shale (66 GPT) (-325 mesh 2°C/min heating ramp). Test 1.

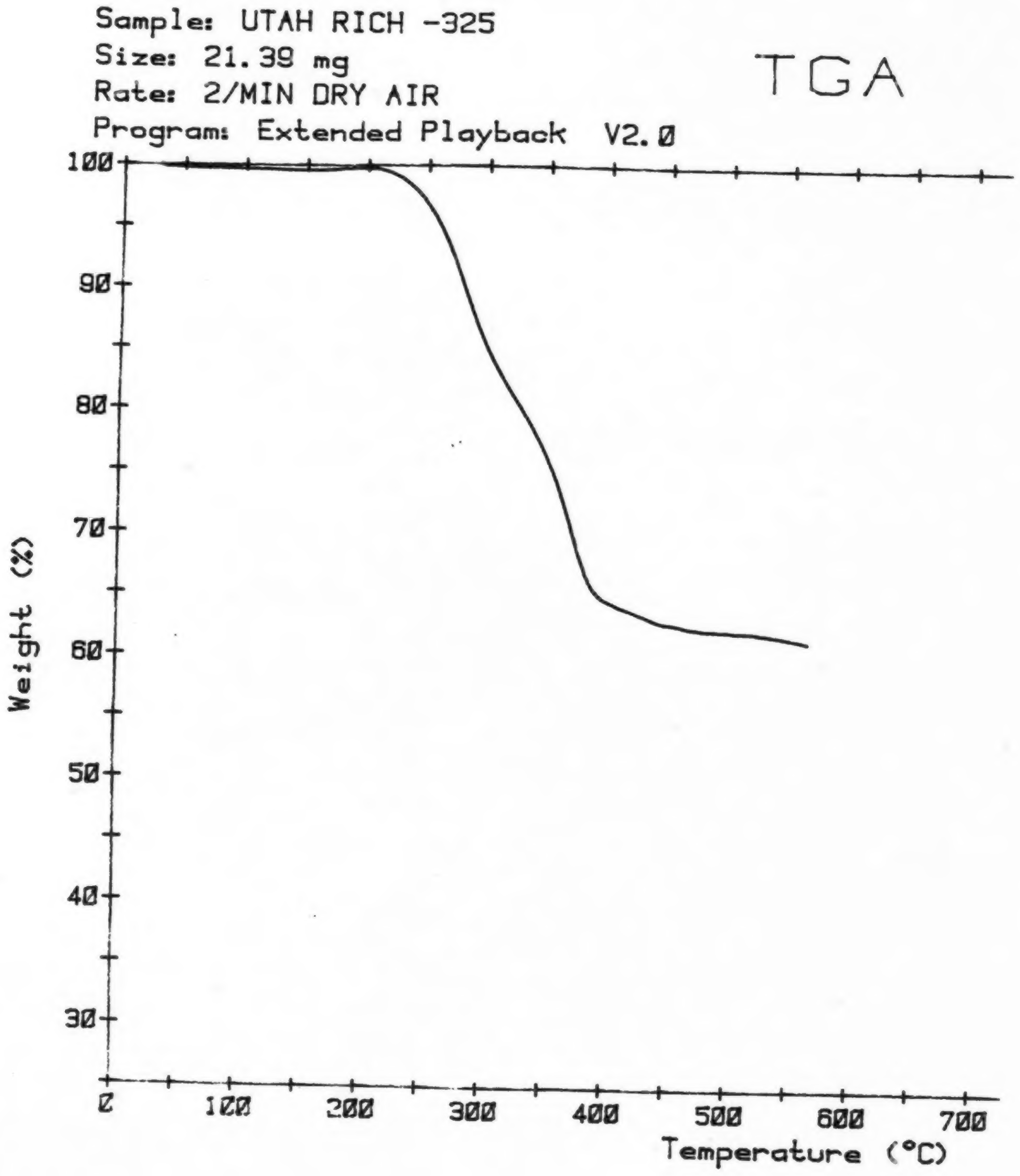

Figure C-35. Thermogravimetric test data, Utah raw shale (66 GPT) (-325 mesh 2°C/min heating ramp). Test 2.

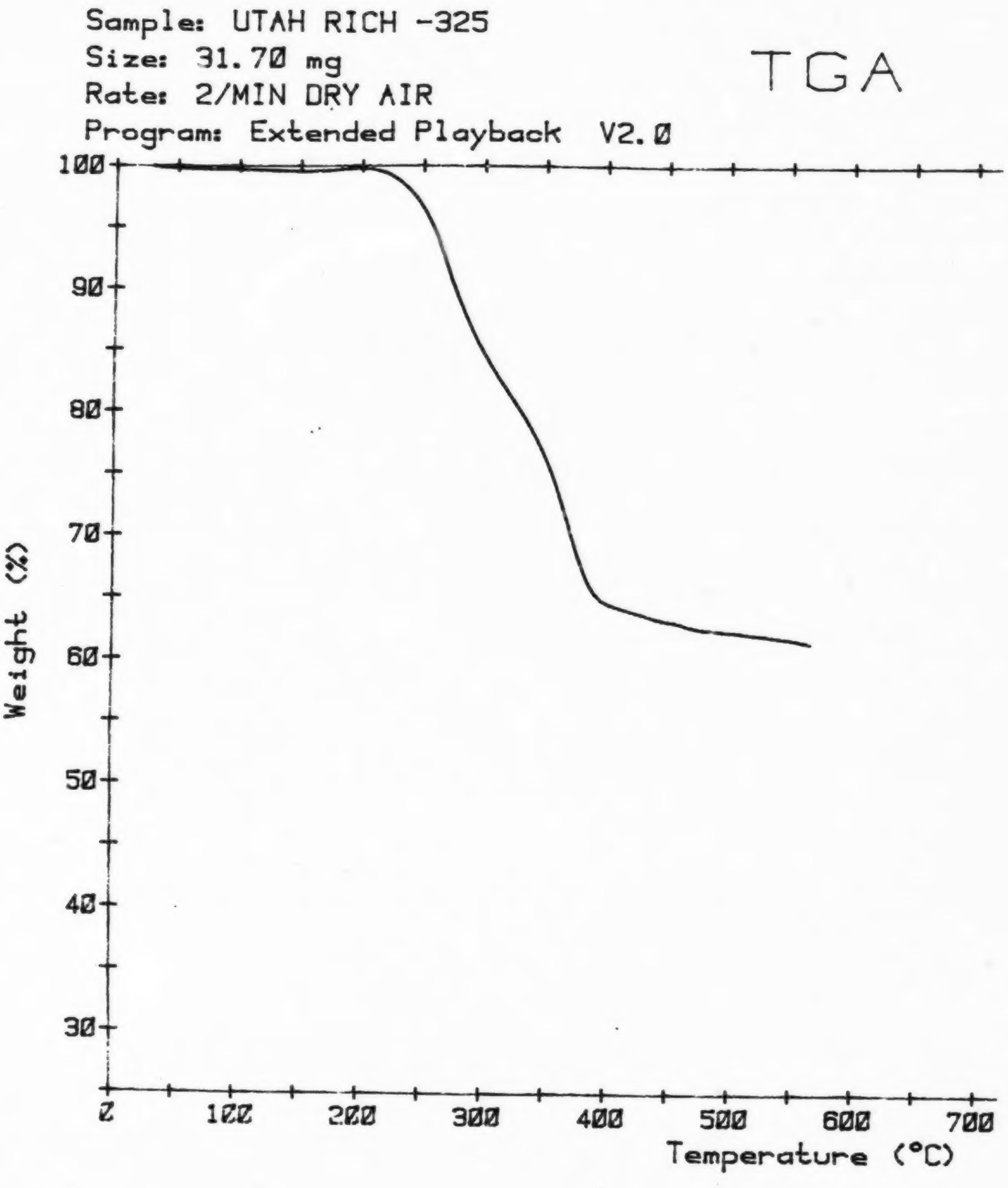

Figure C-36. Thermogravimetric test data, Utah raw shale (66 GPT) (-325 mesh 2°C/min heating ramp). Test 3.